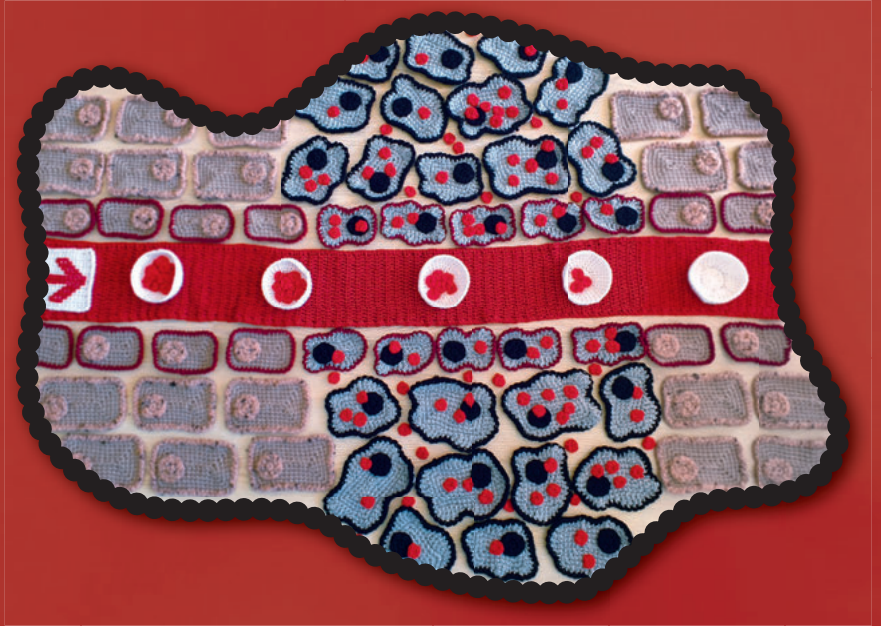


Improving tumor drug deposition by physical activation of liposomes and prodrugs



H.C. Besse

Improving tumor drug deposition by physical activation of liposomes and prodrugs

H.C. Besse

Improving tumor drug deposition by physical activation of liposomes and prodrugs

PhD Thesis, Utrecht University, The Netherlands

© H.C. Besse, Utrecht, 2021

All rights reserved. No part of this publication may be reproduced or transmitted in any form or by any means without permission in writing from the author. The copyright of the articles that have been published or have been accepted for publication have been transferred to the respective journals.

ISBN: 978-90-393-7370-5

DOI: <https://doi.org/10.33540/532>

Lay-out: Lara Leijtens, persoonlijkproefschrift.nl

Cover design: Lara Leijtens, persoonlijkproefschrift.nl

Cover images: H. C. Besse

Printing: Ridderprint, www.ridderprint.nl

Improving tumor drug deposition by physical activation of liposomes and prodrugs

Fysische activatie van liposomen en prodrug ter verbetering van medicijn afgifte in de tumor
(met een samenvatting in het Nederlands)

Proefschrift

ter verkrijging van de graad van doctor aan de Universiteit Utrecht
op gezag van de rector magnificus, prof.dr. H.R.B.M. Kummeling,
ingevolge het besluit van het college voor promoties
in het openbaar te verdedigen op
donderdag 6 mei 2021 des middags te 12.15 uur

door

Helena Clazina Besse

geboren op 17 juni 1990
te Haarlem

Promotor: Prof. dr. C.T.W. Moonen

Copromotoren: Dr. R.H.R. Deckers
Dr. C. Bos

This research presented in this thesis was funded by the European Research Council – Grant #268906 “Sound Pharma” (Prof. dr. C.T.W. Moonen)

"On ne fait jamais attention à ce qui a été fait ; on ne voit que ce qui reste à faire"

"We letten nooit op wat er al gedaan is; we zien alleen wat er nog moet worden gedaan."

Marie Curie

CONTENTS

Chapter 1	General introduction and thesis outline	9
Chapter 2	Triggered radiosensitizer delivery using thermosensitive liposomes and hyperthermia improves efficacy of radiotherapy: an <i>in vitro</i> proof of concept study	27
Chapter 3	Tumor drug distribution after local drug delivery by hyperthermia, <i>in vivo</i>	53
Chapter 4	Modular synthesis of self-immolative doxorubicin prodrugs with rapid enzymatic activation upon ultrasound-mediated mechanical cell destruction	85
Chapter 5	A doxorubicin-glucuronide prodrug released from nanogels activated by high-intensity focused ultrasound liberated β -glucuronidase	109
Chapter 6	Summary and general discussion	129
	Chapter 6.1 Summary	130
	Chapter 6.2 General discussion	133
Appendix		149
	Nederlandse samenvatting	150
	List of publications	154
	Curriculum Vitae	157
	Acknowledgements	159

CHAPTER 1

General introduction and thesis outline

CANCER

Cancer is one of the most prevalent diseases [1], with a third of the population diagnosed with cancer at least once throughout their lives in The Netherlands [2]. It represents a large and heterogeneous group of diseases, which makes a single 'one-size-fits-all' therapy ineffective. Nonetheless, in the last 40 years the progression-free and overall survival has improved significantly for many cancer types, owing to a clear improvement in early diagnostics and therapeutic strategies, among others [3]. Despite these advances, cancer is still the first cause of death in The Netherlands [1].

Chemotherapy is, along with radiotherapy and surgery, one of the corner stones in cancer treatment [2, 4]. It is often administered systemically to the patient, e.g. intravenously. Therefore, the chemotherapeutic agent reaches the primary tumor, but also the metastases and micrometastases, thus potentially alleviating the tumor burden of these multiple locations simultaneously.

Local control of the primary tumor is of utmost importance to restrict or delay the occurrence of metastases, since metastatic disease results in substantially deteriorating patient prognosis and overall survival [5-7]. To render a chemotherapeutic protocol effective in tumors, the tumor tissue must be exposed to the chemotherapeutic agent I) with an appropriate drug concentration and II) for a specific duration, both parameters being dependent on the type of molecule binding and mode of action of the agent [8]. Since most chemotherapeutic agents are not tumor cells specific, the systemically administered chemotherapeutic agent reaches the primary tumor as well as the normal tissue. Exposure of the normal tissue to the chemotherapeutic agent could result in toxicity in these tissues [9-11], which could ultimately lead to required dose reduction of the drug, and suboptimal treatment efficacy [12]. To improve the efficacy of the chemotherapeutic agent in the treatment of the primary tumor, the agent needs to be solely delivered at high concentrations in the primary tumor. Hence, there is a clear need for local drug delivery strategies.

Local drug delivery can be obtained by injecting the drug in or nearby the tumor, for example by intratumoral [13], intraperitoneal, i.e. into the abdomen cavity, [14] and intrathecal, i.e. into the spinal canal, [15] administration. Although these local drug delivery approaches show improvement in survival, they are rather invasive. A less invasive delivery strategy is the systemic administration of an encapsulated or modified chemotherapeutic agent into a so called drug

carrier. These drug carriers release the chemotherapeutic agent only in the tumor microenvironment, avoiding drug exposure to the normal tissue. Multiple formulations of these drug carriers are under investigation, like polymeric nanoparticles, nanocrystals, micelles, nanogels, liposomes and prodrugs [16, 17], of which some of them are FDA approved, like DOXIL, liposomal formulation containing doxorubicin for the treatment of Kaposi Sarcoma [18] and Abraxane, albumin-bound paclitaxel nanoparticle formulation for the treatment of breast cancer [16]. In this thesis temperature sensitive liposomes and prodrugs are used as a means to improve local drug deposition in the primary tumor.

DOXORUBICIN

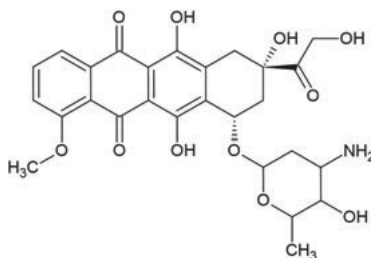


Figure 1.1: Molecular structure of doxorubicin (DOX).

In this thesis doxorubicin (DOX) is used as a model drug. This molecule, also known as Adriamycin and Rubex, was first isolated from the bacterium *Streptomyces peucetius* in 1969 by Arcamone and colleagues [19] and FDA approved in 1974. Although DOX is known for over 40 years, the exact mechanism of action is still unknown. Several mechanisms of action are confirmed, like topoisomerase II inhibition, DNA intercalation, free radical formation, ceramide overproduction and histone eviction [20, 21], which ultimately results in DNA damage and inhibition of DNA and RNA synthesis.

DOX is currently still used in the clinic for the treatment of many cancers, such as breast, kidney and thyroid cancer, leukemia and soft tissue sarcoma [22]. In daily clinical practice DOX is injected systemically; it is not tumor cell specific, and causes toxicity in normal tissues, especially in the heart, i.e. cardiotoxicity [23]. In pre-clinical studies DOX is extensively used as a model drug to investigate drug concentration and drug distribution in the tumor; in particular its intrinsic fluorescence allows investigating DOX uptake in cells and tissues without necessarily resorting to additional contrast agents, like drug-bound fluorescence conjugates [24].

LIPOSOMES

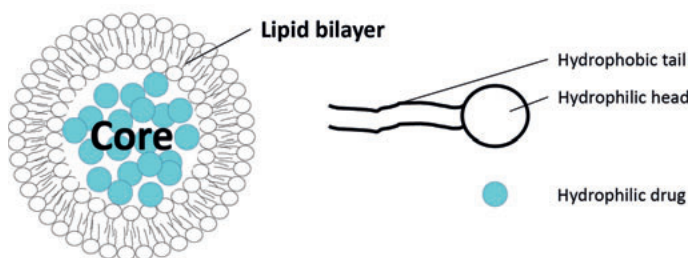


Figure 1.2: Schematic representation of a liposome (typical size around 80 to 300 nm in diameter [25]).

Liposomes are formulations that can be used as drug carriers; they are composed of lipids arranged as a bilayer, with a core containing encapsulated drugs [16], see Figure 1.2. Hence, this structure protects normal surrounding tissues from the drug [26, 27]. Only in the tumor tissue the drug is released from the liposomes. Depending on the composition of the lipids in the liposome bilayer, such as lipid type and proteins between and attached to the lipids, different mechanisms of drug release and tumor targeting can be pursued, like passive, cancer cell and endothelial cell targeting and triggered drug release [28]. The most clinically investigated mechanisms of liposomal drug release are passive targeting and triggered drug release, of which some are listed in Table 1.1 [29].

Table 1.1: Different commonly used liposomes

Drug name	Chemotherapeutic agent	Status of clinical translation	Mechanism of local drug delivery
Myocet	Doxorubicin	FDA approved	Passive targeting
DOXIL/Caelyx	Doxorubicin	FDA approved	Passive targeting
DaunoXome	Daunorubicin	FDA approved	Passive targeting
MM-398	Irinotecan	FDA approved	Passive targeting
Vyxeos	Cytarabine and Daunorubicin	FDA approved	Passive targeting
Lipoplatin	Cisplatin	Phase III	Passive targeting
LEP-ETU	Paclitaxel	Phase III	Passive targeting
ThermoDox	Doxorubicin	Phase III	Triggered drug release

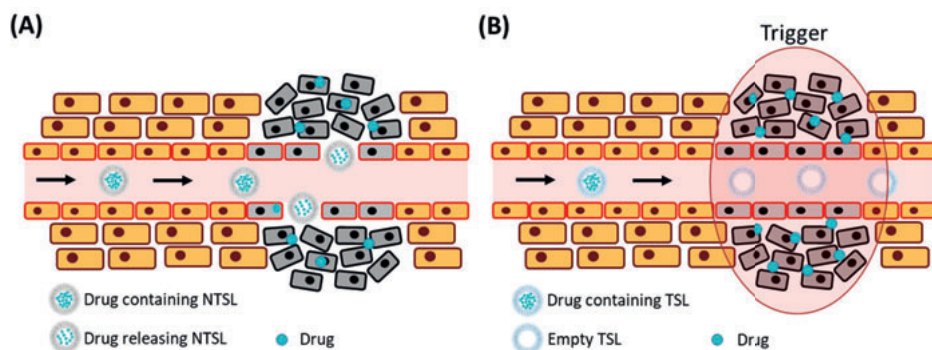


Figure 1.3: Schematic representation of drug delivery by liposome-based drug carriers on (A) passive drug delivery and (B) triggered drug release (not at scale).

Figure 1.3 shows a schematic representation of local drug delivery by liposomes based on passive targeting (A) and triggered drug release (B). Local drug delivery by liposomes that passively target the tumor microenvironment, further referred to as non-temperature sensitive liposomes (NTSL), is achieved by trapping the liposomes in the tumor, subsequently the drug is slowly released from the liposomes into the tumor tissue, whose release kinetics depend on the liposome composition [18, 30], Figure 1.3A. The targeting of the tumor by NTSLs occurs by trapping the liposomes in the tumor tissue by the enhanced permeability and retention (EPR) effect [31]. Only present in tumor tissue, the EPR effect is caused by an increased vascular permeability, along with reduced lymphatic drainage, leading to increased liposome extravasation and accumulation of these liposomes in the tumor tissue [32]. Conversely, another local drug delivery approach is the use of an external local trigger, i.e. triggered drug release, to induce a fast drug release from the liposome in the tumor vasculature. Many triggers have been proposed, such as low pH, light and heat [33], of which the latter being the most widely investigated [34]. To achieve such a triggered release by heat, these liposomes, i.e. temperature sensitive liposomes (TSL), have a rather low phase transition temperature, 41 to 42°C. At this temperature the lipid bilayer of the liposome transfers from a gel phase into a fluid phase, resulting in a quick drug payload release [34-36]. As such, the drug becomes immediately bioavailable in the tumor microenvironment, see Figure 1.3B [26, 37, 38].

Local drug delivery by liposomes based on the mechanisms of passive targeting and triggered drug release improve the efficacy of the chemotherapeutic agent. Both treatment with NTSL and TSL containing DOX have been shown

to significantly reduce tumor growth, and increase survival in tumor bearing animals compared to animals subjected to an un-encapsulated (free) DOX treatment [38-42]. It was demonstrated that the TSL treatment concurrent with exposing the tumor to temperatures in the range of 41 to 42°C, i.e. hyperthermia treatment, results in a greater increase in survival compared to NTSL treatment [38], which may be related to the immediate DOX release in the tumor microenvironment after TSL treatment. Whereas after NTSL treatment, drug is released over a prolonged period of time and is therefore not immediately bioavailable [30].

The increase in survival after treatment with TSLs or NTSLs containing DOX could be attributed to increased DOX concentrations in the tumor, compared to free DOX treatment [26, 27, 41-43]. TSL treatment, in particular, results in the largest DOX concentration in the tumor [38]. It is note-worthy that the DOX concentration mentioned is the total, free (bioavailable) and encapsulated (non-bioavailable), DOX concentration in the tumor. Whereas total DOX concentration and total bioavailable DOX concentration are similar for treatment with free DOX and TSL (after triggering), DOX release from NTSLs is slow, rendering a moderate but prolonged bioavailability [30]. Besides tumor drug concentration, the drug efficacy also depends on its distribution in the tumor, among others [44, 45]. The tumor drug distribution can be subdivided in I) drug distribution relative to the vessels and II) spatial drug distribution in the whole tumor. In comparison with free DOX treatment, both NTSL and TSL treatments potentially increase the DOX penetration distance relative to the vessels into the tumor [37, 46], of which the DOX penetration distance is the largest after TSL treatment [37]. For spatial DOX distribution over the whole tumor, there is evidence that DOX is more homogeneously distributed in the whole tumor after TSL treatment compared to treatment with free DOX [26, 37, 38]. Currently, there is a lack of head-to-head comparison on DOX distribution in the tumor between NTSL and TSL treatment, despite its importance for further improvements in local drug delivery.

Besides a trigger for local drug delivery by TSLs, hyperthermia, temperatures in the range of 41 to 42°C, is also known as a chemosensitizer, it increases the cytotoxicity of some specific chemotherapeutic agents, including DOX [47, 48]. The sensitization by hyperthermia occurs both at macroscopic and molecular level. At macroscopic level, hyperthermia causes vasodilatation, resulting in increased blood flow in the tumor, increasing the chemotherapy concentration in the tumor tissue [48, 49]. At molecular level, hyperthermia treatment was

evidenced to temporally inhibit double strand break (DSB) repair, increasing cell death when hyperthermia is combined with chemotherapy [50].

In the clinic, chemotherapy is in some specific cases combined with radiotherapy, *i.e.* chemoradiation, due to its synergistic combination. Radiotherapy is a local treatment that consists of high energy electrons or photons that induce DNA damage [51, 52]. Some clinically available chemotherapeutic agents are able to sensitize tumors to radiotherapy, hence their name radiosensitizers [53-56]. DOX is such a chemotherapeutic agent that also exhibits a radiosensitizing effect, presumably by inhibition of the DNA damage repair [55]. Currently, DOX is not used as a radiosensitizer in the clinic, because the combination of DOX and radiotherapy causes severe toxicities in the normal tissue located in the beam path of radiotherapy [57-59]. Therefore, local delivery of DOX, by clinically available NTSLs (DOXIL) and under clinical investigation TSLs (ThermoDox), may be beneficial to exert the chemoradiation effect without causing severed adverse events in the normal tissue.

PRODRUGS

Prodrugs are chemically modified drugs that have non or little cytotoxicity, and are activated to be converted into the cytotoxic drug [60]. Prodrugs can be used to overcome various barriers in order to improve the efficacy of the active drug of interest, by improving aqueous solubility, improving chemical stability, and reducing toxicity in normal tissues by tumor site-selective drug activation [61]. Prodrugs for tumor site-selective drug activation are often hydrophilic and therefore not able to cross the cell membrane, reducing the cytotoxicity of the chemotherapeutic agent in the normal tissue [62]. In the tumor the inactive, non-cytotoxic, prodrug needs to be activated by a tumor site-specific stimulus to be converted into a cytotoxic drug. Subsequently, the activated cytotoxic molecule becomes bioavailable in the tumor tissue, is able to cross the cell membrane and causes cytotoxicity [63]. Many stimuli are available for prodrug activation, like hypoxia, low pH, tumor specific antigens and tumor specific enzymes [64]. In cancer therapy, tumor specific enzymes are often used as stimuli for prodrug therapy, *i.e.* enzyme prodrug therapy.

For effective enzyme prodrug therapy the following key requirements need to be met; I) quick conversion of the prodrug into the cytotoxic drug, II) high enzyme concentration available for prodrug conversion in the tumor and III) low enzyme concentration available for prodrug conversion in the normal tissue

[65, 66]. For local drug activation of prodrugs an often investigated enzyme is β -glucuronidase (β -GUS), a lysosomal enzyme that is only extracellularly available in necrotic tumor areas [67]. Prodrugs converted by β -GUS, so called glucuronide-prodrugs, consist of a glucuronic acid, a spacer and a cytotoxic agent [68]. Upon conversion, the enzyme cleaves the glucuronic acid, subsequently the spacer is removed by hydrolysis and finally the cytotoxic agent is released.

For effective enzyme prodrug therapy the enzyme available for prodrug conversion should be highly expressed in the tumor microenvironment. Since in small tumors the β -GUS concentration is rather low, the efficacy of enzyme prodrug therapy in these tumors is hampered [68]. This could be enhanced by increasing the amount of bioavailable β -GUS in the tumor tissue. Previously investigated methods to achieve this are antibody directed enzyme prodrug therapy (ADEPT) and gene directed enzyme prodrug therapy (GDEPT). In ADEPT the activatable enzyme for prodrug conversion is coupled to a tumor specific antibody, Figure 1.4 (left). This combination is injected and the tumor specific antibody only binds to the tumor cells [69]. Conversely, in the case of GDEPT a vector containing a coded gene for the enzyme is injected in the tumor, Figure 1.4 (right). Once tumor cells are transduced with the vector, they start to overexpress the enzyme, and the produced enzymes are excreted from the cells in the extracellular tumor microenvironment [70]. Both ADEPT and GDEPT result *in vivo* in increased enzyme concentrations available for prodrug conversion in the tumor [69, 71], and in increased therapeutic response compared to free drug administration [72-77]. However, clinical applications for ADEPT and GDEPT remain challenging due to the activation of the immune system by foreign enzymes in ADEPT [78, 79] and low transduction efficacy in GDEPT [65]. Therefore, there is still a clinical need for enzyme prodrug therapy to increase the enzyme concentration available for fast prodrug conversion in the tumor.

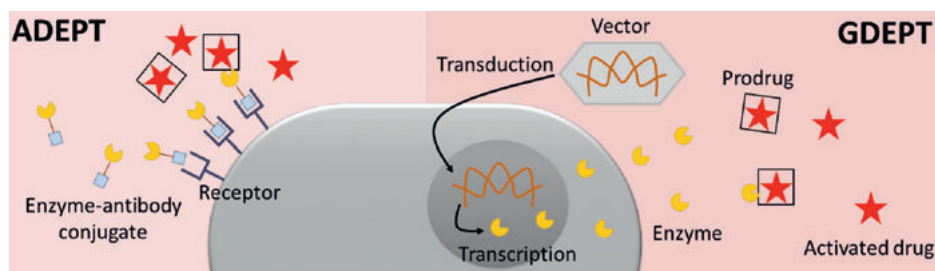


Figure 1.4: Schematic representation of ADEPT (left) and GDEPT (right) to increase the enzyme concentration available for prodrug conversion in the tumor.

THERAPEUTIC ULTRASOUND

Therapeutic ultrasound is a therapeutic modality that applies sound waves at a frequency above the audible frequency range of the human ear, *i.e.* above 20 kHz. By focusing the sound waves into one point, so called focal point or focus [80, 81], high intensities can be generated in this point, while sparing tissues in the near field, hence the name high-intensity focused ultrasound (HIFU). This results in spatially confined lesions in the focus and no cellular damage outside the focus [80]. Depending on the parameters of the sound waves, like intensity, frequency and duty cycle, *i.e.* continuous or pulsed waves, therapeutic ultrasound may induce thermal effects, non-thermal effects or a combination of both [82, 83]. Therapeutic ultrasound that leads to thermal effects in the tumor microenvironment [80, 82, 84] is FDA approved for thermal ablation (thermal dose of 1 second at 56°C) in the treatment of different cancer types; bone metastasis and prostate cancer, and benign tumors; uterine adenomyosis, uterine fibroids and osteoid osteoma [83, 85], and under clinical investigation for hyperthermia (1 hour at 40-42°C) in combination with the TSL formulation ThermoDox [86, 87]. Currently therapeutic ultrasound is increasingly investigated to induce mechanical effects [80, 88] that leads to mechanical ablation, *i.e.* liquefaction, of the tissue [89, 90]. In addition, there is some evidence *in vitro* that mechanical ablation of cells by therapeutic ultrasound results in liberation of proteins [91], which could possibly be used in local drug activation applications.

OUTLINE OF THIS THESIS

The aim of this thesis is to improve local drug deposition in the primary tumor, with the local drug delivery approaches I) temperature sensitive liposomes in combination with hyperthermia and II) prodrugs in combination with the mechanical bio-effects of therapeutic ultrasound.

Chapter 2 and 3 focus on local drug delivery by temperature sensitive liposomes in combination with hyperthermia.

In chemoradiation the normal tissue located in the beam path of radiotherapy is exposed to both the systemic administered radiosensitizer and radiotherapy treatment, resulting in unwanted toxicities in these tissues. In **chapter 2** the concept of triggered radiosensitizer delivery is introduced and investigated *in vitro*. In this concept the radiosensitizer, doxorubicin (DOX), is encapsulated in a TSL, i.e. ThermoDox, and will only become bioavailable in the heated tumor and thus reduces toxicity in the normal tissue located in the beam path. Since the mechanisms of action of DOX, radiotherapy and hyperthermia influence each other when applied simultaneously or in short succession, the optimal treatment order to achieve the largest efficacy was further investigated.

As mentioned before, drug efficacy depends on both the drug concentration and drug distribution in the tumor. In **chapter 3** the drug concentration and drug distribution in the tumor after treatment with different administrated dosages of ThermoDox (TSL containing DOX), in combination with hyperthermia treatment, and DOXIL (NTSL containing DOX) were compared with free DOX treatment *in vivo* in a subcutaneous humane fibrosarcoma model. The doxorubicin distribution relative to the vessels and spatial doxorubicin distribution in a whole tumor slice were characterized and subsequently correlated with the different administrated doses and drug formulations.

Chapter 4 and 5 focus on local drug delivery by prodrugs in combination with the mechanical bio-effects of therapeutic ultrasound.

For effective prodrug therapy the prodrug needs to be quickly converted by the enzyme, that is in high concentrations bioavailable in the tumor. In **chapter 4** first glucuronide-prodrugs were synthesized with an elongation of the spacer to reduce its steric hindrance and therefore increase its conversion rate. Subsequently, the concept of ultrasound directed enzyme prodrug

therapy (UDEPT) was introduced and investigated *in vitro*. In this concept, the mechanical bio-effects of high-intensity focused ultrasound liberate the enzyme β -GUS from cells. Finally, the newly synthesized prodrug and UDEPT concept were combined to improve prodrug activation *in vitro*.

A previously synthesized glucuronide-prodrug DOX-GA3 (without elongated spacer) has poor pharmacokinetics, *i.e.* it is rapidly excreted from the body. In **chapter 5** DOX-GA3 was conjugated to a polymer (prodrug-polymer conjugate) and subsequently formed into a nanogel formulation. This nanogel formulation was subsequently characterized and investigated *in vitro* in combination with the UDEPT concept, as introduced in chapter 4 of this thesis.

In **chapter 6** all results are summarized and addressed within the context of the literature in the general discussion. In addition, future perspectives of local drug delivery by physical activation of temperature sensitive liposomes and prodrugs are discussed.

REFERENCES

1. **WHO** https://www.who.int/health-topics/cancer#tab=tab_1 [Accessed: 08/Nov/2020]
2. **KWF.nl** <https://www.kwf.nl/kanker/wat-is-kanker/behandeling-van-kanker#:~:text=Meest%20gebruikte%20behandelingen> c. [Accessed: 08/Nov/2020]
3. Quaresma M, Coleman MP, Rachet B: **40-year trends in an index of survival for all cancers combined and survival adjusted for age and sex for each cancer in England and Wales, 1971-2011: a population-based study.** *Lancet* 2015, **385**:1206-1218.
4. **Cancer research UK** <https://www.cancerresearchuk.org/health-professional/cancer-statistics/diagnosis-and-treatment#ref-6> [Accessed: 08/Nov/2020]
5. McAllister SS, Gifford AM, Greiner AL, Kelleher SP, Saelzler MP, Ince TA, Reinhardt F, Harris LN, Hylander BL, Repasky EA, Weinberg RA: **Systemic endocrine instigation of indolent tumor growth requires osteopontin.** *Cell* 2008, **133**:994-1005.
6. Rusthoven CG, Jones BL, Flaig TW, Crawford ED, Koshy M, Sher DJ, Mahmood U, Chen RC, Chapin BF, Kavanagh BD, Pugh TJ: **Improved Survival With Prostate Radiation in Addition to Androgen Deprivation Therapy for Men With Newly Diagnosed Metastatic Prostate Cancer.** *J Clin Oncol* 2016, **34**:2835-2842.
7. Xu H, Xia Z, Jia X, Chen K, Li D, Dai Y, Tao M, Mao Y: **Primary Tumor Resection Is Associated with Improved Survival in Stage IV Colorectal Cancer: An Instrumental Variable Analysis.** *Scientific Reports* 2015, **5**.
8. Jain RK: **Delivery of molecular and cellular medicine to solid tumors.** *Adv Drug Deliv Rev* 2001, **46**:149-168.
9. Palumbo MO, Kavan P, Miller WH, Jr., Panasci L, Assouline S, Johnson N, Cohen V, Patenaude F, Pollak M, Jagoe RT, Batist G: **Systemic cancer therapy: achievements and challenges that lie ahead.** *Front Pharmacol* 2013, **4**:57.
10. Plenderleith IH: **Treating the treatment: toxicity of cancer chemotherapy.** *Can Fam Physician* 1990, **36**:1827-1830.
11. Tacar O, Sriamornsak P, Dass CR: **Doxorubicin: an update on anticancer molecular action, toxicity and novel drug delivery systems.** *J Pharm Pharmacol* 2013, **65**:157-170.
12. Foote M: **The Importance of Planned Dose of Chemotherapy on Time: Do We Need to Change Our Clinical Practice?** *Oncologist* 1998, **3**:365-368.
13. Goldberg EP, Hadba AR, Almond BA, Marotta JS: **Intratumoral cancer chemotherapy and immunotherapy: opportunities for nonsystemic preoperative drug delivery.** *J Pharm Pharmacol* 2002, **54**:159-180.
14. Yan TD, Black D, Sugarbaker PH, Zhu J, Yonemura Y, Petrou G, Morris DL: **A systematic review and meta-analysis of the randomized controlled trials on adjuvant intraperitoneal chemotherapy for resectable gastric cancer.** *Ann Surg Oncol* 2007, **14**:2702-2713.
15. Pui CH, Mahmoud HH, Rivera GK, Hancock ML, Sandlund JT, Behm FG, Head DR, Relling MV, Ribeiro RC, Rubnitz JE, et al: **Early intensification of intrathecal chemotherapy virtually eliminates central nervous system relapse in children with acute lymphoblastic leukemia.** *Blood* 1998, **92**:411-415.

16. Bobo D, Robinson KJ, Islam J, Thurecht KJ, Corrie SR: **Nanoparticle-Based Medicines: A Review of FDA-Approved Materials and Clinical Trials to Date.** *Pharm Res* 2016, **33**:2373-2387.
17. Tiwari G, Tiwari R, Sriwastawa B, Bhati L, Pandey S, Pandey P, Bannerjee SK: **Drug delivery systems: An updated review.** *Int J Pharm Investig* 2012, **2**:2-11.
18. Barenholz Y: **Doxil(R)--the first FDA-approved nano-drug: lessons learned.** *J Control Release* 2012, **160**:117-134.
19. Arcamone F, Cassinelli G, Fantini G, Grein A, Orezzi P, Pol C, Spalla C: **Adriamycin, 14-hydroxydaunomycin, a new antitumor antibiotic from *S. peucetius* var. *caesius*.** *Biotechnol Bioeng* 1969, **11**:1101-1110.
20. Gewirtz DA: **A critical evaluation of the mechanisms of action proposed for the antitumor effects of the anthracycline antibiotics adriamycin and daunorubicin.** *Biochem Pharmacol* 1999, **57**:727-741.
21. Yang F, Teves SS, Kemp CJ, Henikoff S: **Doxorubicin, DNA torsion, and chromatin dynamics.** *Biochim Biophys Acta* 2014, **1845**:84-89.
22. **Farmacotherapeutisch Kompas** <https://www.farmacotherapeutischkompas.nl/bladeren/preparaatteksten/d/doxorubicine> [Accessed: 08/Nov/2020]
23. Zhang YW, Shi J, Li YJ, Wei L: **Cardiomyocyte death in doxorubicin-induced cardiotoxicity.** *Arch Immunol Ther Exp (Warsz)* 2009, **57**:435-445.
24. Karukstis KK, Thompson EH, Whiles JA, Rosenfeld RJ: **Deciphering the fluorescence signature of daunomycin and doxorubicin.** *Biophys Chem* 1998, **73**:249-263.
25. Bulbake U, Doppalapudi S, Kommineni N, Khan W: **Liposomal Formulations in Clinical Use: An Updated Review.** *Pharmaceutics* 2017, **9**.
26. Ranjan A, Jacobs GC, Woods DL, Negussie AH, Partanen A, Yarmolenko PS, Gacchina CE, Sharma KV, Frenkel V, Wood BJ, Dreher MR: **Image-guided drug delivery with magnetic resonance guided high intensity focused ultrasound and temperature sensitive liposomes in a rabbit Vx2 tumor model.** *J Control Release* 2012, **158**:487-494.
27. Gabizon A, Shmeeda H, Barenholz Y: **Pharmacokinetics of pegylated liposomal Doxorubicin: review of animal and human studies.** *Clin Pharmacokinet* 2003, **42**:419-436.
28. Lammers T, Kiessling F, Hennink WE, Storm G: **Drug targeting to tumors: principles, pitfalls and (pre-) clinical progress.** *J Control Release* 2012, **161**:175-187.
29. Iqbal J, Abbasi BA, Ahmad R, Mahmood T, Ali B, Khalil AT, Kanwal S, Shah SA, Alam MM, Badshah H, Munir A: **Nanomedicines for developing cancer nanotherapeutics: from benchtop to bedside and beyond.** *Appl Microbiol Biotechnol* 2018, **102**:9449-9470.
30. Laginha KM, Verwoert S, Charrois GJ, Allen TM: **Determination of doxorubicin levels in whole tumor and tumor nuclei in murine breast cancer tumors.** *Clin Cancer Res* 2005, **11**:6944-6949.
31. Maeda H, Wu J, Sawa T, Matsumura Y, Hori K: **Tumor vascular permeability and the EPR effect in macromolecular therapeutics: a review.** *J Control Release* 2000, **65**:271-284.
32. Nakamura Y, Mochida A, Choyke PL, Kobayashi H: **Nanodrug Delivery: Is the Enhanced Permeability and Retention Effect Sufficient for Curing Cancer?** *Bioconjug Chem* 2016, **27**:2225-2238.

33. Bibi S, Lattmann E, Mohammed AR, Perrie Y: **Trigger release liposome systems: local and remote controlled delivery?** *J Microencapsul* 2012, **29**:262-276.
34. Yatvin MB, Weinstein JN, Dennis WH, Blumenthal R: **Design of liposomes for enhanced local release of drugs by hyperthermia.** *Science* 1978, **202**:1290-1293.
35. Li L, ten Hagen TL, Schipper D, Wijnberg TM, van Rhooen GC, Eggermont AM, Lindner LH, Koning GA: **Triggered content release from optimized stealth thermosensitive liposomes using mild hyperthermia.** *J Control Release* 2010, **143**:274-279.
36. Needham D, Park JY, Wright AM, Tong J: **Materials characterization of the low temperature sensitive liposome (LTSL): effects of the lipid composition (lysolipid and DSPE-PEG2000) on the thermal transition and release of doxorubicin.** *Faraday Discuss* 2013, **161**:515-534; discussion 563-589.
37. Manzoor AA, Lindner LH, Landon CD, Park JY, Simnick AJ, Dreher MR, Das S, Hanna G, Park W, Chilkoti A, et al: **Overcoming limitations in nanoparticle drug delivery: triggered, intravascular release to improve drug penetration into tumors.** *Cancer Res* 2012, **72**:5566-5575.
38. Kong G, Anyarambhatla G, Petros WP, Braun RD, Colvin OM, Needham D, Dewhirst MW: **Efficacy of liposomes and hyperthermia in a human tumor xenograft model: importance of triggered drug release.** *Cancer Res* 2000, **60**:6950-6957.
39. Needham D, Anyarambhatla G, Kong G, Dewhirst MW: **A new temperature-sensitive liposome for use with mild hyperthermia: characterization and testing in a human tumor xenograft model.** *Cancer Res* 2000, **60**:1197-1201.
40. Yarmolenko PS, Zhao Y, Landon C, Spasojevic I, Yuan F, Needham D, Viglianti BL, Dewhirst MW: **Comparative effects of thermosensitive doxorubicin-containing liposomes and hyperthermia in human and murine tumours.** *Int J Hyperthermia* 2010, **26**:485-498.
41. Gabizon A, Tzemach D, Mak L, Bronstein M, Horowitz AT: **Dose dependency of pharmacokinetics and therapeutic efficacy of pegylated liposomal doxorubicin (DOXIL) in murine models.** *J Drug Target* 2002, **10**:539-548.
42. Vaage J, Barbera-Guillem E, Abra R, Huang A, Working P: **Tissue distribution and therapeutic effect of intravenous free or encapsulated liposomal doxorubicin on human prostate carcinoma xenografts.** *Cancer* 1994, **73**:1478-1484.
43. Staruch RM, Hynynen K, Chopra R: **Hyperthermia-mediated doxorubicin release from thermosensitive liposomes using MR-HIFU: therapeutic effect in rabbit Vx2 tumours.** *Int J Hyperthermia* 2015, **31**:118-133.
44. Tredan O, Galmarini CM, Patel K, Tannock IF: **Drug resistance and the solid tumor microenvironment.** *J Natl Cancer Inst* 2007, **99**:1441-1454.
45. Minchinton AI, Tannock IF: **Drug penetration in solid tumours.** *Nat Rev Cancer* 2006, **6**:583-592.
46. Li L, ten Hagen TL, Hossann M, Suss R, van Rhooen GC, Eggermont AM, Haemmerich D, Koning GA: **Mild hyperthermia triggered doxorubicin release from optimized stealth thermosensitive liposomes improves intratumoral drug delivery and efficacy.** *J Control Release* 2013, **168**:142-150.
47. Hahn GM, Braun J, Har-Kedar I: **Thermochemotherapy: synergism between hyperthermia (42-43 degrees) and adriamycin (of bleomycin) in mammalian cell inactivation.** *Proc Natl Acad Sci U S A* 1975, **72**:937-940.
48. Issels RD: **Hyperthermia adds to chemotherapy.** *Eur J Cancer* 2008, **44**:2546-2554.

49. Hildebrandt B, Wust P, Ahlers O, Dieing A, Sreenivasa G, Kerner T, Felix R, Riess H: **The cellular and molecular basis of hyperthermia.** *Crit Rev Oncol Hematol* 2002, **43**:33-56.
50. Oei AL, Vriend LE, Crezee J, Franken NA, Krawczyk PM: **Effects of hyperthermia on DNA repair pathways: one treatment to inhibit them all.** *Radiat Oncol* 2015, **10**:165.
51. Baskar R, Dai J, Wenlong N, Yeo R, Yeoh KW: **Biological response of cancer cells to radiation treatment.** *Front Mol Biosci* 2014, **1**:24.
52. Lomax ME, Folkes LK, O'Neill P: **Biological consequences of radiation-induced DNA damage: relevance to radiotherapy.** *Clin Oncol (R Coll Radiol)* 2013, **25**:578-585.
53. Bellamy AS, Hill BT: **Interactions between clinically effective antitumor drugs and radiation in experimental systems.** *Biochim Biophys Acta* 1984, **738**:125-166.
54. Belli JA, Piro AJ: **The interaction between radiation and adriamycin damage in mammalian cells.** *Cancer Res* 1977, **37**:1624-1630.
55. Bonner JA, Lawrence TS: **Doxorubicin decreases the repair of radiation-induced DNA damage.** *Int J Radiat Biol* 1990, **57**:55-64.
56. Greco WR, Bravo G, Parsons JC: **The search for synergy: a critical review from a response surface perspective.** *Pharmacol Rev* 1995, **47**:331-385.
57. Adams MJ, Hardenbergh PH, Constine LS, Lipshultz SE: **Radiation-associated cardiovascular disease.** *Crit Rev Oncol Hematol* 2003, **45**:55-75.
58. Haas RL, de Klerk G: **An illustrated case of doxorubicin-induced radiation recall dermatitis and a review of the literature.** *Neth J Med* 2011, **69**:72-75.
59. Myrehaug S, Pintilie M, Tsang R, Mackenzie R, Crump M, Chen Z, Sun A, Hodgson DC: **Cardiac morbidity following modern treatment for Hodgkin lymphoma: supra-additive cardiotoxicity of doxorubicin and radiation therapy.** *Leuk Lymphoma* 2008, **49**:1486-1493.
60. Kratz F, Muller IA, Ryppa C, Warnecke A: **Prodrug strategies in anticancer chemotherapy.** *ChemMedChem* 2008, **3**:20-53.
61. Rautio J, Kumpulainen H, Heimbach T, Oliyai R, Oh D, Jarvinen T, Savolainen J: **Prodrugs: design and clinical applications.** *Nat Rev Drug Discov* 2008, **7**:255-270.
62. Houba PH, Leenders RG, Boven E, Scheeren JW, Pinedo HM, Haisma HJ: **Characterization of novel anthracycline prodrugs activated by human beta-glucuronidase for use in antibody-directed enzyme prodrug therapy.** *Biochem Pharmacol* 1996, **52**:455-463.
63. Lesniewska-Kowiel MA, Muszalska I: **Strategies in the designing of prodrugs, taking into account the antiviral and anticancer compounds.** *Eur J Med Chem* 2017, **129**:53-71.
64. Denny WA: **Prodrug strategies in cancer therapy.** *Eur J Med Chem* 2001, **36**:577-595.
65. Rooseboom M, Commandeur JN, Vermeulen NP: **Enzyme-catalyzed activation of anticancer prodrugs.** *Pharmacol Rev* 2004, **56**:53-102.
66. Sherwood RF: **Advanced drug delivery reviews: Enzyme prodrug therapy.** *Advanced Drug Delivery Reviews* 1996, **22**:269-288.
67. de Graaf M, Boven E, Scheeren HW, Haisma HJ, Pinedo HM: **Beta-glucuronidase-mediated drug release.** *Curr Pharm Des* 2002, **8**:1391-1403.
68. Houba PH, Boven E, van der Meulen-Muileman IH, Leenders RG, Scheeren JW, Pinedo HM, Haisma HJ: **A novel doxorubicin-glucuronide prodrug DOX-GA3 for tumour-selective chemotherapy: distribution and efficacy in experimental human ovarian cancer.** *Br J Cancer* 2001, **84**:550-557.

69. Bagshawe KD: **Antibody directed enzymes revive anti-cancer prodrugs concept.** *Br J Cancer* 1987, **56**:531-532.
70. Zhang J, Kale V, Chen M: **Gene-directed enzyme prodrug therapy.** *AAPS J* 2015, **17**:102-110.
71. Altaner C: **Prodrug cancer gene therapy.** *Cancer Lett* 2008, **270**:191-201.
72. Houba PH, Boven E, Haisma HJ: **Improved characteristics of a human beta-glucuronidase-antibody conjugate after deglycosylation for use in antibody-directed enzyme prodrug therapy.** *Bioconjug Chem* 1996, **7**:606-611.
73. Houba PH, Boven E, van der Meulen-Muileman IH, Leenders RG, Scheeren JW, Pinedo HM, Haisma HJ: **Pronounced antitumor efficacy of doxorubicin when given as the prodrug DOX-GA3 in combination with a monoclonal antibody beta-glucuronidase conjugate.** *Int J Cancer* 2001, **91**:550-554.
74. Webley SD, Francis RJ, Pedley RB, Sharma SK, Begent RH, Hartley JA, Hochhauser D: **Measurement of the critical DNA lesions produced by antibody-directed enzyme prodrug therapy (ADEPT) in vitro, in vivo and in clinical material.** *Br J Cancer* 2001, **84**:1671-1676.
75. de Graaf M, Pinedo HM, Oosterhoff D, van der Meulen-Muileman IH, Gerritsen WR, Haisma HJ, Boven E: **Pronounced antitumor efficacy by extracellular activation of a doxorubicin-glucuronide prodrug after adenoviral vector-mediated expression of a human antibody-enzyme fusion protein.** *Hum Gene Ther* 2004, **15**:229-238.
76. Sekar TV, Foygel K, Ilovich O, Paulmurugan R: **Noninvasive theranostic imaging of HSV1-sr39TK-NTR/GCV-CB1954 dual-prodrug therapy in metastatic lung lesions of MDA-MB-231 triple negative breast cancer in mice.** *Theranostics* 2014, **4**:460-474.
77. Chen MJ, Green NK, Reynolds GM, Flavell JR, Mautner V, Kerr DJ, Young LS, Searle PF: **Enhanced efficacy of Escherichia coli nitroreductase/CB1954 prodrug activation gene therapy using an E1B-55K-deleted oncolytic adenovirus vector.** *Gene Ther* 2004, **11**:1126-1136.
78. Francis RJ, Sharma SK, Springer C, Green AJ, Hope-Stone LD, Sena L, Martin J, Adamson KL, Robbins A, Gumbrell L, et al: **A phase I trial of antibody directed enzyme prodrug therapy (ADEPT) in patients with advanced colorectal carcinoma or other CEA producing tumours.** *Br J Cancer* 2002, **87**:600-607.
79. Napier MP, Sharma SK, Springer CJ, Bagshawe KD, Green AJ, Martin J, Stribbling SM, Cushen N, O'Malley D, Begent RH: **Antibody-directed enzyme prodrug therapy: efficacy and mechanism of action in colorectal carcinoma.** *Clin Cancer Res* 2000, **6**:765-772.
80. Haar GT, Coussios C: **High intensity focused ultrasound: physical principles and devices.** *Int J Hyperthermia* 2007, **23**:89-104.
81. Izadifar Z, Chapman D, Babyn P: **An Introduction to High Intensity Focused Ultrasound: Systematic Review on Principles, Devices, and Clinical Applications.** *J Clin Med* 2020, **9**.
82. ter Haar G: **Therapeutic ultrasound.** *Eur J Ultrasound* 1999, **9**:3-9.
83. Elhelf IAS, Albahar H, Shah U, Oto A, Cressman E, Almekkawy M: **High intensity focused ultrasound: The fundamentals, clinical applications and research trends.** *Diagn Interv Imaging* 2018, **99**:349-359.

84. Zhu L, Altman MB, Laszlo A, Straube W, Zoberi I, Hallahan DE, Chen H: **Ultrasound Hyperthermia Technology for Radiosensitization**. *Ultrasound Med Biol* 2019, **45**:1025-1043.
85. Siedek F, Yeo SY, Heijman E, Grinstein O, Bratke G, Heneweer C, Puesken M, Persigehl T, Maintz D, Grull H: **Magnetic Resonance-Guided High-Intensity Focused Ultrasound (MR-HIFU): Technical Background and Overview of Current Clinical Applications (Part 1)**. *Rofo* 2019, **191**:522-530.
86. **Clinical trials.gov** <https://clinicaltrials.gov/ct2/show/NCT03749850> [Accessed: 08/Nov/2020]
87. Gray MD, Lyon PC, Mannaris C, Folkes LK, Stratford M, Campo L, Chung DYF, Scott S, Anderson M, Goldin R, et al: **Focused Ultrasound Hyperthermia for Targeted Drug Release from Thermosensitive Liposomes: Results from a Phase I Trial**. *Radiology* 2019, **291**:232-238.
88. Hoogenboom M, Eikelenboom D, den Brok MH, Heerschap A, Futterer JJ, Adema GJ: **Mechanical high-intensity focused ultrasound destruction of soft tissue: working mechanisms and physiologic effects**. *Ultrasound Med Biol* 2015, **41**:1500-1517.
89. Dubinsky TJ, Khokhlova TD, Khokhlova V, Schade GR: **Histotripsy: The Next Generation of High-Intensity Focused Ultrasound for Focal Prostate Cancer Therapy**. *J Ultrasound Med* 2020, **39**:1057-1067.
90. Bader KB, Vlasisavljevich E, Maxwell AD: **For Whom the Bubble Grows: Physical Principles of Bubble Nucleation and Dynamics in Histotripsy Ultrasound Therapy**. *Ultrasound Med Biol* 2019, **45**:1056-1080.
91. Hu Z, Yang XY, Liu Y, Morse MA, Lysterly HK, Clay TM, Zhong P: **Release of endogenous danger signals from HIFU-treated tumor cells and their stimulatory effects on APCs**. *Biochem Biophys Res Commun* 2005, **335**:124-131.

CHAPTER 2

Triggered radiosensitizer delivery using thermosensitive liposomes and hyperthermia improves efficacy of radiotherapy: an *in vitro* proof of concept study

Helena C. Besse
Clemens Bos
Maurice M.J.M. Zandvliet
Kim van der Wurff-Jacobs
Chrit T.W. Moonen
Roel Deckers

Based on: **PloS one (2018); 13(9)**

ABSTRACT

Introduction: To increase the efficacy of chemoradiation and decrease its toxicity in normal tissue, a new concept is proposed, local radiosensitizer delivery, which combines triggered release of a radiosensitizer from thermosensitive liposomes with local hyperthermia and radiotherapy. Here, key aspects of this concept were investigated *in vitro* I) the effect of hyperthermia on the enhancement of radiotherapy by ThermoDox (thermosensitive liposome containing doxorubicin), II) the concentration dependence of the radiosensitizing effect of doxorubicin and III) the sequence of doxorubicin, hyperthermia and radiotherapy maximizing the radiosensitizing effect.

Methods: Survival of HT1080 (human fibrosarcoma) cells was measured after exposure to ThermoDox or doxorubicin for 60 minutes, at 37 or 43°C, with or without irradiation. Furthermore, cell survival was measured for cells exposed to different doxorubicin concentrations and radiation doses. Finally, cell survival was measured after applying doxorubicin and/or hyperthermia before or after irradiation. Cell survival was measured by clonogenic assay. In addition, DNA damage was assessed by γ H2AX staining.

Results: Exposure of cells to doxorubicin at 37°C resulted in cell death, but exposure to ThermoDox at 37°C did not. In contrast, ThermoDox and doxorubicin at 43°C resulted in similar cytotoxicity, and in combination with irradiation caused a similar enhancement of cell kill due to radiation. Doxorubicin enhanced the radiation effect in a small, but significant, concentration-dependent manner. Hyperthermia showed the strongest enhancement of radiation effect when applied after irradiation. In contrast, doxorubicin enhanced radiation effect only when applied before irradiation. Concurrent doxorubicin and hyperthermia immediately before or after irradiation showed equal enhancement of radiation effect.

Conclusion: *In vitro*, ThermoDox resulted in cytotoxicity and enhancement of irradiation effect only in combination with hyperthermia. Therefore hyperthermia-triggered radiosensitizer release from thermosensitive liposomes may ultimately serve to limit toxicities due to the radiosensitizer in unheated normal tissue and result in enhanced efficacy in the heated tumor.

1. INTRODUCTION

Radiotherapy (RT) is often used in the treatment of solid tumors, either as monotherapy or in combination with another treatment modality such as chemotherapy or surgery [1]. For many tumors RT makes a significant contribution to a successful treatment, although it is also accompanied by a serious risk for undesired damage of normal tissue in the beam path and surrounding the tumor. These side effects limit the radiation dose that can be given to the tumor, which could lead to suboptimal radiotherapy treatment [2]. This and intrinsic radioresistance of some tumors contributes to the high recurrence rate observed for several cancers [3]. One of the approaches to increase the local efficacy of RT is to combine it with chemotherapy, i.e. chemoradiation [4].

Administering chemotherapy and RT simultaneously, i.e. concurrent chemoradiation, is currently part of the standard of care for many difficult to treat cancers, including gastric, head and neck and cervical cancers and sarcomas [5-8]. While concomitant chemoradiation has improved disease control as well as survival, it also leads to significantly higher toxicities compared to sequential treatment [9] or RT as a single treatment [10].

To reduce the toxicity of chemotherapy, a common approach is to encapsulate these agents in nanomedicine, e.g. liposomes [11, 12]. In addition, nanomedicine formulations lead to tumor specific drug accumulation due to the enhanced permeability and retention (EPR) effect. The EPR effect is only present in the tumor and is caused by discontinuous endothelial lining and lack of efficient lymphatic drainage, resulting in preferential accumulation of liposomes in the tumor [13]. In animal models the EPR effect leads to increased efficacy of liposomal doxorubicin compared to free doxorubicin (DOX) [14]. In patients with metastatic breast cancer, liposomal doxorubicin reduces the toxicity, while maintaining equal efficacy [12]. The lack of improvement in progression free survival and overall survival of patients treated with liposomal doxorubicin is attributed to heterogeneity of the EPR effect in human tumors [15]. Furthermore, it is argued that the slow DOX release from liposomes, 50% drug release in 118 hours [16], leads to limited bioavailability of the drug in the tumor [16, 17].

To improve the bioavailability of chemotherapeutic agents, trigger-sensitive nanosystems combined with a local trigger are proposed in literature [18],

for example thermosensitive liposomes (TSL) in combination with heat as a local trigger [19]. Combining TSL with local hyperthermia (HT) (i.e. 40-42°C) results in fast drug release, 60% drug release in 20 seconds at a temperature of 41.3°C [20]. This fast release is caused by the increase in permeability of the phospholipid bilayer of the liposomes at the phase transition temperature (~41.3°C) [21]. Several preclinical studies show that this approach leads to increased tumor drug concentration, to a more homogeneous drug distribution in the tumor [19, 22, 23] and to increased survival compared to free drug *in vivo* [24, 25].

Here, a new concept, local radiosensitizer delivery, is proposed in which radiosensitizers are released from the TSL by locally applying hyperthermia to the tumor in combination with conventional radiotherapy. The overall aim of this concept is to reduce the toxicity of the radiosensitizer in normal tissue. In addition, the increased radiosensitizer concentration in the tumor could lead to stronger radiosensitization effect.

The concept of local radiosensitizer delivery implies a combination of three treatment modalities, i.e. radiosensitizer, HT and RT. Within this concept HT is, besides a trigger for radiosensitizer release, also a known chemosensitizer [26, 27] and radiosensitizer [28, 29]. Consequently, the sequence of applying the three treatment modalities will largely influence the overall effect.

In this study we investigated *in vitro* several important aspects of the triggered radiosensitizer delivery concept. Our objectives were to investigate I) the effect of HT on the enhancement of RT by TSL loaded radiosensitizer, II) the concentration dependent radiosensitizing effect of DOX and III) the sequence of DOX, HT and RT maximizing the radiosensitizing effect. For this purpose ThermoDox, a TSL containing DOX, is used to achieve triggered radiosensitizer delivery, since it is already available for clinical trials. DOX is in this concept used as a radiosensitizer, although in the clinic it is often used as a chemotherapeutic agent. We verified the cell survival of cells treated with ThermoDox in the presence and absence of HT with and without RT. For the concept of triggered radiosensitizer delivery, in the absence of HT ThermoDox should not affect the cell survival nor lead to radiosensitization, whereas in the presence of HT ThermoDox should affect the cell survival and lead to radiosensitization comparable to DOX. Subsequently, DOX concentration dependent enhancement of the RT was investigated. For this concept an increase in radiosensitizer would preferably result in an increase

in radiosensitization. Finally, the optimal sequence of the modalities DOX, HT and RT was determined to maximize the radiosensitization.

2. MATERIALS AND METHODS

2.1 Cell culture

HT1080 (human fibrosarcoma) cells, obtained from ATCC (ATCC number CCL-121), were cultured in Minimum Essential Medium (MEM) (Gibco) supplemented with 292 mg/L L-glutamine (Sigma), 110 mg/L sodium pyruvate (Sigma) and 10% Fetal Bovine Serum (Sigma F7524). During all treatments 10 mM HEPES (Sigma) was supplemented to the medium to stabilize the pH. Cells were cultured at 37°C in 5% CO₂ in an air humidified incubator and were regularly tested for mycoplasma contamination.

2.2 Treatment modalities

Hyperthermia, in the range of 37 to 43°C, was performed by incubating cells in a water bath (WNE14I, Memmert, Schwabach, Germany). The bottom of the plate was in direct contact with water inside the water bath, Supplementary Figure 1. This water bath setup was validated using a calibrated fiber optic temperature probe (Neoptix Reflex, Neoptix, Cancada, LP) showing that cell medium reached its target temperature within 10 minutes after being positioned in the water bath.

Chemotherapy treatment was performed by incubating cells for 1 hour with doxorubicin-HCl (DOX) (Guanyu Biotechnology Co., LTD, Xi'an, China) or ThermoDox (Celsion Corporation, Lawrenceville, NJ, USA). Stock solution of DOX was prepared at a concentration of 5 mg/mL and ThermoDox was obtained at a DOX concentration of 2 mg/mL. Before each treatment, DOX and ThermoDox solutions were freshly prepared from stock solution in the concentration range of 0 to 0.24 µg/mL.

Radiotherapy was performed by a single dose of X-ray by a linear accelerator (Elekta Precise Linear Accelerator 11F49, Elekta, Crawley, United Kingdom, 6-MV) in the range of 0 to 8 Gy. During the irradiation cells were positioned on top of 2 cm polystyrene and submerged in a 37°C water bath, Supplementary Figure 1. By applying the radiation from below, the polystyrene ensures proper dose build-up, while the water ensures backscatter to occur. Due to logistics, a time interval of 45 minutes was present between DOX and/or HT treatment and RT.

2.3 Cell survival assay

Cell survival was measured by clonogenic assay, according to Franken et al. [30]. Briefly, at day -1 between 150 and 20,000 cells, depending on the treatment, were seeded in triplicate in 6-well plates and incubated under regular culture conditions. At day 0 cells were treated and subsequently incubated under regular culture conditions. At day 7 cells were fixed and stained with 6% glutaraldehyde and 0.05% crystal violet. Colonies of at least 50 cells were counted. The survival fraction was calculated either relative to untreated samples (0 $\mu\text{g/mL}$ DOX, 37°C and 0 Gy) or relative to samples treated with corresponding treatment of DOX and/or HT at a RT dose of 0 Gy. Representative clonogenic assay images and its analysis are included in Supplementary Figure 2.

2.4 Double strand breaks measurement by flow cytometry of γH2AX staining

Cells were harvested by trypsinization, fixed in 1% PFA and permeabilized in 70% ethanol overnight at -20°C. Subsequently, non-specific antibody binding was blocked by incubating cells for 5 minutes with 1% BSA/0.2% Triton X-100/PBS at room temperature. Staining of γH2AX was performed by incubating cells for 30 minutes with FITC-labeled anti-H2AX mouse IgG1 antibody (1:20; #613403, Biolegend, London, United Kingdom) at room temperature. Next, cells were washed and 5 $\mu\text{g/mL}$ propidium iodine (Sigma-Aldrich) and 100 $\mu\text{g/mL}$ RNase (ThermoFisher) in PBS was added to the samples to normalize the γH2AX signal for the DNA concentration. Finally, samples were measured by flow cytometry (BD FACSCanto II) and analyzed by FlowJo software (FlowJo, Ashland, OR). The percentage γH2AX positive cells was normalized to untreated cells (0 $\mu\text{g/mL}$ DOX, 0 Gy at 37°C). Representative flow cytometry images and its analysis are included in Supplementary Figure 3.

2.5 The effect of ThermoDox and DOX in combination with HT and RT on cell survival

Cells were exposed to ThermoDox (0 or 0.02 $\mu\text{g/mL}$) or DOX (0 or 0.02 $\mu\text{g/mL}$) for 1 hour at 37 or 43°C and subsequently irradiated with different radiation doses (0 to 8 Gy). Finally, cell survival was determined as described above.

2.6 The radiosensitizing effect of DOX

Cells were exposed to DOX at different concentrations (0, 0.01, 0.02 or 0.06 $\mu\text{g/mL}$) for 1 hour at 37°C and subsequently irradiated with different radiation doses (0 to 8 Gy). Finally, cell survival was determined as described above.

2.7 The effect of the combination of individual treatment modalities on cell survival

For the combination of concurrent DOX and HT, cells were exposed to DOX concentrations in the range of 0 to 0.24 $\mu\text{g/mL}$ for 1 hour at 37, 42 or 43°C. For the combination treatments of RT and DOX and/or HT, cells were exposed to DOX (0 or 0.02 $\mu\text{g/mL}$) for 1 hour at 37, 42 or 43°C before or after irradiation with different radiation doses (0 to 8 Gy). Finally, cell survival was determined as described above.

2.8 The effect of DOX with and without HT on DNA damage

Cells were exposed to DOX (0, 0.02 or 0.06 $\mu\text{g/mL}$) for 1 hour at 37 or 43°C. Afterwards, cells were incubated under regular culturing conditions as described above. At time points 2 and 26 hours after DOX removal DNA damage was measured by flow cytometry of γH2AX staining as described above.

2.9 The effect of the combination of individual treatment modalities on DNA damage

Cells were exposed to DOX (0 or 0.02 $\mu\text{g/mL}$) for 1 hour at 37 or 43°C, subsequently cells were irradiated with 0 or 4 Gy. Afterwards, cells were incubated under regular culturing conditions as described above. At time points 45 minutes and 24 hours after irradiation, DNA damage was measured by flow cytometry of γH2AX staining as described above.

2.10 Statistical analysis

All data is presented as mean, with error bars representing the standard deviation based on a minimum of 3 independent experiments. Cell survival data by clonogenic assay were statistically tested in SPSS 23 (IBM, Armonk, NY, USA) by linear regression as described by Franken et al [30]. DSB measurements by γH2AX were statistically tested in GraphPad Prism 7 (GraphPad Software, Inc, San Diego, CA) by comparison of groups by a paired t-test. Differences between groups with $p < 0.05$ were considered statistically significant.

3. RESULTS

3.1 The effect of triggered release of DOX from a TSL in combination with RT

First the cytotoxicity of ThermoDox at different temperatures was investigated. Figure 1A shows the surviving fraction of cells incubated with DOX or

ThermoDox at a concentration of 0.02 $\mu\text{g/mL}$ for 1 hour at 37 or 43°C, relative to the untreated samples (0 $\mu\text{g/mL}$ DOX at 37°C). Cells treated with ThermoDox at 37°C showed similar survival compared to untreated cells (0 $\mu\text{g/mL}$ DOX). In contrast, cells treated with ThermoDox at 43°C showed a similar surviving fraction compared to cells exposed to free DOX at 43°C, which is caused by the fast DOX release from the TSL at elevated temperatures. Incubation of cells at 43°C by itself resulted in limited toxicity, a surviving fraction of $94.46\% \pm 9.92\%$ was obtained. Note that these cells are rather heat resistant compared to other cell lines [31, 32], Supplementary Figure 4.

Subsequently, the cytotoxicity of the combination of ThermoDox and RT was investigated at different temperatures. Figure 1B shows surviving fraction as function of radiation dose for cells incubated for 1 hour with DOX or ThermoDox at 37 or 43°C followed by RT treatment. The surviving fraction is presented relative to untreated sample (0 $\mu\text{g/mL}$ DOX, 37°C, 0 Gy). As a function of RT dose, ThermoDox at 37°C resulted in similar survival as RT as a single treatment, whereas ThermoDox at 43°C resulted in comparable toxicity as DOX at 43°C followed by RT.

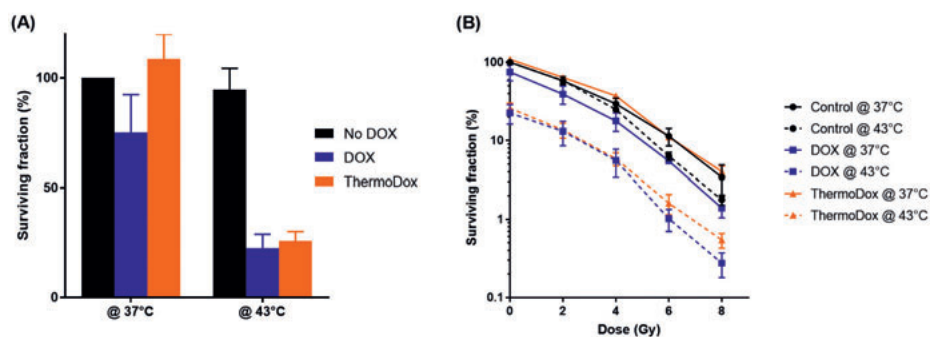


Figure 1. Cytotoxicity of free DOX and DOX from ThermoDox at different temperatures with and without RT. Surviving fraction of HT1080 cells exposed to DOX (0.02 $\mu\text{g/mL}$) or ThermoDox (0.02 $\mu\text{g/mL}$) for 1 hour at 37°C or 43°C without (A) or with (B) RT. ThermoDox at 37°C, with or without RT, resulted in equal toxicity compared to treatment without a drug, however ThermoDox at 43°C resulted in comparable toxicity compared to DOX treatment.

3.2 Concentration dependent radiosensitization effect of DOX

The enhancement of the sensitivity to RT of cells was investigated for different DOX concentrations. Figure 2A shows the survival fraction of cells treated with DOX and RT relative to samples treated with equal chemotherapy treatment

(equal DOX concentration and 0 Gy), whereas Figure 2B presents the surviving fraction relative to untreated samples (0 $\mu\text{g/mL}$ DOX and 0 Gy). All DOX concentrations used in this experiment resulted in significant enhancement of the sensitivity to RT. In addition, DOX at a concentration of 0.06 $\mu\text{g/mL}$ resulted in a small, but significant, increase in enhancement of the sensitivity to RT compared to 0.01 $\mu\text{g/mL}$ (Figure 2A). DOX as a single treatment also showed, as expected, a concentration dependent increase of cell kill, which can be observed from the decreasing surviving fraction at 0 Gy for the different DOX concentration curves in Figure 2B.

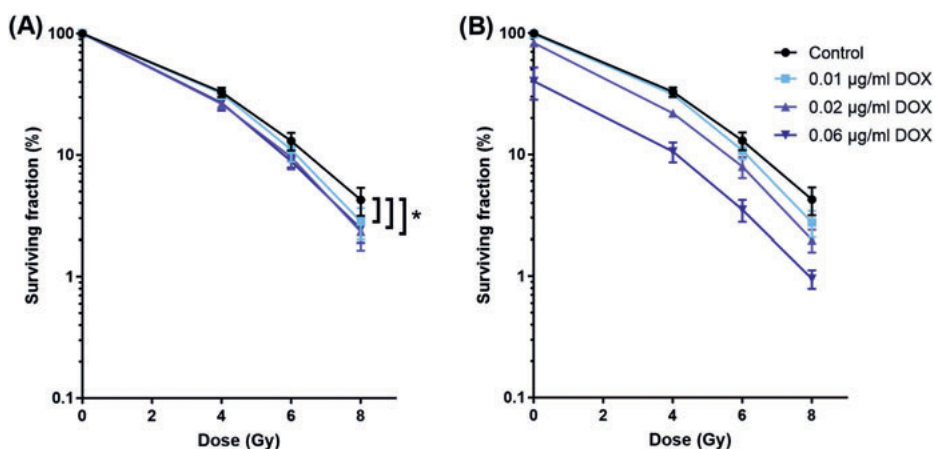


Figure 2: Cytotoxicity of DOX at different concentrations and RT. Surviving fraction as function of radiation dose for different DOX concentrations. Cells were exposed for 1 hour to DOX (0.01, 0.02 or 0.06 $\mu\text{g/mL}$) before RT. Surviving fraction calculated by samples treated with the corresponding DOX concentration (A) or by untreated sample (B). All DOX concentrations resulted in a significant enhancement of RT. In addition, 0.06 $\mu\text{g/mL}$ DOX resulted in a larger RT effect compared to 0.01 $\mu\text{g/mL}$ DOX ($p < 0.05$).

3.3 Effect of combinations of the modalities doxorubicin, HT and RT

Since HT not only causes drug release from TSL, but also sensitizes RT and DOX [26], the optimal sequence of the modalities in the concept of triggered radiosensitizer release was investigated. To avoid concentration differences of DOX due to the (incomplete) release of DOX from ThermoDox at 37°C, free DOX was used in these experiments. The DOX concentration was set to 0.02 $\mu\text{g/mL}$ which led to a cell survival of approximately 10%, such that the effect of the combination treatments would be detectable. First, the effect of the sequence was investigated for the combination RT and HT and the combination RT and DOX.

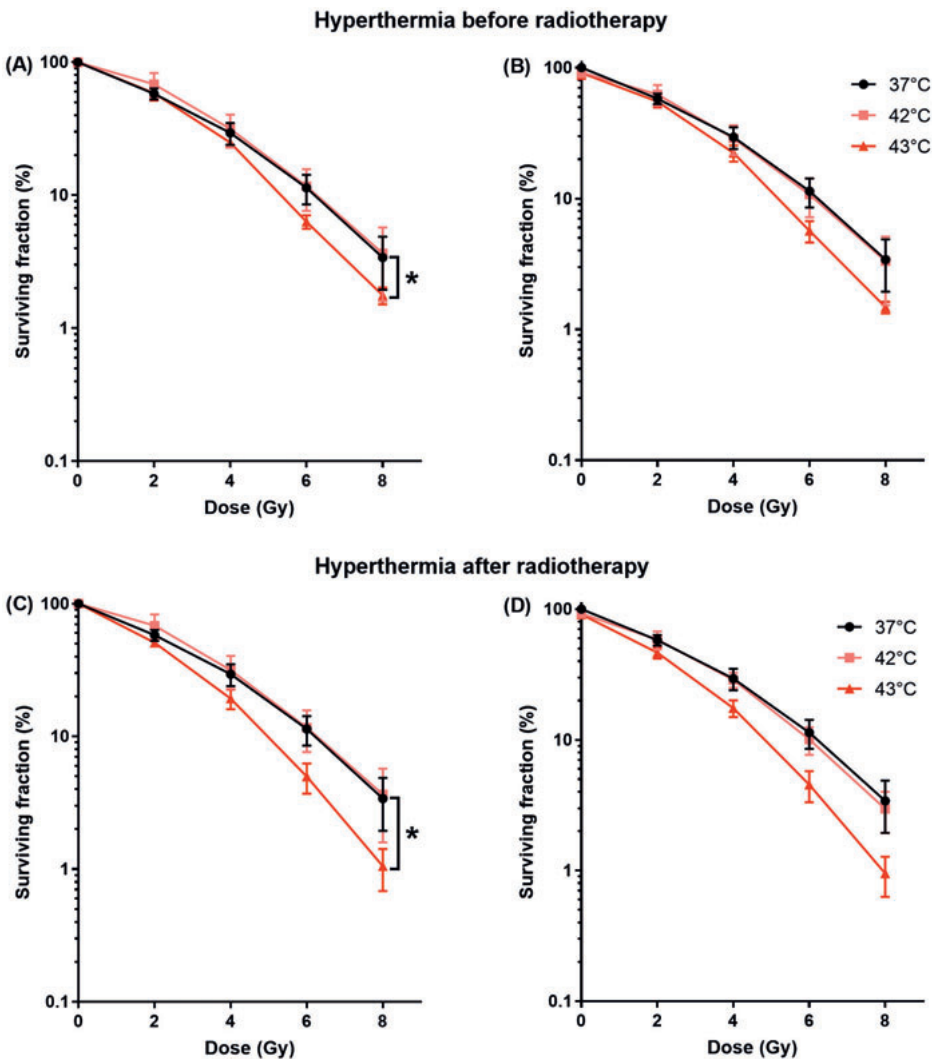


Figure 3. Cytotoxicity of hyperthermia at different temperatures before and after RT. Surviving fraction as function of radiation dose at different temperatures. Cells exposed for 1 hour to 37, 42 or 43°C before (A and B) or after (C and D) RT normalized for HT treatment at 0 Gy (A and C) and normalized for untreated samples (37°C and 0 Gy) (B and D). HT of 43°C resulted in significant enhancement of RT both before (A) and after RT (C). HT of 43°C resulted in the largest enhancement of the RT.

3.3.1 Radiotherapy and hyperthermia

Figure 3 shows the surviving fraction as function of radiation dose of cells incubated at 37, 42 or 43°C for 1 hour before (A and B) or after (C and D) applying RT. Incubation of cells during 1 hour at 42°C did not improve the

effect of RT on cell kill independent on the timing. HT at 42°C before or after RT resulted in a surviving fraction at 6 Gy (SF_6) of $11.6\% \pm 4.1\%$ and $11.7\% \pm 4.1\%$, respectively. In contrast, the effect of RT was significantly enhanced by incubating cells at 43°C. HT at 43°C applied before or after RT resulted in a SF_6 of $6.3\% \pm 0.7\%$ and of $5.0\% \pm 1.3\%$, respectively. HT at 43°C following RT resulted in a small, but significant larger enhancement of RT compared to HT at 43°C before RT. RT as a monotherapy resulted in a SF_6 of $11.3\% \pm 2.8\%$.

3.3.2 Radiotherapy and doxorubicin

Figure 4 shows the surviving fraction as function of radiation dose of cells exposed to DOX (0 or 0.02 $\mu\text{g/mL}$ for 1 hour) before or after RT. Incubation of cells with DOX before RT resulted in a significant enhancement of the sensitivity to RT, however no enhancement of sensitivity was observed when DOX was applied after RT. The SF_6 of DOX before and after RT were $7.32\% \pm 0.27\%$ and $10.7\% \pm 0.71\%$, respectively.

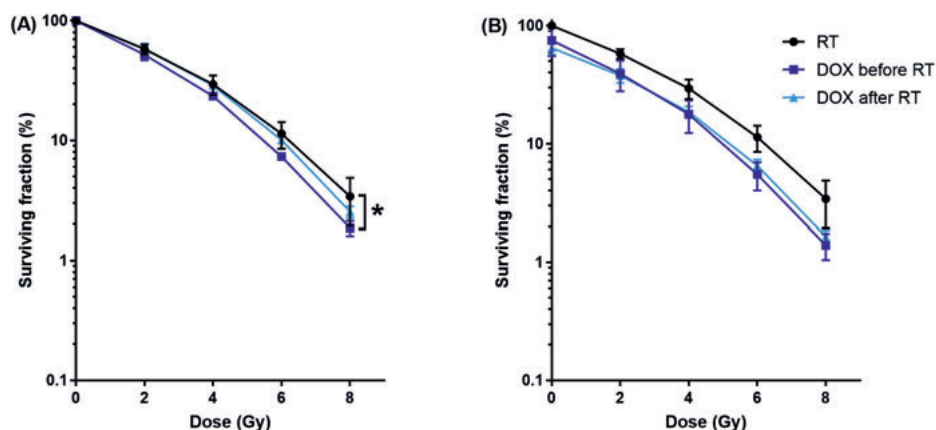


Figure 4. Cytotoxicity of DOX before or after RT. Surviving fraction as function of radiation dose. Cells were exposed for 1 hour to DOX (0.02 $\mu\text{g/mL}$) before or after RT, normalized for DOX at 0 Gy (A) and normalized for untreated samples (0 $\mu\text{g/mL}$ and 0 Gy) (B). Only DOX before RT resulted in a significant enhancement of the RT

3.3.3 Doxorubicin and hyperthermia

Since in the proposed concept of triggered radiosensitizer release the primary role of HT is to trigger the release of the radiosensitizer, DOX and HT were always concurrently combined. The surviving fraction as function of DOX concentration at different temperatures is presented in Figure 5A. HT enhanced the cytotoxicity of DOX, which was the largest at 43°C. At a surviving fraction

of 1% the enhancement ratios of HT at 42°C and 43°C were 1.79 and 2.83, respectively. Note that HT as a single treatment resulted in limited toxicity, HT of 42 and 43°C resulted in surviving fractions of $96.73 \pm 16.84\%$ and $101.84 \pm 0.21\%$, respectively.

These results were confirmed by measuring the percentage γ H2AX positive cells 2 and 26 hours after incubated with DOX for 1 hour at 37 or 43°C (Figure 5B). An increase in DOX concentration resulted in an increase in percentage γ H2AX positive cells both 2 and 26 hours after treatment, which was only significant 2 hours after DOX treatment. HT as a single treatment showed only 2 hours after treatment a significant enhancement of the percentage γ H2AX positive cells, 26 hours after treatment the percentage γ H2AX positive cells was similar to control cells. The combination DOX and HT resulted in enhanced percentage γ H2AX positive cells compared to DOX as a single treatment, this was only significant at a DOX concentration of 0.06 $\mu\text{g}/\text{mL}$ 2 hours after incubation. For all DOX and/or HT conditions 2 hours after treatment the percentage γ H2AX positive cells were larger compared to 26 hours after treatment.

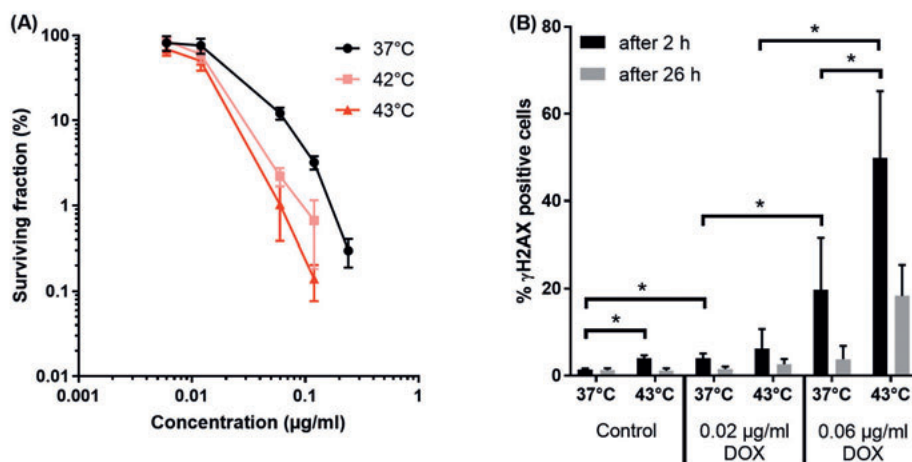


Figure 5. Cytotoxicity of hyperthermia at different temperatures and DOX. (A) Surviving fraction as function of DOX concentration for 1 hour at 37, 42 or 43°C. Cells were exposed for 1 hour to DOX at 37, 42 and 43°C. Both 42 and 43°C showed enhancement cytotoxicity of the DOX, which was the largest at 43°C. (B) Percentage γ H2AX positive cells 2 and 26 hours after incubation with DOX (0, 0.02 or 0.06 $\mu\text{g}/\text{mL}$) for 1 hour at 37°C or 43°C. HT enhanced the percentage γ H2AX positive cells both 2 and 26 hours after treatment.

3.3.4 Radiotherapy, doxorubicin and hyperthermia

Finally, the optimal sequence was investigated for all modalities in the proposed concept of triggered radiosensitizer delivery. In these experiments HT at 43°C was used, since HT at 42°C did not show enhancement of RT (Figure 3). Cells treated with DOX (0.02 µg/mL) at 43°C for 1 hour showed an equal and significant enhancement of the sensitivity to RT independent of the timing, i.e. before or after RT (Figure 6). The SF₀ of DOX and HT before and after RT were 4.37% ± 0.15% and 5.56% ± 0.80%, respectively.

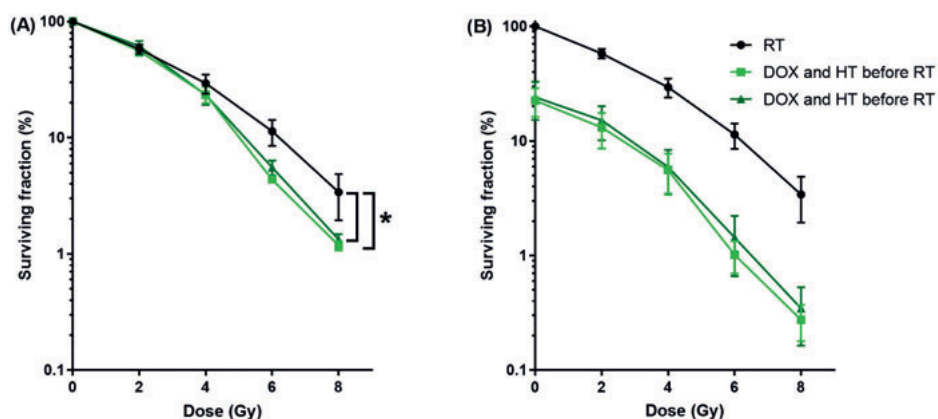


Figure 6. Cytotoxicity of HT and DOX before and after RT. Surviving fraction as function of radiation dose. Cells were exposed for 1 hour to DOX (0.02 µg/mL) at 43°C before or after RT. Both DOX and HT before and after RT resulted in a significant enhancement of the RT normalized for DOX and HT at 0 Gy (A) and normalized for untreated samples (0 µg/mL, 37°C and 0 Gy) (B).

3.4 Initial and prolonged double strand breaks after exposure to DOX, HT and RT

The enhancement of RT by DOX and/or HT was further investigated by quantifying the percentage γH2AX positive cells 45 minutes and 24 hours after RT. Figure 7 shows the percentage γH2AX positive cells after treatment with DOX (0 or 0.02 µg/mL) at 37 or 43°C followed by RT (0 or 4 Gy). Flow cytometry measurements were performed either 45 minutes (A and B) or 24 hours (C and D) after RT. As a single treatment RT showed significant enhancement of the percentage γH2AX positive cells both 45 minutes and 24 hours after RT relative to control. To be able to assess the radiosensitizing effect of DOX and/or HT more clearly, the contribution of DOX and HT to the percentage of γH2AX positive cells in the absence of RT was subtracted

from the percentage of γ H2AX positive cells in the presence of RT, defining $\Delta \gamma$ H2AX. Both HT, DOX and the combination HT and DOX in combination with RT resulted in an increase in $\Delta \gamma$ H2AX, i.e. radiosensitizing effect, both 45 minutes and 24 hours after RT. This was only significant for the combination of DOX and RT 24 hours after irradiation.

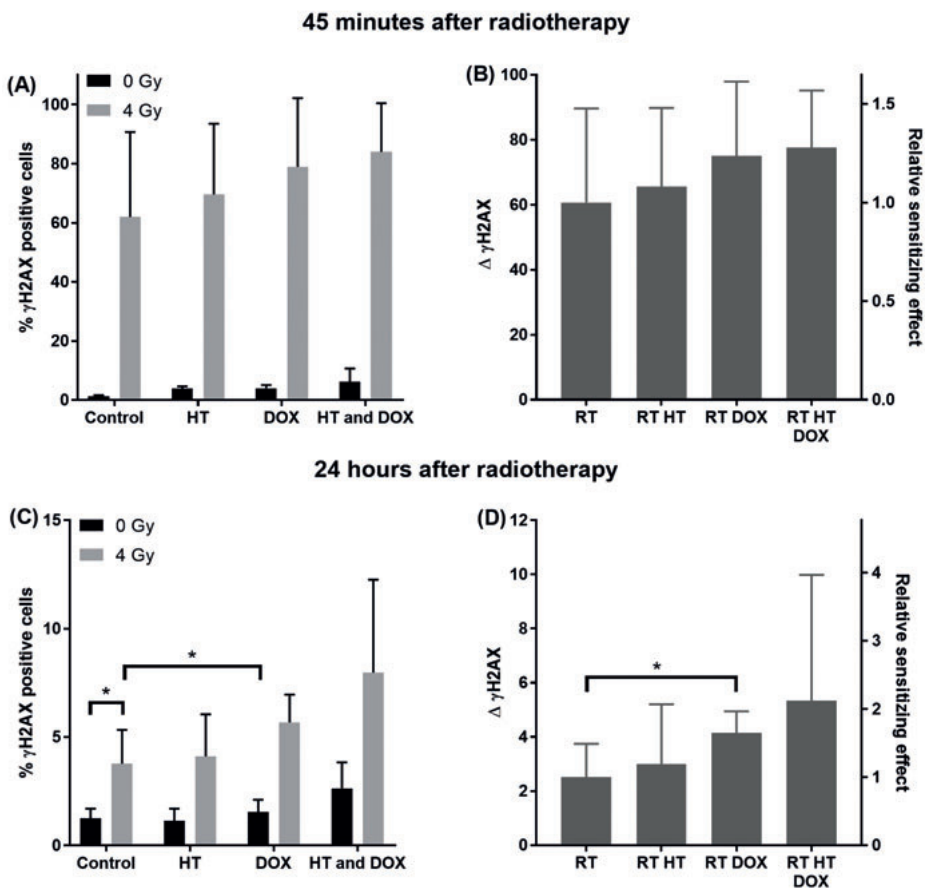


Figure 7. γ H2AX staining after cells treated with DOX, HT and/or RT. Percentage γ H2AX positive cells after incubated with DOX (0 or 0.02 μ g/mL) for 1 hour at 37 or 43°C and irradiated at 0 or 4 Gy, 45 minutes (A and B) or 24 hours (C and D) after irradiation. Expressed in percentage γ H2AX positive cells (A and C) and expressed in difference in percentage γ H2AX cells of treatment with and without RT (0 and 4 Gy) and expressed in relative sensitizing effect (B and D).

4. DISCUSSION

To decrease toxicity of the radiosensitizers in normal tissue and increase the local efficacy of chemoradiation for local tumor control, we investigated *in vitro* the potential of the concept of triggered radiosensitizer release from TSL by heat followed by conventional radiotherapy. Triggered release of DOX from ThermoDox at 43°C resulted in comparable cell death as free DOX at 43°C, with and without RT. Exposure of cells to ThermoDox at 37°C alone or in combination with RT did not change the cell survival. DOX had a direct toxic effect on cells, and proved an effective enhancement of the RT which was only slightly concentration dependent. The sequence of the treatments in the concept triggered radiosensitizer release was important to achieve the largest enhancement of sensitivity to RT.

The concept of triggered radiosensitizer release was investigated by exposing cells to ThermoDox and DOX at 37 and 43°C followed by conventional RT. No toxicity was observed when cells were incubated with ThermoDox at 37°C, however ThermoDox at 43°C resulted in equal cytotoxicity compared to DOX at 43°C. In addition, ThermoDox at 37°C did not result in any radiosensitization. However, at 43°C, ThermoDox and DOX resulted in comparable radiosensitization. According to Li et al [33], 1 hour incubation of ThermoDox at 37°C results in 50% DOX release, which in this study would lead to a final DOX concentration of about 0.01 µg/mL. Exposure of HT1080 cells to a DOX concentration of 0.01 µg/mL did not result in cell death (Figure 4), therefore no toxicity was expected of ThermoDox at 37°C for 1 hour. In contrast, ThermoDox at 42°C results in 100% DOX release after 1 minute [33]. As a consequence, for almost the complete hour the DOX concentration of cells treated with ThermoDox is equal to cells treated with free DOX and therefore resulted in equal cytotoxicity. These results show the potential of the local radiosensitizer delivery concept for reducing toxicities in unheated normal tissue located in the beam path.

In vivo studies of ThermoDox combined with local HT show 4.7 to 26.7 times increase in DOX concentration in the tumor compared to treatment with free DOX, while leaving the concentration of DOX in normal tissue nearly unchanged [22, 23, 25]. To investigate the radiosensitization effect of this envisioned increased radiosensitizer concentration in the tumor, we investigated the concentration dependency of DOX based radiosensitization. Although all DOX concentrations used in this study (0.01 up to 0.06 µg/mL) resulted in

an enhancement of the sensitivity to RT, a relatively large increase in DOX concentration was required to obtain a small increase in sensitivity to RT. To the best of the authors' knowledge no data is available on the concentration dependence of the DOX radiosensitization. Other radiosensitizers, such as cisplatin [34] and docetaxel [35], show a larger concentration dependent radiosensitization compared to DOX. It could be expected that local triggered release of such radiosensitizers from TSL would result in a more pronounced concentration dependent radiosensitization effect.

Since HT not only causes drug release from TSL, but also sensitizes RT and chemotherapy, the optimization of the sequence of radiosensitizer, HT and RT is important to achieve the largest efficacy [27-29, 36]. In order to understand the contribution of each modality and maximize the effect of triggered radiosensitizer release, the effect of the sequence of DOX, HT and RT on radiosensitization was investigated. In this study temperatures of 42 and 43°C were investigated, since one hour incubation at these temperatures resulted in limited toxicity to the cells. Note that, compared to other cell lines, the HT1080 cells have been found to be relatively heat resistant [37, 38].

For the combination of RT and HT, a temperature dependent radiosensitization has been observed [37, 39, 40]. Here, HT at 43°C resulted in an enhanced sensitivity to RT, which was not observed at 42°C. As a result all subsequent HT experiments were performed at a temperature of 43°C. The largest sensitization was achieved when HT followed RT. The radiosensitization effect of HT is relatively small in HT1080 cells compared to other cell lines [28, 37, 40]. Both optimal temperature and optimal sequence of HT with respect to RT differs between cell lines [28, 37, 39, 40], however the underlying mechanism behind the optimal sequence of HT and RT is unknown. The main mechanism of HT mediated-radiosensitization is inhibition of the DNA damage repair proteins [29]. Therefore prolonged presence of DSB was expected after treatment of RT and HT compared to RT as a single treatment. However, in our study 24 hours after RT no enhancement of DSB was observed. This might be attributed to the recovery of the DNA damage repair protein function 6 hours after HT treatment as was shown by Van Oorschot [41]. In almost all cell lines, simultaneous HT and RT results in the largest sensitization effect [28], however simultaneous HT and RT is clinically impractical and therefore not investigated in this study.

Since the concept of local radiosensitizer release requires HT to release the radiosensitizer from the TSL, HT and DOX were always concurrently applied.

HT potentiated the effect of DOX; at 42 and 43°C DOX showed consistently enhanced toxicity compared to 37°C. In addition, HT increased the DSB caused by DOX immediately and 24 hours after treatment. This enhanced toxicity is most likely caused by the increase in intracellular DOX uptake when cells were exposed to elevated temperatures [26, 42]. In the concept local triggered radiosensitizer delivery, the chemosensitization of HT could cause extra potentiation of tumor treatment.

In the combination of DOX and RT, only DOX treatment before RT resulted in an enhancement of the sensitivity to RT. This is most likely related to the radiosensitizing mechanism of DOX, as previously reported [43-45]. In addition, 24 hours after RT the amount of γ H2AX positive cells was significantly enhanced by DOX compared to RT as a single therapy. Therefore we expect that the enhancement of RT by DOX is caused by an inhibition of the DSB repair, as was also observed by Bonner and Lawrence [44]. Possible mechanisms of inhibition of the DNA repair by DOX are stabilization of the DNA-topoisomerase II complex resulting in conformational changes of the DNA, cell kill in the radioresistant cell phase and free radical generation [44].

Finally, the combination of all treatment modalities for triggered radiosensitizer release was investigated. The sequences were limited to clinical relevant sequences for local radiosensitizer release. Since HT is required to release DOX from the TSL, HT and DOX were concurrently combined. In contrast, HT and RT were performed successively due to logistic limitations to be expected in a clinical setting. As a consequence, only the combinations of concurrent HT and DOX before or after RT were investigated. Concurrent HT and DOX before or after RT both resulted in equal enhancement of the sensitivity to RT. Since DOX before RT resulted in the largest enhancement of RT and HT after RT resulted in the largest enhancement of RT, it is plausible that HT and DOX concurrently before or after RT resulted in equal sensitization.

The primary goal of this study is to provide an *in vitro* proof of the triggered radiosensitizer delivery concept. We showed the potential of this concept in 1 cell line with 2 different radiobiological assays (i.e. clonogenic assay and γ H2AX assay). To understand in more detail the mechanism underlying the sensitization effect of DOX, HT and RT, future experiments should be performed in multiple cell lines.

In the current *in vitro* study, HT can only act as a chemosensitizer and radiosensitizer at cellular level, by mechanisms such as inhibition of the DNA damage repair, enhanced DNA damage and by increasing the membrane fluidity. However, HT *in vivo* also sensitizes tissue to chemotherapy and RT at organ level, by mechanisms such as increasing blood flow, tissue oxygenation and increasing the vascular permeability [38]. The additional effects of HT *in vivo* compared to *in vitro*, further support our concept of local triggered radiosensitizer delivery *in vivo*.

Since ThermoDox is already commercially available for use in clinical trials, it was used in this study as an example of a radiosensitizer in a TSL (i.e. ThermoDox). Currently DOX is only occasionally used in the clinic as a radiosensitizer in the treatment of soft tissue sarcomas, hence a soft tissue sarcoma cell line (HT1080) was used in this study. In contrast, other radiosensitizers, which are also chemotherapeutic agents, exist which are more commonly used in the clinic and are already encapsulated in a TSL, including cisplatin [46], pyrimidine analogue gemcitabine (dFdC) [47] and 5-FU [48]. However, the objective of these studies is to decrease the toxicity of the chemotherapeutic agent by TSL encapsulation, and as a consequence have not been tested as a radiosensitizer for triggered local release in combination with RT. As mentioned, ThermoDox is rather leaky at 37°C, which leads to unnecessary release of radiosensitizer in normal tissue. Therefore a stable TSL containing the radiosensitizer should be prepared to avoid normal toxicity by the radiosensitizer.

5. CONCLUSION

In vitro we showed enhancement of RT by the TSL only when the radiosensitizer was released by HT. These results demonstrated the potential of the local radiosensitizer release concept. Hyperthermia triggered local radiosensitizer delivery is able to decrease radiosensitizer-related toxicities in unheated normal tissue located in the beam path and at the same time enhance the efficacy of chemotherapy in heated tumor tissue. To maximize the effect of the individual treatments concurrent DOX and HT should be applied either before or after RT.

Acknowledgements

The authors would like to thank Kim van den Berkmortel, Ingrid Boots, Marjolijn Gross and Masha Hoogenboom from the Veterinarian Radiotherapy Department for their help with radiotherapy.

REFERENCES

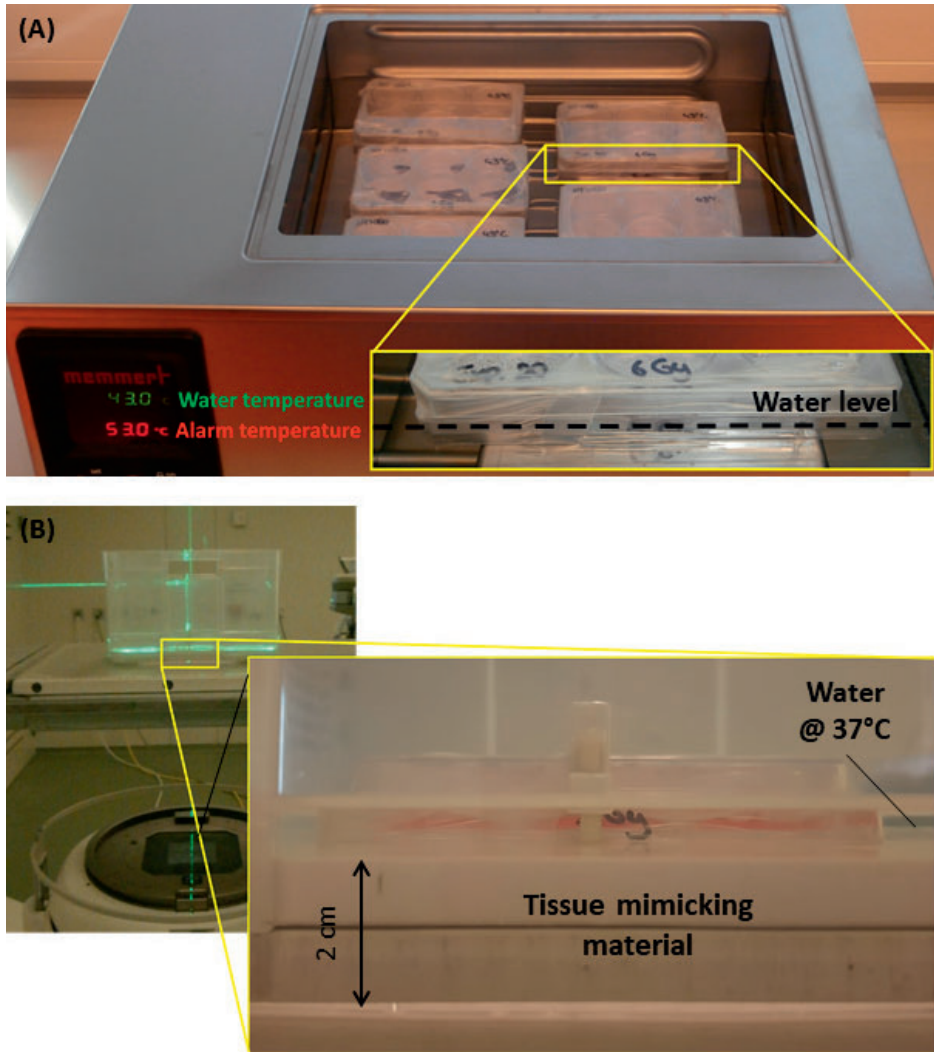
1. Miller KD, Siegel RL, Lin CC, Mariotto AB, Kramer JL, Rowland JH, Stein KD, Alteri R, Jemal A: **Cancer treatment and survivorship statistics, 2016.** *CA Cancer J Clin* 2016, **66**:271-289.
2. Barnett GC, West CM, Dunning AM, Elliott RM, Coles CE, Pharoah PD, Burnet NG: **Normal tissue reactions to radiotherapy: towards tailoring treatment dose by genotype.** *Nat Rev Cancer* 2009, **9**:134-142.
3. Peters LJ, Withers HR, Thames HD, Jr., Fletcher GH: **Tumor radioresistance in clinical radiotherapy.** *Int J Radiat Oncol Biol Phys* 1982, **8**:101-108.
4. Vokes EE, Weichselbaum RR: **Concomitant chemoradiotherapy: rationale and clinical experience in patients with solid tumors.** *J Clin Oncol* 1990, **8**:911-934.
5. Eilber FR, Morton DL, Eckardt J, Grant T, Weisenburger T: **Limb salvage for skeletal and soft tissue sarcomas. Multidisciplinary preoperative therapy.** *Cancer* 1984, **53**:2579-2584.
6. Green J, Kirwan J, Tierney J, Vale C, Symonds P, Fresco L, Williams C, Collingwood M: **Concomitant chemotherapy and radiation therapy for cancer of the uterine cervix.** *Cochrane Database Syst Rev* 2005:CD002225.
7. Milas L, Mason KA, Liao Z, Ang KK: **Chemoradiotherapy: emerging treatment improvement strategies.** *Head Neck* 2003, **25**:152-167.
8. Xiong HQ, Gunderson LL, Yao J, Ajani JA: **Chemoradiation for resectable gastric cancer.** *Lancet Oncol* 2003, **4**:498-505.
9. Curran WJ, Jr., Paulus R, Langer CJ, Komaki R, Lee JS, Hauser S, Movsas B, Wasserman T, Rosenthal SA, Gore E, et al: **Sequential vs. concurrent chemoradiation for stage III non-small cell lung cancer: randomized phase III trial RTOG 9410.** *J Natl Cancer Inst* 2011, **103**:1452-1460.
10. Myrehaug S, Pintilie M, Tsang R, Mackenzie R, Crump M, Chen Z, Sun A, Hodgson DC: **Cardiac morbidity following modern treatment for Hodgkin lymphoma: supra-additive cardiotoxicity of doxorubicin and radiation therapy.** *Leuk Lymphoma* 2008, **49**:1486-1493.
11. Gabizon A, Martin F: **Polyethylene glycol-coated (pegylated) liposomal doxorubicin. Rationale for use in solid tumours.** *Drugs* 1997, **54 Suppl 4**:15-21.
12. O'Brien ME, Wigler N, Inbar M, Rosso R, Grischke E, Santoro A, Catane R, Kieback DG, Tomczak P, Ackland SP, et al: **Reduced cardiotoxicity and comparable efficacy in a phase III trial of pegylated liposomal doxorubicin HCl (CAELYX/Doxil) versus conventional doxorubicin for first-line treatment of metastatic breast cancer.** *Ann Oncol* 2004, **15**:440-449.
13. Immordino ML, Dosio F, Cattel L: **Stealth liposomes: review of the basic science, rationale, and clinical applications, existing and potential.** *Int J Nanomedicine* 2006, **1**:297-315.
14. Gabizon A, Shmeeda H, Barenholz Y: **Pharmacokinetics of pegylated liposomal Doxorubicin: review of animal and human studies.** *Clin Pharmacokinet* 2003, **42**:419-436.
15. Lammers T, Kiessling F, Hennink WE, Storm G: **Drug targeting to tumors: principles, pitfalls and (pre-) clinical progress.** *J Control Release* 2012, **161**:175-187.

16. Charrois GJ, Allen TM: **Drug release rate influences the pharmacokinetics, biodistribution, therapeutic activity, and toxicity of pegylated liposomal doxorubicin formulations in murine breast cancer.** *Biochim Biophys Acta* 2004, **1663**:167-177.
17. Laginha KM, Verwoert S, Charrois GJ, Allen TM: **Determination of doxorubicin levels in whole tumor and tumor nuclei in murine breast cancer tumors.** *Clin Cancer Res* 2005, **11**:6944-6949.
18. Ta T, Porter TM: **Thermosensitive liposomes for localized delivery and triggered release of chemotherapy.** *J Control Release* 2013, **169**:112-125.
19. Manzoor AA, Lindner LH, Landon CD, Park JY, Simnick AJ, Dreher MR, Das S, Hanna G, Park W, Chilkoti A, et al: **Overcoming limitations in nanoparticle drug delivery: triggered, intravascular release to improve drug penetration into tumors.** *Cancer Res* 2012, **72**:5566-5575.
20. Needham D, Park JY, Wright AM, Tong J: **Materials characterization of the low temperature sensitive liposome (LTSL): effects of the lipid composition (lysolipid and DSPE-PEG2000) on the thermal transition and release of doxorubicin.** *Faraday Discuss* 2013, **161**:515-534; discussion 563-589.
21. Mills JK, Needham D: **Lysolipid incorporation in dipalmitoylphosphatidylcholine bilayer membranes enhances the ion permeability and drug release rates at the membrane phase transition.** *Biochim Biophys Acta* 2005, **1716**:77-96.
22. Ranjan A, Jacobs GC, Woods DL, Negussie AH, Partanen A, Yarmolenko PS, Gacchina CE, Sharma KV, Frenkel V, Wood BJ, Dreher MR: **Image-guided drug delivery with magnetic resonance guided high intensity focused ultrasound and temperature sensitive liposomes in a rabbit Vx2 tumor model.** *J Control Release* 2012, **158**:487-494.
23. Staruch RM, Ganguly M, Tannock IF, Hynynen K, Chopra R: **Enhanced drug delivery in rabbit VX2 tumours using thermosensitive liposomes and MRI-controlled focused ultrasound hyperthermia.** *Int J Hyperthermia* 2012, **28**:776-787.
24. Needham D, Anyarambhatla G, Kong G, Dewhirst MW: **A new temperature-sensitive liposome for use with mild hyperthermia: characterization and testing in a human tumor xenograft model.** *Cancer Res* 2000, **60**:1197-1201.
25. Yarmolenko PS, Zhao Y, Landon C, Spasojevic I, Yuan F, Needham D, Viglianti BL, Dewhirst MW: **Comparative effects of thermosensitive doxorubicin-containing liposomes and hyperthermia in human and murine tumours.** *Int J Hyperthermia* 2010, **26**:485-498.
26. Hahn GM, Braun J, Har-Kedar I: **Thermochemotherapy: synergism between hyperthermia (42-43 degrees) and adriamycin (of bleomycin) in mammalian cell inactivation.** *Proc Natl Acad Sci U S A* 1975, **72**:937-940.
27. Issels RD: **Hyperthermia adds to chemotherapy.** *Eur J Cancer* 2008, **44**:2546-2554.
28. Horsman MR, Overgaard J: **Hyperthermia: a potent enhancer of radiotherapy.** *Clin Oncol (R Coll Radiol)* 2007, **19**:418-426.
29. Kampinga HH, Dikomey E: **Hyperthermic radiosensitization: mode of action and clinical relevance.** *Int J Radiat Biol* 2001, **77**:399-408.
30. Franken NA, Rodermond HM, Stap J, Haveman J, van Bree C: **Clonogenic assay of cells in vitro.** *Nat Protoc* 2006, **1**:2315-2319.

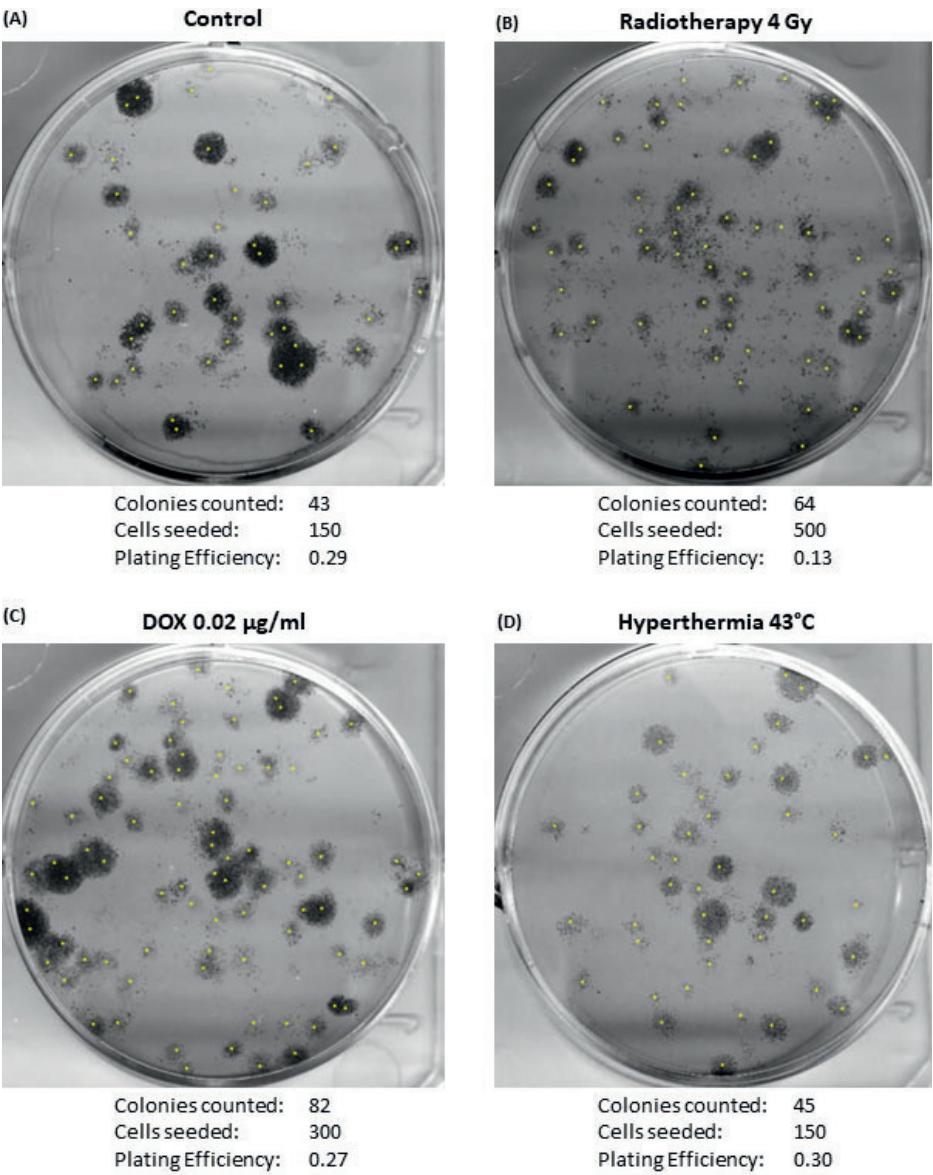
31. Dewey WC, Hopwood LE, Sapareto SA, Gerweck LE: **Cellular responses to combinations of hyperthermia and radiation.** *Radiology* 1977, **123**:463-474.
32. Roizin-Towle L, Pirro JP: **The response of human and rodent cells to hyperthermia.** *Int J Radiat Oncol Biol Phys* 1991, **20**:751-756.
33. Li L, ten Hagen TL, Hossann M, Suss R, van Rhoon GC, Eggermont AM, Haemmerich D, Koning GA: **Mild hyperthermia triggered doxorubicin release from optimized stealth thermosensitive liposomes improves intratumoral drug delivery and efficacy.** *J Control Release* 2013, **168**:142-150.
34. van de Vaart PJ, Klaren HM, Hofland I, Begg AC: **Oral platinum analogue JM216, a radiosensitizer in oxlc murine cells.** *Int J Radiat Biol* 1997, **72**:675-683.
35. Miyanaga S, Ninomiya I, Tsukada T, Okamoto K, Harada S, Nakanuma S, Sakai S, Makino I, Kinoshita J, Hayashi H, et al: **Concentration-dependent radiosensitizing effect of docetaxel in esophageal squamous cell carcinoma cells.** *Int J Oncol* 2016, **48**:517-524.
36. Seiwert TY, Salama JK, Vokes EE: **The concurrent chemoradiation paradigm--general principles.** *Nat Clin Pract Oncol* 2007, **4**:86-100.
37. Bergs JW, Haveman J, Ten Cate R, Medema JP, Franken NA, Van Bree C: **Effect of 41 degrees C and 43 degrees C on cisplatin radiosensitization in two human carcinoma cell lines with different sensitivities for cisplatin.** *Oncol Rep* 2007, **18**:219-226.
38. Hildebrandt B, Wust P, Ahlers O, Dieing A, Sreenivasa G, Kerner T, Felix R, Riess H: **The cellular and molecular basis of hyperthermia.** *Crit Rev Oncol Hematol* 2002, **43**:33-56.
39. Krawczyk PM, Eppink B, Essers J, Stap J, Rodermond H, Odijk H, Zelensky A, van Bree C, Stalpers LJ, Buist MR, et al: **Mild hyperthermia inhibits homologous recombination, induces BRCA2 degradation, and sensitizes cancer cells to poly (ADP-ribose) polymerase-1 inhibition.** *Proc Natl Acad Sci U S A* 2011, **108**:9851-9856.
40. Maeda J, Fujii Y, Fujisawa H, Hirakawa H, Cartwright IM, Uesaka M, Kitamura H, Fujimori A, Kato TA: **Hyperthermia-induced radiosensitization in CHO wild-type, NHEJ repair mutant and HR repair mutant following proton and carbon-ion exposure.** *Oncol Lett* 2015, **10**:2828-2834.
41. van Oorschot B, Granata G, Di Franco S, Ten Cate R, Rodermond HM, Todaro M, Medema JP, Franken NA: **Targeting DNA double strand break repair with hyperthermia and DNA-PKcs inhibition to enhance the effect of radiation treatment.** *Oncotarget* 2016, **7**:65504-65513.
42. Herman TS: **Temperature dependence of adriamycin, cis-diamminedichloroplatinum, bleomycin, and 1,3-bis(2-chloroethyl)-1-nitrosourea cytotoxicity in vitro.** *Cancer Res* 1983, **43**:517-520.
43. Belli JA, Piro AJ: **The interaction between radiation and adriamycin damage in mammalian cells.** *Cancer Res* 1977, **37**:1624-1630.
44. Bonner JA, Lawrence TS: **Doxorubicin decreases the repair of radiation-induced DNA damage.** *Int J Radiat Biol* 1990, **57**:55-64.
45. Jagetia GC, Aruna R: **Correlation between cell survival and micronuclei-induction in HeLa cells treated with adriamycin after exposure to various doses of gamma-radiation.** *Toxicol Lett* 2000, **115**:183-193.
46. Woo J, Chiu GN, Karlsson G, Wasan E, Ickenstein L, Edwards K, Bally MB: **Use of a passive equilibration methodology to encapsulate cisplatin into preformed thermosensitive liposomes.** *Int J Pharm* 2008, **349**:38-46.

47. Limmer S, Hahn J, Schmidt R, Wachholz K, Zengerle A, Lechner K, Eibl H, Issels RD, Hossann M, Lindner LH: **Gemcitabine treatment of rat soft tissue sarcoma with phosphatidylglycerol-based thermosensitive liposomes.** *Pharm Res* 2014, **31**:2276-2286.
48. Al Sabbagh C, Tsapis N, Novell A, Calleja-Gonzalez P, Escoffre JM, Bouakaz A, Chacun H, Denis S, Vergnaud J, Gueutin C, Fattal E: **Formulation and pharmacokinetics of thermosensitive stealth(R) liposomes encapsulating 5-Fluorouracil.** *Pharm Res* 2015, **32**:1585-1603.

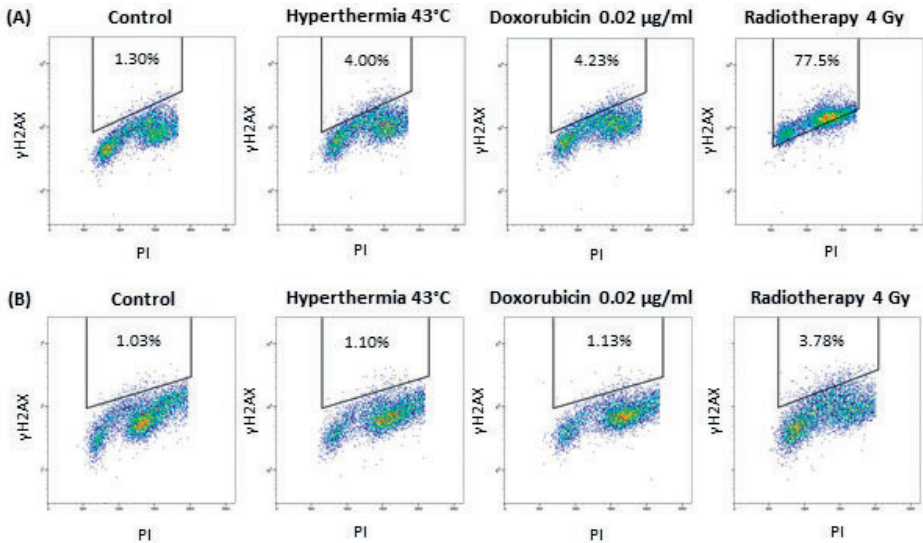
SUPPLEMENTARY INFORMATION



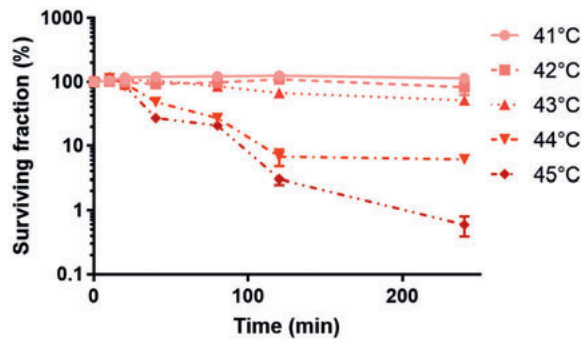
Supplementary Figure 1. Water bath and irradiation setup. A photo of the water bath (A) and irradiation setup (B). During incubation of the samples in the water bath and irradiation, well plates were wrapped with Parafilm.



Supplementary Figure 2. Representative clonogenic assay images. Representative clonogenic assay images of untreated cells (A) and cells treated with radiotherapy 4 Gy (B), DOX 0.02 $\mu\text{g/ml}$ (C) and HT 43°C (D). Only colonies that exist of at least 50 cells were counted (yellow dots). The plating efficiency was calculated from the number of colonies formed and the number of cells seeded according to Franken et al [30].



Supplementary Figure 3. Representative Flow Cytometry results of γ H2AX and PI fluorescence. Representative Flow Cytometry results of γ H2AX and PI fluorescence of untreated cells and cells treated with hyperthermia (43°C), doxorubicin (0.02 μ g/mL) and radiotherapy (4 Gy) 45 minutes (A) and 24 hours (B) after radiotherapy treatment. The percentage γ H2AX positive cells was determined relative to the control sample. Since the fluorescence of PI highly depend on the concentration of PI, the width of the box to determine positive γ H2AX labeled cells was adjusted to PI fluorescence.



Supplementary Figure 4. Survival fraction as function of incubation time of at different temperatures. Cells exposed for 0 to 240 minutes to temperatures ranging between 41 and 45°C.

CHAPTER 3

Tumor Drug Distribution after Local Drug Delivery by Hyperthermia, *In Vivo*

Helena C. Besse
Angelique D. Barten-van Rijbroek
Kim M.G. van der Wurff-Jacobs
Clemens Bos
Chrit T.W. Moonen
Roel Deckers

Based on: **Cancers (2019); 11(10)**

ABSTRACT

Tumor drug distribution and concentration are important factors for effective tumor treatment. A promising method to enhance the distribution and the concentration of the drug in the tumor is to encapsulate the drug in a temperature sensitive liposome. The aim of this study was to investigate the tumor drug distribution after treatment with various injected doses of different liposomal formulations of doxorubicin, ThermoDox (temperature sensitive liposomes) and DOXIL (non-temperature sensitive liposomes), and free doxorubicin at macroscopic and microscopic levels. Only ThermoDox treatment was combined with hyperthermia. Experiments were performed in mice bearing a human fibrosarcoma. At low and intermediate doses, the largest growth delay was obtained with ThermoDox, and at the largest dose, the largest growth delay was obtained with DOXIL. On histology, tumor areas with increased doxorubicin concentration correlated with decreased cell proliferation, and substantial variations in doxorubicin heterogeneity were observed. ThermoDox treatment resulted in higher tissue drug levels than DOXIL and free doxorubicin for the same dose. A relation with the distance to the vasculature was shown, but vessel perfusion was not always sufficient to determine doxorubicin delivery. Our results indicate that tumor drug distribution is an important factor for effective tumor treatment and that its dependence on delivery formulation merits further systematic investigation.

1. INTRODUCTION

Chemotherapy is one of the main treatment modalities of cancer. A commonly used chemotherapeutic agent is doxorubicin, which is used for the treatment of soft tissue sarcoma, among others [1-4]. As such, doxorubicin contributes to successful tumor treatment, but it also causes serious toxicities in non-tumor tissue, especially in the heart [5-7]. These toxicities are a dose limiting factor for doxorubicin and could lead to suboptimal treatment of the tumor and to compromised efficacy [8].

A common approach to reduce chemotherapy related toxicities is to encapsulate the drug in nanomedicine [9], such as liposomes [10, 11]. Liposomes preferentially accumulate in the tumor tissue driven by the enhanced permeability and retention (EPR) effect [12]. After accumulation of the liposomes in the tumor, the chemotherapeutic agent diffuses from these liposomes over the course of days [13].

In 1995, DOXIL was the first Food and Drug Administration (FDA) approved doxorubicin containing liposome [14]. Preclinical experiments had demonstrated that DOXIL treatment reduced doxorubicin accumulation in the heart [15] and increased survival compared to free doxorubicin (DOX) treatment [16]. In humans with metastatic breast cancer, though, DOXIL treatment did decrease toxicity, but survival remained comparable to that of DOX treatment [11]. The observation that DOXIL treatment failed to increase survival in these patients has been attributed to inter- and intra-patient variations of the tumor EPR effect [17] and to the slow diffusion of doxorubicin from the liposomes, resulting in limited bioavailability of the drug [18].

The bioavailability of the drug in the tumor can be improved by combining temperature sensitive liposomes (TSL) with local hyperthermia, as first proposed in 1978 by Yatvin et al. [19]. The quick release of the encapsulated drug from TSLs is caused by increased permeability of the liposomal membrane for temperatures exceeding a threshold, its phase transition temperature [20]. Preclinical treatment with TSLs containing doxorubicin in combination with hyperthermia improved efficacy [21-23] and increased doxorubicin concentration gradients in the tumor [22, 24-26].

A TSL containing doxorubicin available for clinical studies is ThermoDox [27]. ThermoDox releases 60% of the encapsulated doxorubicin within 20

seconds at a temperature of 41.3°C, its phase transition temperature [28]. Currently, ThermoDox is in a phase III clinical trial for hepatocellular carcinoma in combination with tumor radiofrequency (RF) ablation (clinicaltrials.org identifier: NCT02161562). Previous clinical trials have already shown the safety and the feasibility of ThermoDox treatment in combination with RF ablation and hyperthermia [29-32].

Not only absolute drug concentration in the tumor, but also the spatial drug distribution of the drug is an important factor to achieve effective tumor treatment. Absolute drug concentration in the tumor and spatial drug distribution of the drug are important factors to achieve effective tumor treatment [33]. For example, Torok et al. showed that a more homogeneous spatial distribution of anti-angiogenic receptor tyrosine kinase inhibitors correlated with improved antitumor and anti-vascular effects [34]. Cesca et al. demonstrated that larger anti-tumor activity of paclitaxel after bevacizumab is due not necessarily to overall tumor drug levels but to better drug penetration and more homogenous drug distribution [35]. A promising approach to improve the drug distribution and the drug concentration in the tumor is by TSL in combination with hyperthermia. TSL in combination with hyperthermia results in a more homogeneous spatial doxorubicin concentration [25], increased doxorubicin concentrations at larger distances from the vessels [24], and increased doxorubicin concentrations in the whole tumor [22, 25, 26] compared to DOX. Although a couple of landmark papers provided evidence for heterogeneous drug distribution after ThermoDox treatment, these studies only investigated the doxorubicin distribution in a qualitative way [25] or only in a small region of the tumor [24].

Here, the drug distribution after treatment with different doses of clinically available TSL containing doxorubicin, ThermoDox, was compared with clinically available non-temperature sensitive liposomes containing doxorubicin (NTSL), DOXIL, and free doxorubicin, DOX. Only ThermoDox treatment was combined with hyperthermia, since ThermoDox has to be combined with hyperthermia for triggered drug release, whereas DOX and DOXIL are, in daily clinical practice, always applied in the absence of hyperthermia. To investigate the efficacy of the different formulations, the tumor growth was monitored after treatment. Since drug distribution has an effect on the tumor growth, the drug distribution was studied quantitatively in whole tumor sections. After treatment with the different formulations, the drug distribution was investigated in terms of spatial doxorubicin distribution and doxorubicin concentration in the tumor and by

doxorubicin concentration in relation to the perfused tumor vessels. Finally, the microscopic effect of the doxorubicin distribution in the tumor on tumor cell proliferation was investigated.

2. MATERIALS AND METHODS

2.1 Materials

DOX (Accord Healthcare, CityUtrecht, The Netherlands), DOXIL (Janssen-Cilag BV, Breda, The Netherlands), and ThermoDox (Celsion Corporation, Lawrenceville, NJ, USA) were obtained at a doxorubicin concentration of 2 mg/mL.

2.2 Cell Culture

HT1080 (human fibrosarcoma) cells (obtained from ATCC, ATCC CCL-121, CityRockville, MD, USA) were cultured in Minimum Essential Medium (MEM, Gibco, Grand Island, NY, US) supplemented with 292 mg/L L-glutamine (Sigma, St. Louis, MO, USA), 110 mg/L sodium pyruvate (Sigma), and 10% fetal bovine serum (Sigma F7524). Cells were cultured at 37°C in 5% CO₂ in an air humidified incubator and regularly tested for mycoplasma contamination.

2.3 Animal Model

Seven to nine weeks Balb/c immune deficient mice (CAnN.Cg-Foxn1nu/Crl, Charles River) were housed in a 12 hour light/dark cycle. Food and water were available ad libitum. Tumors were inoculated by subcutaneous injection of 1×10^6 cells [phosphate buffered saline (PBS):matrigel (354230, Corning, Corning, NY, USA), volume 1:1] in the hind leg. All animal experiments were approved by the Utrecht Animal Experimental Committee (DEC Utrecht, project number: 2013.III.09.066, approval date: 17 October 2013).

2.4 Chemotherapy Treatment

Mice with tumor volumes between 50 and 100 mm³ were randomized and received a single intravenous (i.v.) injection into the tail vein with different doxorubicin formulations (i.e., DOX, DOXIL, or ThermoDox) at various doses (i.e., 2.5, 5, or 10 mg/kg) or saline. Only mice receiving ThermoDox formulation were treated with hyperthermia for 1 hour immediately after ThermoDox administration. Subsequently, mice were either used to study the efficacy (N = 5 or 6 per formulation per dose) or to study the drug distribution 24 hours after treatment (N = 3 per formulation) (Supplementary Figure 1).

2.5 Hyperthermia Treatment

For hyperthermia treatment, mice were anesthetized with isofluorane (1.5–2%) immediately after ThermoDox administration. Subsequently, the tumor and the tumor bearing leg were covered with Vaseline and submerged in a water bath (WNE14I, Memmert, Schwabach, Germany) of 42°C for 1 hour (Supplementary Figure 2A).

In a separate experiment, intra tumor and core (rectal) temperatures were monitored by calibrated fiber optic temperature probes (Neoptix Reflex, Neoptix, StateQuebec, Canada, LP). Within one minute, tumors reached a temperature of $42.0 \pm 0.19^{\circ}\text{C}$, which was similar to the water bath temperature and remained constant over time. The core temperature was $36.9 \pm 0.18^{\circ}\text{C}$ during the treatment (Supplementary Figure 2B).

2.6 Efficacy Study

Mice were weighed and tumors were measured three times a week. Tumor volume was determined using the following equation: $0.5 \times \text{length} \times \text{width} \times \text{width}$. Mice were monitored until 5 times the initial tumor volume (tumor volume during treatment) was reached or until 60 days after treatment.

2.7 Drug Distribution Study

Mice were intraperitoneally (i.p.) injected 60 and 20 minutes before euthanasia with 0.5 mL pimonidazole (hypoxia marker, 4 mg/mL in saline, Hypoxyprobe, Burlington, MA, USA) and 0.5 mL BrdU (s-phase marker, 3 mg/mL in saline, Sigma), respectively. One minute before euthanasia, mice were i.v. injected with 0.1 mL Hoechst 33342 (perfusion marker, 3.25 mg/mL in saline, Sigma). Subsequently, euthanasia was performed by cervical dislocation. Tumors were harvested, embedded in optimal cutting temperature (OCT) compound, snap frozen in liquid nitrogen, and stored at -80°C .

2.8 Immunohistochemistry

Tumors were cut in 5 μm thick slices, mounted on glass, air-dried, and stored at -80°C until further use. Before immunohistochemistry staining, the fluorescence of doxorubicin and Hoechst was recorded, as described below. Subsequently, two successive slices were stained for CD31 and pimonidazole and for BrdU [36]. First, all slices were fixed in acetone at 4°C for 10 minutes and rehydrated in PBS. Staining of CD31 and pimonidazole was performed by incubating slices overnight with rat anti-mouse CD31 (1:50, 550274 BD pharmingen, San Diego, CA, USA) and rabbit anti-pimonidazole (1:500,

hypoxyprobe) at 4°C in a humidified chamber. Then, they were incubated for 1 hour with goat anti-rat Cy5 (1:500, ab6565, Abcam, Cambridge, UK) and goat-anti-rabbit IgG H&L Alexa fluor®594 (1:500, ab150080, Abcam) at room temperature in a humidified chamber and finally mounted with Fluoromount W (2163401, Serva electrophoresis GmbH, Heidelberg, Germany). Staining of BrdU was performed by incubating slices for 10 minutes in 2N HCl and neutralized for 10 minutes in 0.1 M Borax for antigen retrieval. Subsequently, slices were incubated overnight with sheep anti-BrdU (10 mg/mL, GTX21893, GeneTex, San Antonio, TX, USA) at 4°C in a humidified chamber. Then, they were incubated for 1 hour with donkey anti-sheep IgG H&L Alexa fluor®594 (1:200, ab150180, Abcam) at room temperature in a humidified chamber, incubated with Hoechst 33342 (1 µg/mL) for 1 minute, and mounted with Fluoromount W. Between all incubations, the slices were washed 3 times for 5 minutes in PBS. All antibodies were diluted in primary antibody diluent (PAD, GTX28208 GeneTex).

2.9 Image Acquisition and Processing

Whole tumor slices were scanned by Leica TCS SP8 X microscope (Leica, Germany) at 10 times magnification. Before staining, the fluorescence (excitation, emission) was recorded for doxorubicin (504, 540–680 nm) and Hoechst (405, 410–499 nm). After staining, the fluorescence was recorded for CD31 (649, 665–750 nm), pimonidazole (598, 615–720 nm), and BrdU (598, 615–720 nm). For each slice and fluorophore, a z-stack was acquired, and a maximum intensity projection was created for further analysis. Images before and after staining were semi-automatic aligned, tumors were manually segmented, and artifacts and necrotic areas were manually removed. All processing and analyzing was performed in MATLAB (MathWorks, Inc, Natick, MA, USA). Example of total tumor and zoomed in detail of the stainings of the tumor treated with 5 mg/kg ThermoDox is presented in Supplementary Figure 3.

Doxorubicin images were normalized for intensity fluctuations of the laser by dividing the tumor area by areas without any tissue. Since tumor autofluorescence can vary between tumors [37], autofluorescence of the tumor tissue was removed by subtracting the mean of the 10% smallest intensities of the normalized image.

Masks of vessels and dividing cells were obtained by applying a local maxima filter on CD31 and BrdU images, respectively. Masks of perfusion and hypoxia were acquired by interactive thresholding of the Hoechst and the pimonidazole

images, respectively. The mask of perfused vessels was created from the overlay of the vessels and the perfusion mask [38]. A vessel was considered as perfused when both vessel mask and perfusion mask were positive for this vessel.

2.10 Image Analysis

Dividing cell fraction, vessel density, perfused vessel density, and hypoxic fraction were calculated on whole tumor slices by dividing the amount of positive pixels in each mask by the amount of pixels of the segmented tumor.

The doxorubicin heterogeneity parameter (Hdox) was determined over the whole tumor of the doxorubicin images to investigate the spatial doxorubicin distribution. First, tumor slices were binned by 10×10 pixels to reduce the matrix size of the image and cropped to avoid rim artifacts. Subsequently, the cropped image was filtered with a local mean filter of 51×51 pixels (0.7×0.7 mm). Finally, the standard deviation of the pixels in the filtered image was divided by the standard deviation of the unfiltered image (Supplementary Figure 4A). Low values represented homogeneous spatial doxorubicin distribution, whereas high values represented heterogeneous spatial doxorubicin distribution.

The 90th percentile (P90) was used as a measure of the doxorubicin concentration in the whole tumor, i.e., 90% of all intensities of the doxorubicin image in the tumor were below this value.

The mean fluorescent intensity of the doxorubicin signal (doxorubicin intensity) in relation to the distance of the perfused vessels was determined [39]. Briefly, the perfused vessel mask was converted into a distance mask. Subsequently, the distance mask and the doxorubicin image were superimposed, and the mean doxorubicin intensity was calculated for each distance (Supplementary Figure 4B).

Finally, spatial correlation between the doxorubicin intensity and the dividing cells was determined by dividing each tumor image in squares of 200×200 pixels. For each square, the mean doxorubicin intensity and the dividing cell fraction were determined. Subsequently, each square represented one dot in the scatter plot. Dividing cell fraction below 0.05 and doxorubicin intensity below 0.5 were considered low. This resulted in 4 quadrants in the scatter plot, i.e., low/high dividing cell fraction in combination with low/high doxorubicin intensity.

2.11 Statistical Analysis

All tumor growth curves were presented as mean, with error bars representing the standard error of the mean. Kaplan-Meier curves were statistically tested in GraphPad Prism 7 (Graph-Pad Software, Inc, San Diego, CA, USA) by comparison of groups with a log rank Mantel-Cox test. Differences between groups with $p < 0.05$ were considered statistically significant.

3. RESULTS

3.1 Tumor Growth and Survival

Figure 1A–C shows tumor growth of mice in the different experimental groups. Tumor growth was decreased with respect to controls in animals receiving DOX, DOXIL, and ThermoDox treatments. A dose dependent decrease in tumor growth was observed after DOX, DOXIL, and ThermoDox treatment, although after treatment with ThermoDox at doses of 5 and 10 mg/kg, the tumor growth was comparable. At 2.5 and 5 mg/kg, the largest growth delay was obtained after ThermoDox treatment, whereas at 10 mg/kg, the largest growth delay was obtained after DOXIL treatment.

Figure 1D–F shows the survival of mice (i.e., time to reach tumor volume five times larger than the initial tumor volume) in the different experimental groups. Survival was related to the tumor growth; in all cases, the mouse was sacrificed because of reaching the humane endpoint for tumor growth. Survival was increased with respect to the controls in animals receiving DOX, DOXIL, and ThermoDox treatments, which was significant at doses of 5 and 10 mg/kg. A dose dependent increase in survival was observed after DOX, DOXIL, and ThermoDox treatments with the exception that ThermoDox treatment at doses of 5 and 10 mg/kg, which resulted in comparable survival and with a comparable result for tumor growth as well. A significant dose dependent increase in survival ($p < 0.05$) was observed after treatment with DOX and DOXIL between doses of 2.5 and 10 mg/kg and 5 and 10 mg/kg. For ThermoDox treatment, no significant differences in survival were observed between the different doses. At a dose of 5 mg/kg, survival was significantly increased ($p < 0.05$) after DOXIL and ThermoDox treatments compared to DOX treatment. No significant difference in survival was observed between DOXIL and ThermoDox treatments at any dose.

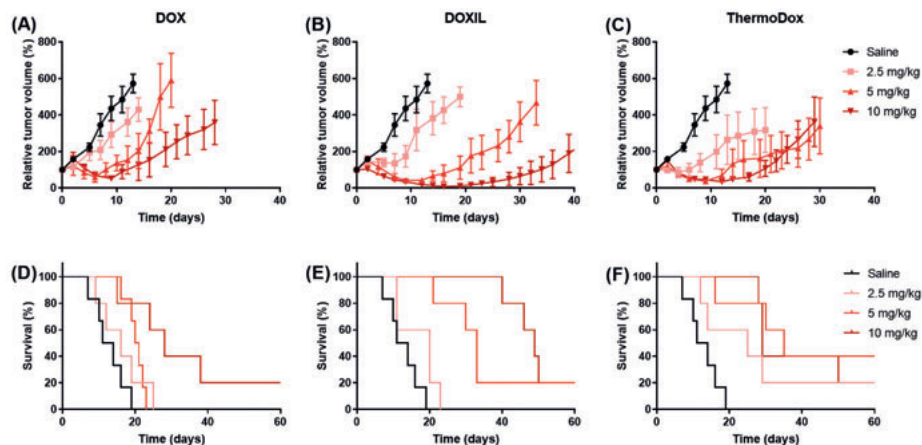


Figure 1. Tumor growth and survival (“tumor volume five times larger than the initial tumor volume”). Relative tumor volume and survival of tumors treated with saline, doxorubicin (DOX) (A and D), DOXIL (B and E), and ThermoDox (C and F) at a dose of 2.5, 5, and 10 mg/kg.

Toxicities were only observed after ThermoDox treatment. One mouse died immediately after injection of 10 mg/kg ThermoDox and was excluded from the study. Treatment with 5 and 10 mg/kg ThermoDox resulted in a maximum weight loss of 7% relative to the weight immediately before treatment in three and five mice, respectively. The weight loss was classified as mild toxicity; hence, these mice were not withdrawn from the study. Since no weight loss was observed after ThermoDox treatment with 2.5 mg/kg in combination with hyperthermia, the mild toxicity observed after ThermoDox treatment with 5 and 10 mg/kg in combination with hyperthermia was most likely not related to the hyperthermia treatment, but caused by the high local doxorubicin concentrations in the tumor bearing leg.

3.2 Qualitative Distributions of Doxorubicin, Perfusion, Hypoxia, and Dividing Cells

Figure 2 and Supplementary Figures 5–7 show the distribution of doxorubicin, perfusion, vessels, hypoxia, and dividing cells in tumors after DOX, DOXIL, and ThermoDox treatment at different injected doses and saline (control). After all treatments, areas with high doxorubicin intensities, i.e., doxorubicin containing areas, were heterogeneously distributed over the whole tumor with spatially varied doxorubicin intensities. The percentage of doxorubicin containing area varied as a function of the injected dose and the treatment formulation; it was

highest for the largest injected dose and for tumors treated with ThermoDox and DOXIL.

In all tumors, the vessels were homogeneously distributed throughout the tumor slice; however, only parts of these vessels were perfused. These perfused areas were heterogeneously distributed in the tumor slice. The doxorubicin containing areas were mainly located in areas that were perfused. However, after treatment with all formulations, there were also tumor areas that were perfused but did not contain doxorubicin. The hypoxic areas were heterogeneously distributed throughout the tumor slice. In addition, the percentage of hypoxic areas in the tumors differed between the tumors. The hypoxic areas were correlated with areas that did not contain doxorubicin. The dividing cells were also heterogeneously distributed throughout the tumor slice. Areas with few dividing cells were strongly correlated with doxorubicin containing areas.

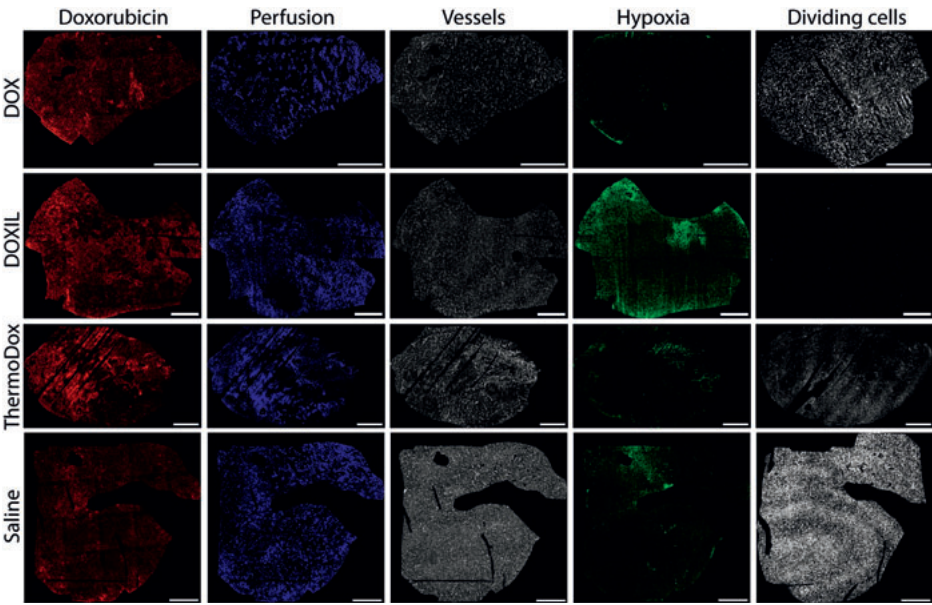


Figure 2. Different stainings of tumors treated with 5 mg/kg DOX, DOXIL, and ThermoDox. Tumors stained for doxorubicin, perfusion, all vessels, hypoxia, and proliferating cells. The scale bar is 1 mm.

3.3 Qualitative Doxorubicin Distribution

Figure 3A presents the correlation between the 90th percentile (P90) of the doxorubicin concentration and the doxorubicin heterogeneity parameter (Hdox) over the whole tumor slice in a scatter plot. High and low P90 values represent high and low tumor doxorubicin concentrations, respectively; high and low Hdox values represent heterogeneous and homogeneous spatial doxorubicin distribution, respectively. In the control tumor, both the P90 and the Hdox were low compared to DOX, DOXIL, and ThermoDox treated tumors, as expected.

The Hdox and the P90 were arbitrarily divided in high and low values at 0.4 and 0.92, respectively (Figure 3A). The untreated tumor (saline) and the tumors treated with DOX at all doses showed a low doxorubicin concentration that was homogeneously distributed in the tumor. Tumors treated with DOXIL and ThermoDox at doses of 2.5 and 5 mg/kg showed a high doxorubicin concentration that was heterogeneously distributed in the tumor. Tumors treated with DOXIL and ThermoDox at a dose of 10 mg/kg finally showed a high doxorubicin concentration that was homogeneously distributed throughout the tumor.

Overall, a trend was observed that P90 increased with increasing injected dose, although the tumor treated with 2.5 mg/kg ThermoDox was surprisingly high (Figure 3A and B). For all formulations, the spatial doxorubicin distribution was more homogeneous after treatment with 10 mg/kg than for doses of 2.5 and 5 mg/kg (Figure 3A and C). Doses of 2.5 and 5 mg/kg resulted in similar spatial doxorubicin distributions.

The P90 of ThermoDox treated tumors was increased compared to DOX and DOXIL treated tumors at all injected doses. The spatial doxorubicin distribution was more heterogeneous after ThermoDox treatment compared to DOX and DOXIL treatments at doses of 2.5 and 5 mg/kg. At a dose of 10 mg/kg, the spatial doxorubicin distribution after ThermoDox treatment was comparable with DOX treatment and more homogeneous compared to DOXIL treatment.

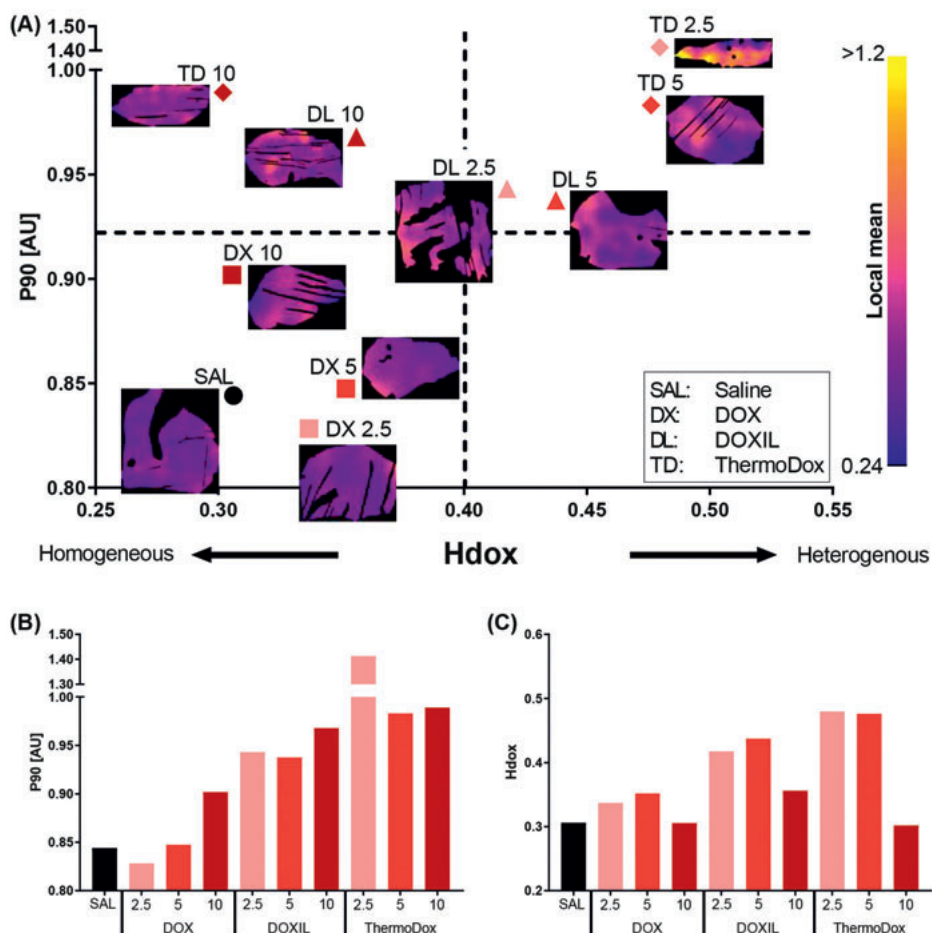


Figure 3. The 90th percentile of the doxorubicin concentration (P90) and the doxorubicin heterogeneity parameter (Hdox) over the whole tumor. Tumors treated with saline (SAL), DOX (DX), DOXIL (DL), and ThermoDox (TD) at 2.5, 5, and 10 mg/kg. The P90 (A and B) and the Hdox (A and C) were calculated over the whole tumor.

3.4 Doxorubicin Distribution Relative to Vessels

Figure 4 shows the doxorubicin intensity in relation to the distance of all perfused vessels in the whole tumor. In all tumors, the doxorubicin intensity close to the vessel was in the range of 0.5 and 0.6 AU except for the tumor treated with ThermoDox at a dose of 2.5 mg/kg, which was surprisingly high. In all tumors, the doxorubicin intensity declined with increased distance from the perfused vessels. However, no clear correlation was observed between the injected dose and the doxorubicin intensity in relation to the perfused vessels.

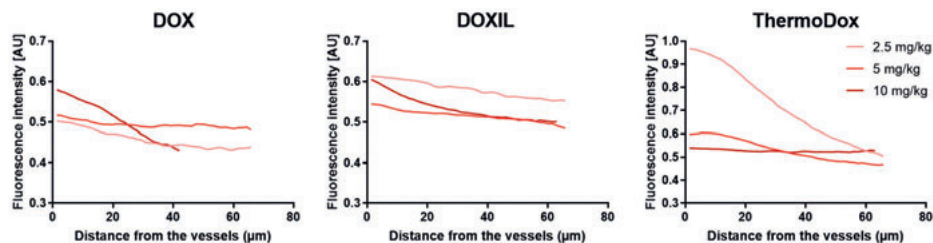


Figure 4. Doxorubicin intensities relative to the vessels over the whole tumor. The doxorubicin intensity relative to the vessels was determined after DOX (A), DOXIL (B), and ThermoDox (C) treatment at injected doses of 2.5, 5, and 10 mg/kg.

Since DOX, DOXIL, and ThermoDox treatments resulted in spatially varied doxorubicin intensities in the tumor, Figure 2 and Supplementary Figures 5–7, tumor locations with high and low doxorubicin concentrations were independently analyzed for doxorubicin intensity in relation to the perfused vessels (Supplementary Figure 8). Doxorubicin intensity in relation to the perfused vessels in locations with high doxorubicin concentrations and in the whole tumor showed a similar trend, i.e., the doxorubicin intensity decreased with an increase in distance from the perfused vessels, and no clear correlation was observed between injected dose and doxorubicin intensity in relation to the perfused vessels. However, the absolute doxorubicin intensities were higher in locations with high doxorubicin concentrations compared to the whole tumor at all investigated distances from the perfused vessels. In locations with low doxorubicin concentrations, the doxorubicin intensity hardly changed with increased distance from the perfused vessel. In addition, the absolute doxorubicin intensities in areas with low doxorubicin concentrations were lower compared to the absolute doxorubicin intensities in the whole tumor at all investigated distances from the perfused vessels, as expected.

3.5 Cell Proliferation

Figure 5 shows the dividing cell fraction in tumors from the different experimental groups. The dividing cell fraction was reduced with respect to the control tumor after treatment with DOX, DOXIL, and ThermoDox. Overall, the dividing cell fraction decreased with increased injected dose for all formulations, although the dividing cell fraction in the tumor treated with 10 mg/kg DOXIL was unexpectedly high. The largest decrease in cell proliferation was obtained by DOXIL followed by ThermoDox and DOX at all doses.

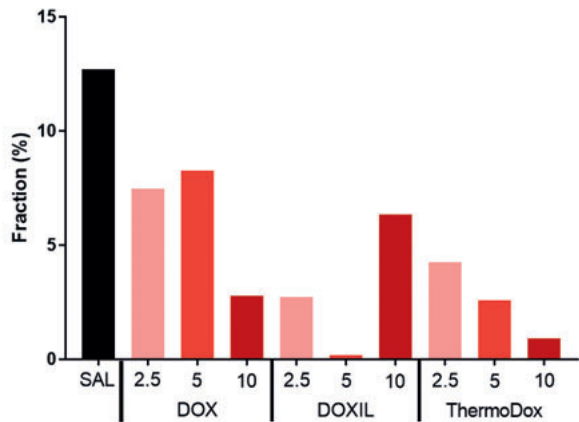


Figure 5. Dividing cell fraction over the whole tumor. The dividing cell fraction was calculated after tumors treated with SAL, DOX, DOXIL, and ThermoDox at doses of 2.5, 5, and 10 mg/kg. The tumor treated with DOXIL at a dose of 10 mg/kg was unexpectedly high.

Visual inspection of Figure 2 and Supplementary Figures 5–7 shows that areas with high doxorubicin intensity were correlated with reduced cell proliferation. This correlation was further quantitatively analyzed. Figure 6 presents, for each tumor, the dividing cell fraction and the doxorubicin intensity evaluated at each 200 × 200 pixel square of the tumor image, presented by a dot in the scatter plot. Generally, for each tumor, the dots were clustered. Overall, the dividing cell fraction per square decreased with increasing dose, as was already observed for whole tumor slices (Figure 5). In addition, an increasing trend was present between doxorubicin intensity and injected dose similar to that observed in the whole tumor slices (Figure 3B). Overall, the dots were mainly located either at high doxorubicin intensity and low dividing cells or at low doxorubicin intensity and high dividing cells.

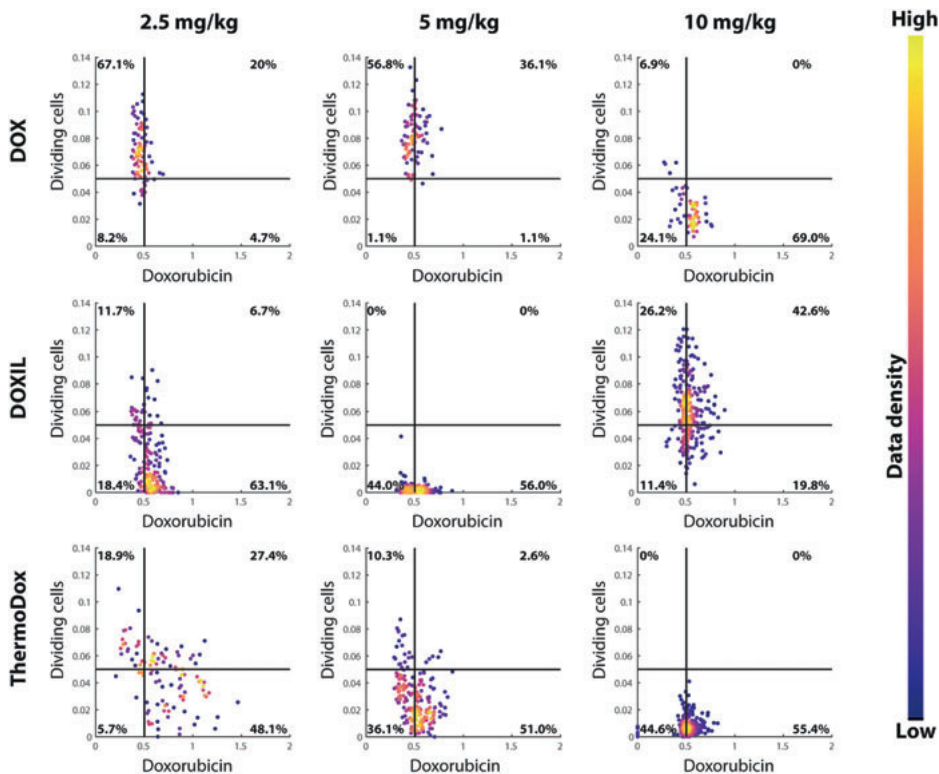


Figure 6. Correlation between dividing cell fraction and doxorubicin intensity. For each region in the tumor, the dividing cell fraction and the mean doxorubicin intensity were determined and are represented by one dot in the scatterplot. The color of the dots represents the data density of the locations. Dividing cell fraction below 0.05 and doxorubicin intensity below 0.5 were considered low.

3.6 Tumor Microenvironment

The doxorubicin distribution in the tumor not only depends on the doxorubicin formulation and the injected dose, it also depends on the tumor microenvironment [33]. The microenvironments of the tumors were compared by vessel density, perfused vessel density, and the hypoxic fraction (Figure 7). The perfused vessels were a subset of all vessels, and 50–85% of all vessels were perfused. The vessel fraction, the perfused vessel fraction, and the hypoxic fraction differed between all tumors. In all tumors, the vessel density, the perfused vessel density, and the hypoxic fraction were between 5–15%, 3–14%, and 4–14%, respectively. No correlation was observed between vessel fraction, perfused vessel fraction, or hypoxic fraction and injected formulation or dose.

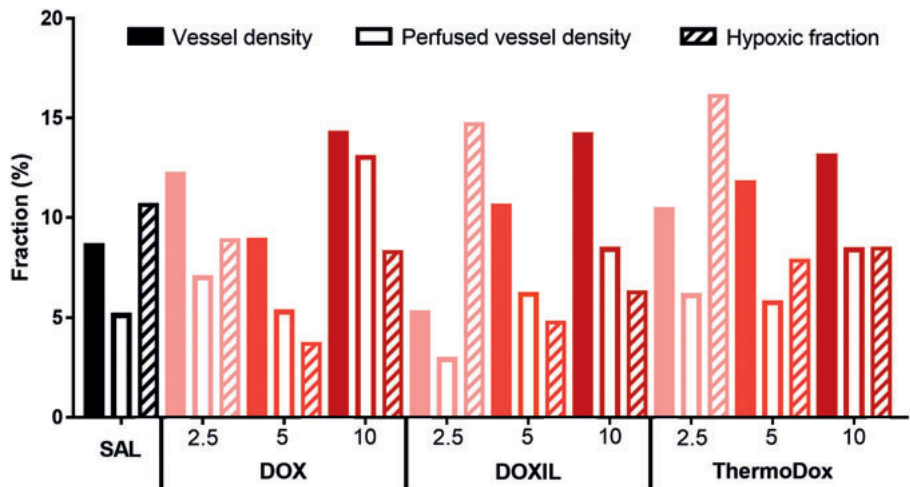


Figure 7. Vessel density, perfused vessel density, and hypoxic fraction. For each tumor, the vessel density (closed bars), the perfused vessel density (open bars), and the hypoxic fraction (striped bars) were determined in the whole tumor section.

4. DISCUSSION

Several studies have shown that tumor drug distribution is an important factor for effective tumor treatment [33-35]. TSL combined with hyperthermia is a promising approach to increase the drug distribution and the drug concentration in the tumor [24, 25, 40, 41]. Therefore, we studied in more detail the efficacy and the drug distribution in the tumor after treatment with different doxorubicin formulations, namely, ThermoDox (clinically available TSL with triggered release using hyperthermia), DOXIL (clinically available NTSL), and DOX, with different injected doses. The largest growth delay was obtained after ThermoDox treatment at lowest and intermediate doses, whereas at the highest dose, the largest growth delay was obtained after DOXIL treatment. We observed that an increase in injected dose resulted in decreased tumor growth and a more homogeneous spatial doxorubicin distribution for each formulation. In addition, an increase in injected dose of DOX and DOXIL treatment resulted in increased doxorubicin concentrations in the tumor.

A dose dependent decrease in tumor growth was observed after ThermoDox, DOXIL, and DOX treatment, as shown before [42]. ThermoDox treatment with doses of 5 and 10 mg/kg resulted in comparable tumor growth, most likely since the efficacy of ThermoDox did not further increase at doses larger than

5 mg/kg. The formulation that resulted in the largest growth delay depended on the injected dose. At doses of 2.5 and 5 mg/kg, the largest reduction in tumor growth was present after ThermoDox treatment. This is in line with previous studies demonstrating that TSLs such as ThermoDox result in greater anti-tumor effects compared to NTSLs such as DOXIL [22, 43]. At the highest investigated dose, i.e., 10 mg/kg, DOXIL treatment resulted in the largest growth delay in this study. We have no specific explanation for these differences; most likely, they are related to the maximum doxorubicin concentration and the area under the curve of the bioavailable doxorubicin concentration in the tumor.

As qualitatively observed, ThermoDox, DOXIL, and DOX treatments resulted in a heterogeneous doxorubicin distribution with spatially varied doxorubicin concentrations. This is in line with other studies that show a heterogeneous drug distribution in the tumor after treatment with DOX [44] and other drugs [45, 46]. These doxorubicin containing areas were mainly present in close proximity to perfused vessels. Interestingly, there were also areas with perfused vessels that showed low doxorubicin intensities. We cannot explain why perfused vessels, in spite of similar appearance, showed very different surrounding drug distributions, yet comparable observations have been described in literature for DOX [47] and other drugs [46, 48].

Many methods have been proposed to quantify the tumor drug distribution [49-51]. However, these methods are based on either drug concentration or spatial drug distribution. In our opinion, both drug concentration and spatial drug distribution are important to characterize the doxorubicin distribution in the tumor. Therefore, we separated our analysis in tumor concentration and spatial drug distribution and devised measures to quantify these from a fluorescence image.

A dose dependent increase in doxorubicin concentration in the tumor was present after DOX and DOXIL treatments, as observed before in whole tumors [52]. However, doxorubicin concentrations in the tumor after ThermoDox treatment were inconsistent in this study. For all formulations, an increase in injected dose resulted in a more homogeneous spatial doxorubicin distribution, as was qualitatively observed before for other drugs [48, 53].

For all injected doses, the doxorubicin concentration in the tumor after ThermoDox treatment was increased compared to DOX treatment. Differences in spatial drug distribution between DOX and ThermoDox treatments were dose

dependent. At doses of 2.5 and 5 mg/kg, the spatial doxorubicin distribution after treatment with ThermoDox was heterogeneous compared to DOX treatment, while at a dose of 10 mg/kg, the spatial doxorubicin distributions of ThermoDox and DOX were comparable. These results were not in line with Ranjan et al. [25], in which the spatial doxorubicin distribution at a dose of 5 mg/kg after ThermoDox treatment was homogeneous compared to DOX treatment. However, Ranjan et al. [25] qualitatively described the doxorubicin distribution and did not distinguish between the doxorubicin concentration and the spatial doxorubicin distribution in the tumor.

Although an increased injected dose corresponded well with decreased tumor growth, more homogeneous doxorubicin distribution, as well as increased tumor doxorubicin concentration, the relation between tumor growth and tumor doxorubicin concentration and distribution was less distinct. For each formulation, the group with the slowest tumor growth corresponded with the group with the highest tumor doxorubicin concentration and the most homogenous spatial drug distribution, as expected, since heterogeneous tumor drug distribution has been shown to decrease tumor treatment efficacy [33, 34, 54]. Interestingly, we did observe a correlation between areas with high doxorubicin concentrations and reduced dividing cells in all groups. Apparently, this first drug response was inconclusive to determine the final efficacy of the different formulations. It is known that the doxorubicin concentration in the tumor varies over time, and that these variations in concentrations are formulation dependent [18]. Therefore, further research should be conducted on variations in doxorubicin distribution in the tumor over time with single and repeated dosing and on the correlation between these time dependent variations and the efficacy of the different formulations.

In this study, no correlation was observed between the doxorubicin intensity in relation to the distance from the vessels and the injected dose. This was unexpected, since it was shown by Rhoden et al. [55] that an increase in injected dose increased the drug concentration both in close proximity to the vessels and at larger distances from the vessels 24 hours after administration of the antibodies. However, these experiments were performed with antibodies, and therefore our results cannot be directly compared with the results of Rhoden et al.

Drug distribution in the tumor depends on the properties of the drug formulation, but is also influenced by the tumor microenvironment [56]. No

differences were observed between vessel density, perfused vessel density, and hypoxic fraction between the tumors in the different formulations and injected doses. Therefore, we concluded that the observed differences in drug distribution between the different formulations and the injected doses were not related to the differences in tumor microenvironment. In addition, note that the hypoxic fraction was relatively low [39, 57-59] and the vessel density and the perfused vessel density were rather high [60, 61] in the investigated tumors. Hence, in this study, a well perfused tumor model was used.

A couple of limitations in this study were that, in the drug delivery part of this study, only one slice per tumor per treatment was chosen for further analysis; therefore, doxorubicin distribution was only investigated in a small part of one tumor per treatment and not in three-dimensional space. Consequently, a few important factors such as the out of plane vessels and the drug distribution in the whole tumor were not taken into account. In addition, since one tumor per treatment was analyzed, a bias could have occurred. In this study, 24 hours after treatment, animals were euthanized and immunohistochemistry was performed, since cell proliferation was included as an early marker for tumor response. However, it is known that doxorubicin concentration is preferably assessed between 30 and 60 minutes after administration of DOX [62] and between 24 and 48 hours after administration of DOXIL [15, 44, 62].

Doxorubicin fluorescence intensities were used as a measure of doxorubicin concentrations in the tumor. However, the doxorubicin fluorescence intensity not only depends on the doxorubicin concentration, it also depends on the interaction of the doxorubicin with molecules in its environment, such as the histones and the DNA [63, 64]. We assumed that, in all tumors, the doxorubicin molecules were similarly affected by the molecules in their environment.

In this study, hyperthermia was used as a trigger to release doxorubicin from ThermoDox; however, hyperthermia can also have direct effects on the tumor, such as enhancing blood flow and permeability of the vasculature [65]. These effects may also lead to increased drug concentrations [65, 66] and altered drug distribution [67-69] in the tumor. However, in this study, we used hyperthermia only in combination with ThermoDox, since hyperthermia is required for drug release by ThermoDox. In addition, in the clinic, DOX and DOXIL are mainly applied without hyperthermia.

5. CONCLUSION

At low and intermediate doses, the largest growth delay was obtained after ThermoDox treatment combined with hyperthermia, whereas at the largest investigated dose, the largest growth delay was obtained after DOXIL treatment. At each investigated dose, tumors treated with ThermoDox contained higher doxorubicin concentrations compared to DOXIL and DOX. For all formulations, at the largest dose, the spatial doxorubicin distribution was most homogeneous and the doxorubicin concentration in the tumor was the largest. On histology, tumor areas with high doxorubicin concentrations corresponded with areas with low cell proliferation. Unfortunately, no distinct relation between tumor growth and drug distribution and concentration was found. This is most likely related to changes in spatial drug distribution over time, which were not investigated in this study.

Acknowledgement

The authors would like to thank Anja van der Sar and Koen Westphal from the University Utrecht for their help with the animals and the microscopy, respectively.

REFERENCES

1. Judson I, Verweij J, Gelderblom H, Hartmann JT, Schoffski P, Blay JY, Kerst JM, Sufliarsky J, Whelan J, Hohenberger P, et al: **Doxorubicin alone versus intensified doxorubicin plus ifosfamide for first-line treatment of advanced or metastatic soft-tissue sarcoma: a randomised controlled phase 3 trial.** *Lancet Oncol* 2014, **15**:415-423.
2. Mackey JR, Martin M, Pienkowski T, Rolski J, Guastalla JP, Sami A, Glaspy J, Juhos E, Wardley A, Fornander T, et al: **Adjuvant docetaxel, doxorubicin, and cyclophosphamide in node-positive breast cancer: 10-year follow-up of the phase 3 randomised BCIRG 001 trial.** *Lancet Oncol* 2013, **14**:72-80.
3. Mutch DG, Orlando M, Goss T, Teneriello MG, Gordon AN, McMeekin SD, Wang Y, Scribner DR, Jr., Marciniack M, Naumann RW, Secord AA: **Randomized phase III trial of gemcitabine compared with pegylated liposomal doxorubicin in patients with platinum-resistant ovarian cancer.** *J Clin Oncol* 2007, **25**:2811-2818.
4. Straus DJ, Portlock CS, Qin J, Myers J, Zelenetz AD, Moskowitz C, Noy A, Goy A, Yahalom J: **Results of a prospective randomized clinical trial of doxorubicin, bleomycin, vinblastine, and dacarbazine (ABVD) followed by radiation therapy (RT) versus ABVD alone for stages I, II, and IIIA nonbulky Hodgkin disease.** *Blood* 2004, **104**:3483-3489.
5. Carvalho C, Santos RX, Cardoso S, Correia S, Oliveira PJ, Santos MS, Moreira PI: **Doxorubicin: the good, the bad and the ugly effect.** *Curr Med Chem* 2009, **16**:3267-3285.
6. Pugazhendhi A, Edison T, Velmurugan BK, Jacob JA, Karuppusamy I: **Toxicity of Doxorubicin (Dox) to different experimental organ systems.** *Life Sci* 2018, **200**:26-30.
7. Tacar O, Sriamornsak P, Dass CR: **Doxorubicin: an update on anticancer molecular action, toxicity and novel drug delivery systems.** *J Pharm Pharmacol* 2013, **65**:157-170.
8. Foote M: **The Importance of Planned Dose of Chemotherapy on Time: Do We Need to Change Our Clinical Practice?** *Oncologist* 1998, **3**:365-368.
9. Wolinsky JB, Colson YL, Grinstaff MW: **Local drug delivery strategies for cancer treatment: gels, nanoparticles, polymeric films, rods, and wafers.** *J Control Release* 2012, **159**:14-26.
10. Gabizon A, Martin F: **Polyethylene glycol coated (pegylated) liposomal doxorubicin - Rationale for use in solid tumours.** *Drugs* 1997, **54**:15-21.
11. O'Brien ME, Wigler N, Inbar M, Rosso R, Grischke E, Santoro A, Catane R, Kieback DG, Tomczak P, Ackland SP, et al: **Reduced cardiotoxicity and comparable efficacy in a phase III trial of pegylated liposomal doxorubicin HCl (CAELYX/Doxil) versus conventional doxorubicin for first-line treatment of metastatic breast cancer.** *Ann Oncol* 2004, **15**:440-449.
12. Maeda H, Wu J, Sawa T, Matsumura Y, Hori K: **Tumor vascular permeability and the EPR effect in macromolecular therapeutics: a review.** *J Control Release* 2000, **65**:271-284.
13. Charrois GJ, Allen TM: **Drug release rate influences the pharmacokinetics, biodistribution, therapeutic activity, and toxicity of pegylated liposomal doxorubicin formulations in murine breast cancer.** *Biochim Biophys Acta* 2004, **1663**:167-177.

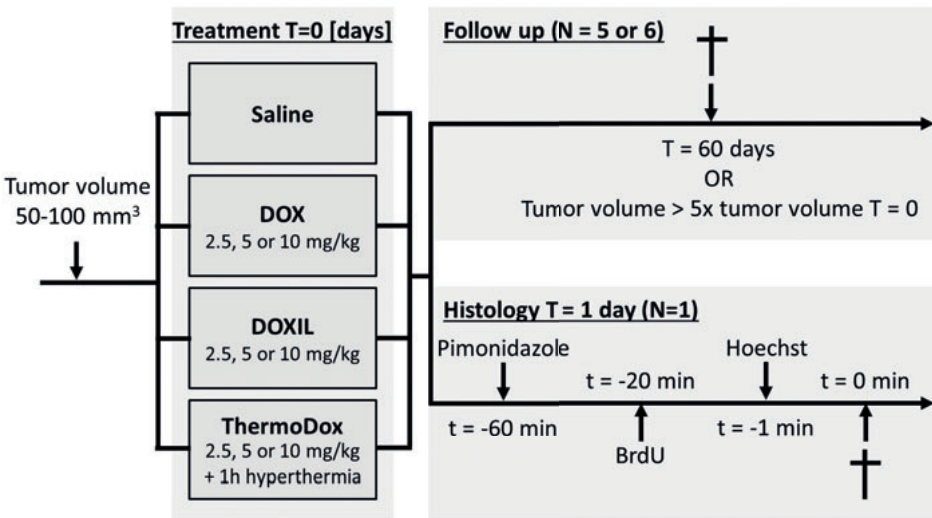
14. Barenholz Y: **Doxil(R)--the first FDA-approved nano-drug: lessons learned.** *J Control Release* 2012, **160**:117-134.
15. Gabizon A, Shmeeda H, Barenholz Y: **Pharmacokinetics of pegylated liposomal Doxorubicin: review of animal and human studies.** *Clin Pharmacokinet* 2003, **42**:419-436.
16. Papahadjopoulos D, Allen TM, Gabizon A, Mayhew E, Matthay K, Huang SK, Lee KD, Woodle MC, Lasic DD, Redemann C, et al.: **Sterically stabilized liposomes: improvements in pharmacokinetics and antitumor therapeutic efficacy.** *Proc Natl Acad Sci U S A* 1991, **88**:11460-11464.
17. Lammers T, Kiessling F, Hennink WE, Storm G: **Drug targeting to tumors: principles, pitfalls and (pre-) clinical progress.** *J Control Release* 2012, **161**:175-187.
18. Laginha KM, Verwoert S, Charrois GJ, Allen TM: **Determination of doxorubicin levels in whole tumor and tumor nuclei in murine breast cancer tumors.** *Clin Cancer Res* 2005, **11**:6944-6949.
19. Yatvin MB, Weinstein JN, Dennis WH, Blumenthal R: **Design of liposomes for enhanced local release of drugs by hyperthermia.** *Science* 1978, **202**:1290-1293.
20. Kneidl B, Peller M, Winter G, Lindner LH, Hossann M: **Thermosensitive liposomal drug delivery systems: state of the art review.** *Int J Nanomedicine* 2014, **9**:4387-4398.
21. Hijnen N, Kneepkens E, de Smet M, Langereis S, Heijman E, Grull H: **Thermal combination therapies for local drug delivery by magnetic resonance-guided high-intensity focused ultrasound.** *Proc Natl Acad Sci U S A* 2017, **114**:E4802-E4811.
22. Kong G, Anyarambhatla G, Petros WP, Braun RD, Colvin OM, Needham D, Dewhirst MW: **Efficacy of liposomes and hyperthermia in a human tumor xenograft model: importance of triggered drug release.** *Cancer Res* 2000, **60**:6950-6957.
23. Yarmolenko PS, Zhao Y, Landon C, Spasojevic I, Yuan F, Needham D, Viglianti BL, Dewhirst MW: **Comparative effects of thermosensitive doxorubicin-containing liposomes and hyperthermia in human and murine tumours.** *Int J Hyperthermia* 2010, **26**:485-498.
24. Manzoor AA, Lindner LH, Landon CD, Park JY, Simnick AJ, Dreher MR, Das S, Hanna G, Park W, Chilkoti A, et al.: **Overcoming limitations in nanoparticle drug delivery: triggered, intravascular release to improve drug penetration into tumors.** *Cancer Res* 2012, **72**:5566-5575.
25. Ranjan A, Jacobs GC, Woods DL, Negussie AH, Partanen A, Yarmolenko PS, Gacchina CE, Sharma KV, Frenkel V, Wood BJ, Dreher MR: **Image-guided drug delivery with magnetic resonance guided high intensity focused ultrasound and temperature sensitive liposomes in a rabbit Vx2 tumor model.** *J Control Release* 2012, **158**:487-494.
26. Staruch RM, Hynynen K, Chopra R: **Hyperthermia-mediated doxorubicin release from thermosensitive liposomes using MR-HIFU: therapeutic effect in rabbit Vx2 tumours.** *Int J Hyperthermia* 2015, **31**:118-133.
27. Bulbake U, Doppalapudi S, Kommineni N, Khan W: **Liposomal Formulations in Clinical Use: An Updated Review.** *Pharmaceutics* 2017, **9**.
28. Needham D, Park JY, Wright AM, Tong J: **Materials characterization of the low temperature sensitive liposome (LTSL): effects of the lipid composition (lysolipid and DSPE-PEG2000) on the thermal transition and release of doxorubicin.** *Faraday Discuss* 2013, **161**:515-534; discussion 563-589.

29. Lyon PC, Gray MD, Mannaris C, Folkes LK, Stratford M, Campo L, Chung DYF, Scott S, Anderson M, Goldin R, et al: **Safety and feasibility of ultrasound-triggered targeted drug delivery of doxorubicin from thermosensitive liposomes in liver tumours (TARDOX): a single-centre, open-label, phase 1 trial.** *Lancet Oncol* 2018, **19**:1027-1039.
30. Poon RT, Borys N: **Lyso-thermosensitive liposomal doxorubicin: a novel approach to enhance efficacy of thermal ablation of liver cancer.** *Expert Opin Pharmacother* 2009, **10**:333-343.
31. Wood BJ, Poon RT, Locklin JK, Dreher MR, Ng KK, Eugeni M, Seidel G, Dromi S, Neeman Z, Kolf M, et al: **Phase I study of heat-deployed liposomal doxorubicin during radiofrequency ablation for hepatic malignancies.** *J Vasc Interv Radiol* 2012, **23**:248-255 e247.
32. Zagar TM, Vujaskovic Z, Formenti S, Rugo H, Muggia F, O'Connor B, Myerson R, Stauffer P, Hsu IC, Diederich C, et al: **Two phase I dose-escalation/pharmacokinetics studies of low temperature liposomal doxorubicin (LTLD) and mild local hyperthermia in heavily pretreated patients with local regionally recurrent breast cancer.** *Int J Hyperthermia* 2014, **30**:285-294.
33. Tredan O, Galmarini CM, Patel K, Tannock IF: **Drug resistance and the solid tumor microenvironment.** *J Natl Cancer Inst* 2007, **99**:1441-1454.
34. Torok S, Rezeli M, Kelemen O, Vegvari A, Watanabe K, Sugihara Y, Tisza A, Marton T, Kovacs I, Tovari J, et al: **Limited Tumor Tissue Drug Penetration Contributes to Primary Resistance against Angiogenesis Inhibitors.** *Theranostics* 2017, **7**:400-412.
35. Cesca M, Morosi L, Berndt A, Fuso Nerini I, Frapolli R, Richter P, Decio A, Dirsch O, Micotti E, Giordano S, et al: **Bevacizumab-Induced Inhibition of Angiogenesis Promotes a More Homogeneous Intratumoral Distribution of Paclitaxel, Improving the Antitumor Response.** *Mol Cancer Ther* 2016, **15**:125-135.
36. van Herpen CM, Bussink J, van der Kogel AJ, Peeters WJ, van der Voort R, van Schijndel A, de Wilde PC, Adema GJ, de Mulder PH: **Interleukin-12 has no effect on vascular density, perfusion, hypoxia and proliferation of an implanted human squamous cell carcinoma xenograft tumour despite up-regulation of ICAM-1.** *Anticancer Res* 2005, **25**:1015-1021.
37. Kascakova S, de Visscher S, Kruijt B, de Bruijn HS, van der Ploeg-van den Heuvel A, Sterenborg HJ, Witjes MJ, Amelink A, Robinson DJ: **In vivo quantification of photosensitizer fluorescence in the skin-fold observation chamber using dual-wavelength excitation and NIR imaging.** *Lasers Med Sci* 2011, **26**:789-801.
38. Rijken PF, Bernsen HJ, van der Kogel AJ: **Application of an image analysis system to the quantitation of tumor perfusion and vascularity in human glioma xenografts.** *Microvasc Res* 1995, **50**:141-153.
39. Primeau AJ, Rendon A, Hedley D, Lilge L, Tannock IF: **The distribution of the anticancer drug Doxorubicin in relation to blood vessels in solid tumors.** *Clin Cancer Res* 2005, **11**:8782-8788.
40. Li L, ten Hagen TL, Hossann M, Suss R, van Rhoon GC, Eggermont AM, Haemmerich D, Koning GA: **Mild hyperthermia triggered doxorubicin release from optimized stealth thermosensitive liposomes improves intratumoral drug delivery and efficacy.** *J Control Release* 2013, **168**:142-150.

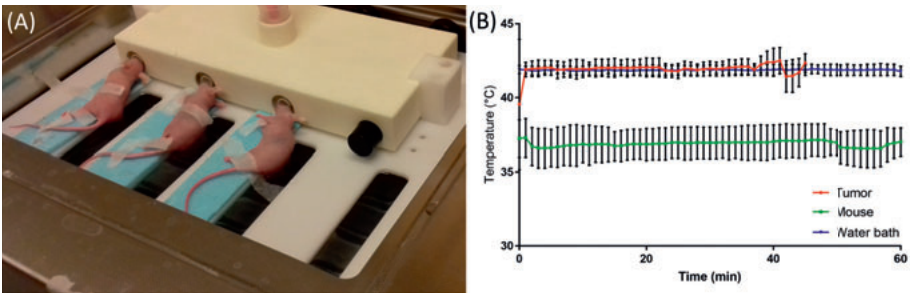
41. Lokerse WJ, Kneepkens EC, ten Hagen TL, Eggermont AM, Grull H, Koning GA: **In depth study on thermosensitive liposomes: Optimizing formulations for tumor specific therapy and in vitro to in vivo relations.** *Biomaterials* 2016, **82**:138-150.
42. Vaage J, Donovan D, Mayhew E, Abra R, Huang A: **Therapy of human ovarian carcinoma xenografts using doxorubicin encapsulated in sterically stabilized liposomes.** *Cancer* 1993, **72**:3671-3675.
43. Needham D, Anyarambhatla G, Kong G, Dewhirst MW: **A new temperature-sensitive liposome for use with mild hyperthermia: characterization and testing in a human tumor xenograft model.** *Cancer Res* 2000, **60**:1197-1201.
44. Zhang F, Zhu L, Liu G, Hida N, Lu G, Eden HS, Niu G, Chen X: **Multimodality imaging of tumor response to doxil.** *Theranostics* 2011, **1**:302-309.
45. Giordano S, Zucchetti M, Decio A, Cesca M, Fuso Nerini I, Maiezza M, Ferrari M, Licandro SA, Frapolli R, Giavazzi R, et al: **Heterogeneity of paclitaxel distribution in different tumor models assessed by MALDI mass spectrometry imaging.** *Sci Rep* 2016, **6**:39284.
46. Kyle AH, Baker JH, Gandolfo MJ, Reinsberg SA, Minchinton AI: **Tissue penetration and activity of camptothecins in solid tumor xenografts.** *Mol Cancer Ther* 2014, **13**:2727-2737.
47. Derieppe M, Escoffre JM, Denis de Senneville B, van Houtum Q, Rijbroek AB, van der Wurff-Jacobs K, Dubois L, Bos C, Moonen C: **Assessment of Intratumoral Doxorubicin Penetration after Mild Hyperthermia-Mediated Release from Thermosensitive Liposomes.** *Contrast Media Mol Imaging* 2019, **2019**:2645928.
48. Baker JHE, Kyle AH, Reinsberg SA, Moosvi F, Patrick HM, Cran J, Saatchi K, Hafeli U, Minchinton AI: **Heterogeneous distribution of trastuzumab in HER2-positive xenografts and metastases: role of the tumor microenvironment.** *Clin Exp Metastasis* 2018, **35**:691-705.
49. Ekdawi SN, Stewart JM, Dunne M, Stapleton S, Mitsakakis N, Dou YN, Jaffray DA, Allen C: **Spatial and temporal mapping of heterogeneity in liposome uptake and microvascular distribution in an orthotopic tumor xenograft model.** *J Control Release* 2015, **207**:101-111.
50. Just N: **Improving tumour heterogeneity MRI assessment with histograms.** *Br J Cancer* 2014, **111**:2205-2213.
51. Natrajan R, Sailem H, Mardakheh FK, Arias Garcia M, Tape CJ, Dowsett M, Bakal C, Yuan Y: **Microenvironmental Heterogeneity Parallels Breast Cancer Progression: A Histology-Genomic Integration Analysis.** *PLoS Med* 2016, **13**:e1001961.
52. Gabizon A, Tzemach D, Mak L, Bronstein M, Horowitz AT: **Dose dependency of pharmacokinetics and therapeutic efficacy of pegylated liposomal doxorubicin (DOXIL) in murine models.** *J Drug Target* 2002, **10**:539-548.
53. Bartelink IH, Prideaux B, Krings G, Wilmes L, Lee PRE, Bo P, Hann B, Coppe JP, Heditsian D, Swigart-Brown L, et al: **Heterogeneous drug penetrance of veliparib and carboplatin measured in triple negative breast tumors.** *Breast Cancer Res* 2017, **19**:107.
54. Fuso Nerini I, Morosi L, Zucchetti M, Ballerini A, Giavazzi R, D'Incalci M: **Intratumor heterogeneity and its impact on drug distribution and sensitivity.** *Clin Pharmacol Ther* 2014, **96**:224-238.
55. Rhoden JJ, Wittrup KD: **Dose dependence of intratumoral perivascular distribution of monoclonal antibodies.** *J Pharm Sci* 2012, **101**:860-867.

56. Minchinton AI, Tannock IF: **Drug penetration in solid tumours.** *Nat Rev Cancer* 2006, **6**:583-592.
57. Moulder JE, Rockwell S: **Hypoxic fractions of solid tumors: experimental techniques, methods of analysis, and a survey of existing data.** *Int J Radiat Oncol Biol Phys* 1984, **10**:695-712.
58. Rijken PF, Bernsen HJ, Peters JP, Hodgkiss RJ, Raleigh JA, van der Kogel AJ: **Spatial relationship between hypoxia and the (perfused) vascular network in a human glioma xenograft: a quantitative multi-parameter analysis.** *Int J Radiat Oncol Biol Phys* 2000, **48**:571-582.
59. Rijken PF, Peters JP, Van der Kogel AJ: **Quantitative analysis of varying profiles of hypoxia in relation to functional vessels in different human glioma xenograft lines.** *Radiat Res* 2002, **157**:626-632.
60. Heinke J, Kerber M, Rahner S, Mnich L, Lassmann S, Helbing T, Werner M, Patterson C, Bode C, Moser M: **Bone morphogenetic protein modulator BMPER is highly expressed in malignant tumors and controls invasive cell behavior.** *Oncogene* 2012, **31**:2919-2930.
61. Qayum N, Muschel RJ, Im JH, Balathasan L, Koch CJ, Patel S, McKenna WG, Bernhard EJ: **Tumor vascular changes mediated by inhibition of oncogenic signaling.** *Cancer Res* 2009, **69**:6347-6354.
62. Vaage J, Donovan D, Uster P, Working P: **Tumour uptake of doxorubicin in polyethylene glycol-coated liposomes and therapeutic effect against a xenografted human pancreatic carcinoma.** *Br J Cancer* 1997, **75**:482-486.
63. Lee RJ, Low PS: **Folate-mediated tumor cell targeting of liposome-entrapped doxorubicin in vitro.** *Biochim Biophys Acta* 1995, **1233**:134-144.
64. Mohan P, Rapoport N: **Doxorubicin as a Molecular Nanotheranostic Agent: Effect of Doxorubicin Encapsulation in Micelles or Nanoemulsions on the Ultrasound-Mediated Intracellular Delivery and Nuclear Trafficking.** *Molecular Pharmaceutics* 2010, **7**:1959-1973.
65. Hildebrandt B, Wust P, Ahlers O, Dieing A, Sreenivasa G, Kerner T, Felix R, Riess H: **The cellular and molecular basis of hyperthermia.** *Crit Rev Oncol Hematol* 2002, **43**:33-56.
66. Song CW: **Effect of local hyperthermia on blood flow and microenvironment: a review.** *Cancer Res* 1984, **44**:4721s-4730s.
67. Ariffin AB, Forde PF, Jahangeer S, Soden DM, Hinchion J: **Releasing Pressure in Tumors: What Do We Know So Far and Where Do We Go from Here ? A Review.** *Cancer Res* 2014, **74**:2655-2662.
68. Kong G, Dewhirst MW: **Hyperthermia and liposomes.** *Int J Hyperthermia* 1999, **15**:345-370.
69. Matteucci ML, Anyarambhatla G, Rosner G, Azuma C, Fisher PE, Dewhirst MW, Needham D, Thrall DE: **Hyperthermia increases accumulation of technetium-99m-labeled liposomes in feline sarcomas.** *Clin Cancer Res* 2000, **6**:3748-3755.

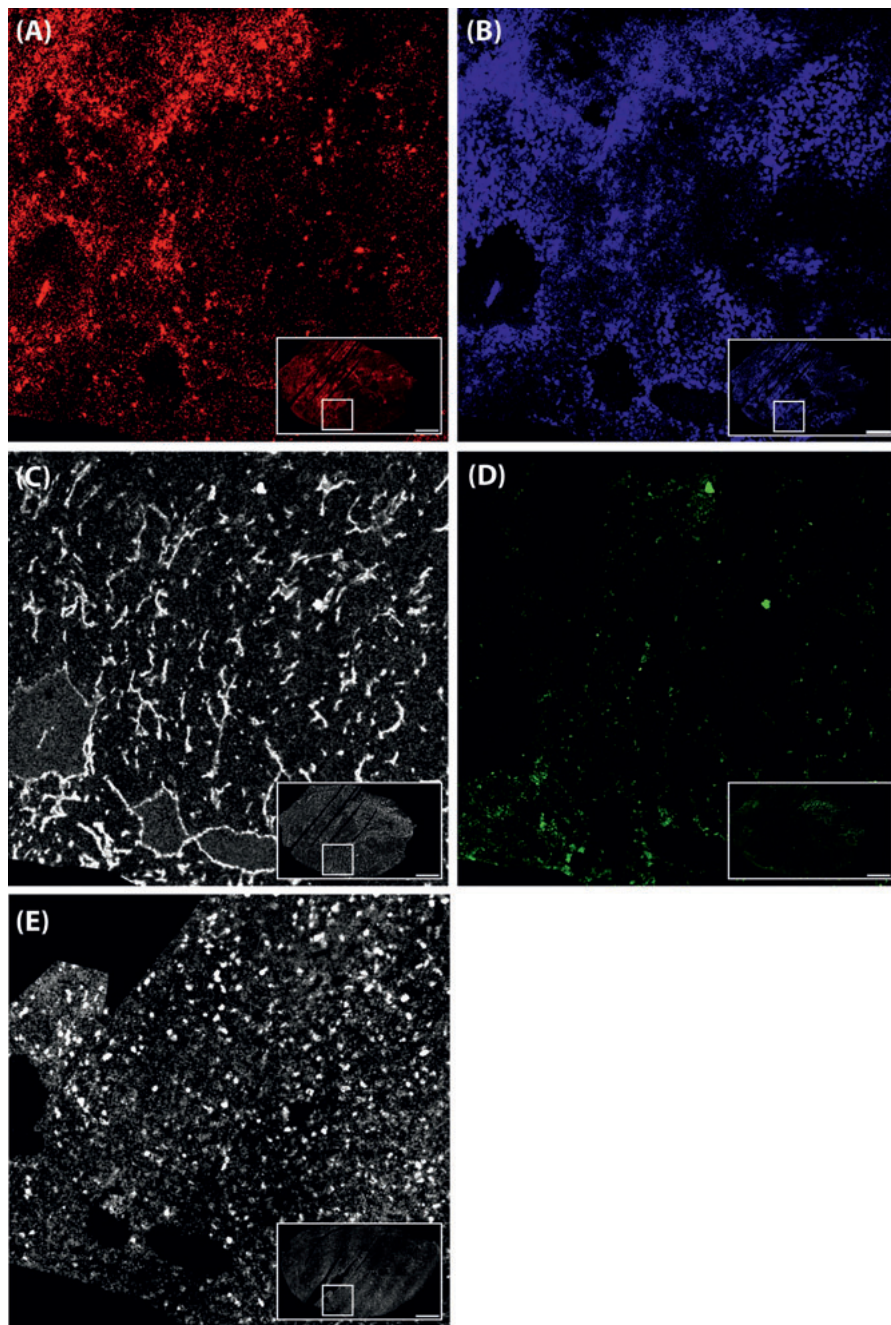
SUPPLEMENTARY INFORMATION



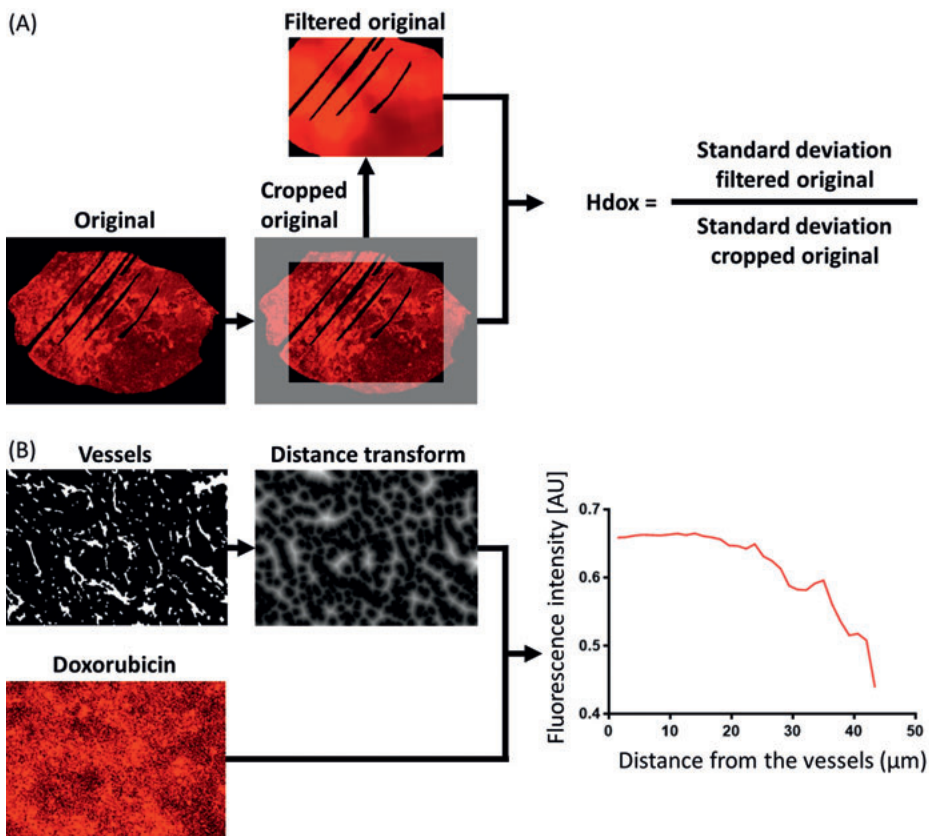
Supplementary Figure 1. Experimental timeline of the experiments Experimental timeline of the experiments. Mice with tumor volumes between 50 and 100 mm³ were treated with saline, DOX, DOXIL or ThermoDox at a dose of 2.5, 5 or 10 mg/kg. Only after ThermoDox administration tumors were treated for 1 hour with hyperthermia. Subsequently, mice were used to study the efficacy or to study the doxorubicin distribution 24 hours after treatment.



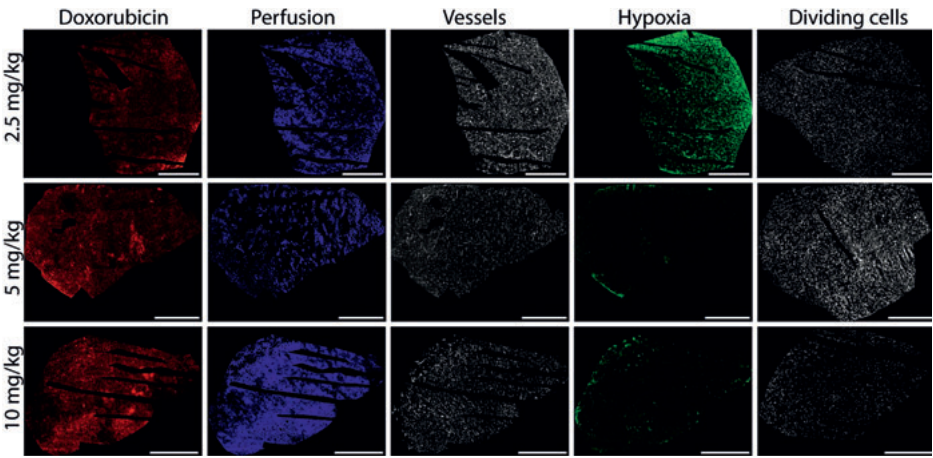
Supplementary Figure 2. Hyperthermia setup Hyperthermia setup. A photo of the hyperthermia setup (A) and temperature measurements of tumor (N = 4), mouse (core) (N = 5) and water bath (N = 5) during hyperthermia treatment up to 60 minutes (B).



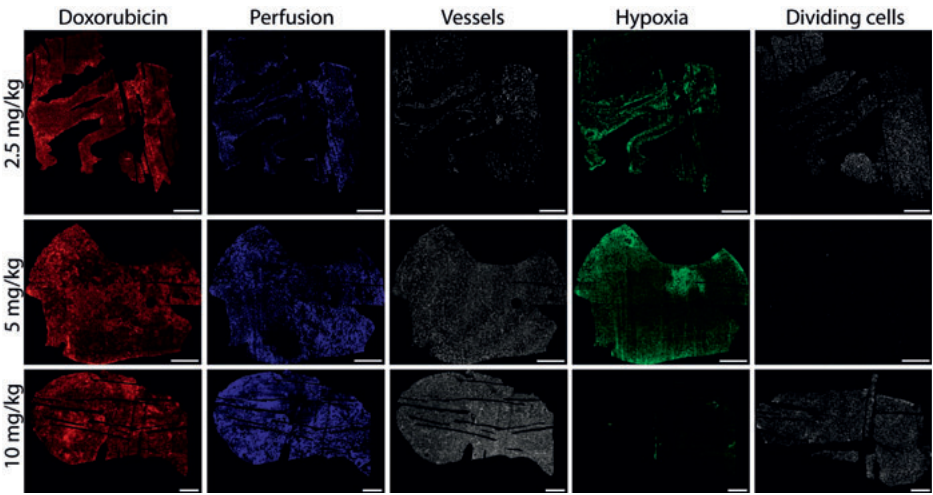
Supplementary Figure 3. Total tumor and zoomed in detail of the stainings of the tumor treated with 5 mg/kg ThermoDox; doxorubicin (A), Perfusion (B), All vessels (C), hypoxia (D) and dividing cells (E). The scale bar in the total tumor represents 1 mm. The size of the zoom is 1.43x1.43 mm.



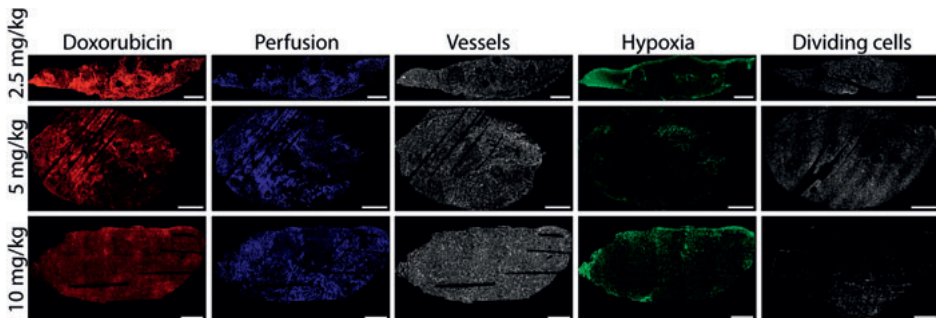
Supplementary Figure 4. Calculations of Hdox over the whole tumor and doxorubicin intensity in relation to the perfused vessels Hdox (A) was calculated by cropping the original image, subsequently the cropped image was filtered and the ratio of the standard deviation of the filtered image and cropped image was calculated. The doxorubicin intensity in relation to the vessels (B) was calculated by converting the perfused vessel mask to a distance map, and then combining the distance map and doxorubicin image to obtain the average fluorescence intensity as a function of the distance from the perfused vessels.



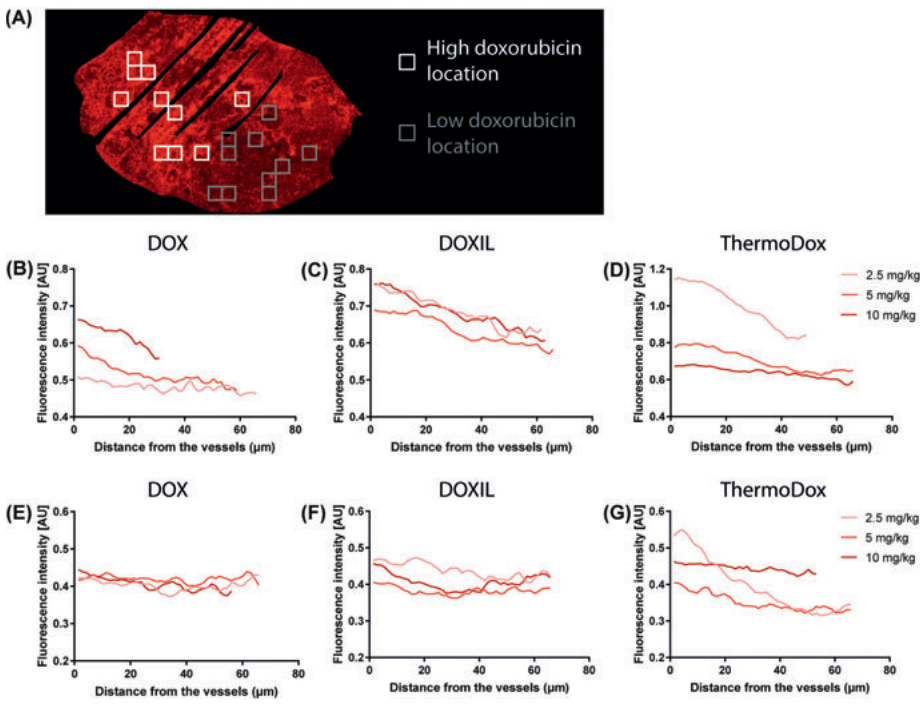
Supplementary Figure 5. Different stainings of tumors treated with DOX of 2.5, 5 and 10 mg/kg Tumors stained for doxorubicin, perfusion, all vessels, hypoxia and proliferating cells. The scale bar is 1 mm.



Supplementary Figure 6. Different stainings of tumors treated with DOXIL of 2.5, 5 and 10 mg/kg Tumors stained for doxorubicin, perfusion, all vessels, hypoxia and proliferating cells. The scale bar is 1 mm.



Supplementary Figure 7. Different stainings of tumors treated with ThermoDox of 2.5, 5 and 10 mg/kg Tumors stained for doxorubicin, perfusion, all vessels, hypoxia and proliferating cells. The scale bar is 1 mm.



Supplementary Figure 8. Doxorubicin intensity relative to the perfused vessels in locations with high and low doxorubicin intensities Doxorubicin intensity relative to the perfused vessels in locations with high and low doxorubicin intensities. Locations with high and low doxorubicin intensities were selected in each tumor (A). Doxorubicin intensities relative to the vessels in areas with high doxorubicin intensities after DOX (B), DOXIL (C) and ThermoDox (D) treatment and doxorubicin intensities relative to the vessels in areas with low doxorubicin intensities after DOX (E), DOXIL (F) and ThermoDox (G) treatment.

CHAPTER 4

Modular synthesis of self-immolative doxorubicin prodrugs with rapid enzymatic activation upon ultrasound-mediated mechanical cell destruction

Helena C. Besse[‡]
Karolin Roemhild[‡]
Bi Wang[‡]
Qingxue Sun
Daiki Omata
Burcin Ozbakir
Clemens Bos
Hans W. Scheeren
Gert Storm
Fabian Kiessling
Chrit T.W. Moonen
Twan Lammers*
Roel Deckers*
Yang Shi*

[‡] These authors contributed equally

*These authors contributed equally

Submitted

ABSTRACT

Prodrug chemistry is widely employed in drug design and development, for which rapid and efficient prodrug activation is highly desired. We hypothesize that for enzyme-activated self-immolative prodrugs, prolonging the spacer between the capping group and the drug molecule is an effective strategy to realize rapid prodrug activation. We here describe a high-yield approach to synthesize glucuronide-capped self-immolative doxorubicin prodrugs, which strategically prevented basic hydrolysis of doxorubicin. The prepared prodrugs have varying lengths of the spacer with different numbers of aromatic units. Our results show that prolonging the spacer from 1 to 2 or 3 aromatic units led to highly accelerated prodrug activation by β -glucuronidase (e.g. >10 times faster at pH 7.4). We furthermore show that clinically relevant high-intensity focused ultrasound protocols can be employed to mechanically destroy cancer cells, resulting in the release of β -glucuronidase, activation of the prodrug, potentiation of cytotoxicity and calreticulin translocation (i.e. immunogenic cell death induction). Together, the prodrug chemistry and ultrasound methodology presented here may help to pave the way for improved anti-cancer mechano-chemo-immunotherapy.

Prodrug chemistry has been widely utilized for several decades to convert drugs to precursors which release the native drugs by chemical, physical and enzymatic triggers [1]. Among the different categories of prodrugs, self-immolative prodrugs are attractive due to several advantages, including tunable activation kinetics [2]. Self-immolative prodrugs are covalent and sequential assemblies of the drug molecule, self-immolative spacer and capping group. Following removal of the capping group, the spacer is cleaved via self-immolation, leading to the release of the native drug molecule. Such spacers are typically degraded via elimination [3-7] or cyclization [8, 9], with the former being faster [2]. For elimination-mediated self-immolation, spacers are commonly based on aromatic structures substituted with nucleophilic groups such as hydroxy, amine and thiol. To achieve fast prodrug activation, efforts have been made to modify the aromatic groups [10] or change the substitution positions of the aromatic groups [11]. These strategies, however, tend to complicate the prodrug synthesis processes.

To activate self-immolative prodrugs, chemical, physical and enzymatic stimuli have been evaluated to remove the capping groups. Enzymes, such as β -glucuronidase (β -GUS), are highly interesting in this context, since their extracellular availability is frequently associated with cancer development and progression, enabling site-specific prodrug activation [12]. Unfortunately, the extracellular enzyme levels are often too low to induce rapid and efficient prodrug activation. To tackle this problem, gene-directed, virus-directed and antibody-directed enzyme prodrug therapies have been evaluated to enhance extracellular enzyme levels in tumors. These strategies, however, have shown relatively limited success, and their immunogenicity and safety concerns have compromised their *in vivo* applicability [13, 14]. Consequently, safe, efficient and potentially clinically translatable strategies to enhance extracellular enzyme levels for prodrug therapy are highly desired.

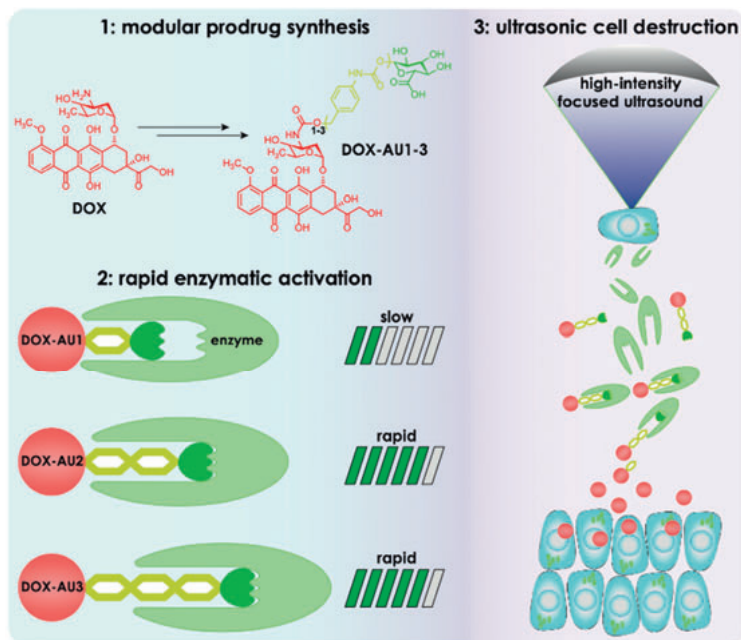
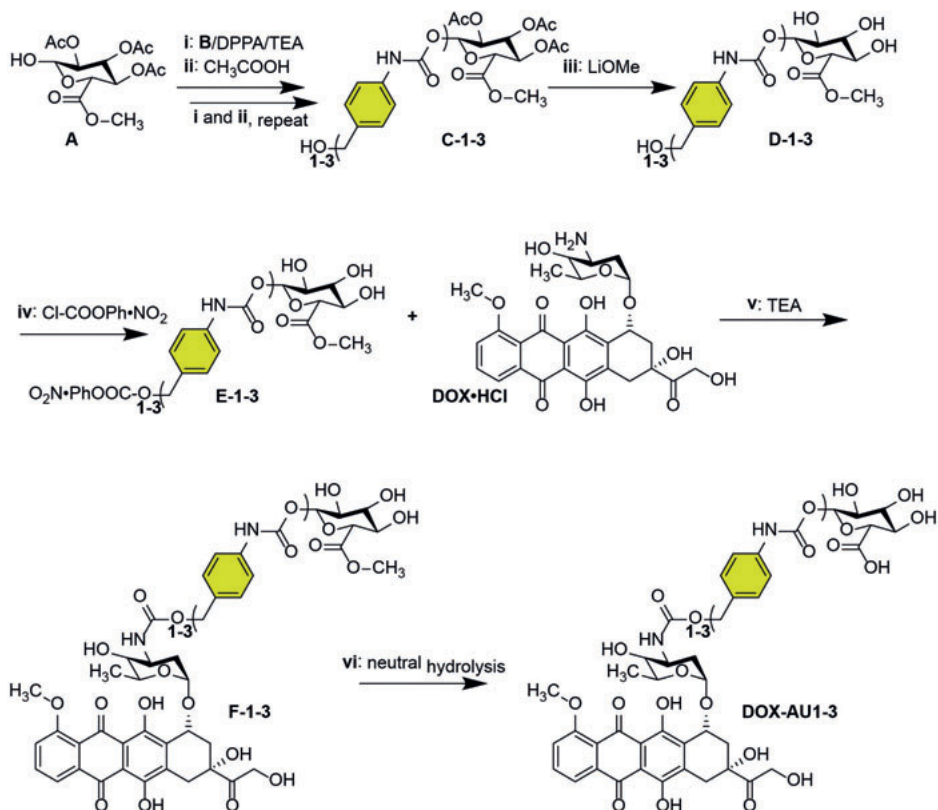


Figure 1. Schematic illustration of DOX prodrug synthesis (1), enabling fast and efficient enzymatic activation by prolonging the length of the self-immolative spacer (2), and the use of HIFU to mechanically destroy cancer cells to release β -GUS for DOX prodrug activation (3).

We here describe a combinatorial chemico-physical strategy to achieve fast and efficient activation of self-immolative doxorubicin (DOX) prodrugs capped by glucuronide. This activation is realized by β -GUS released from cancer cells upon high-intensity focused ultrasound (HIFU)-mediated mechanical destruction. Since the removal of the capping group is generally considered to be the rate-limiting step for self-immolative prodrug activation [2], we hypothesized that prolonging the length of the self-immolative spacer effectively facilitates enzymatic digestion of the capping group and thereby prodrug activation.



Scheme 1. Synthesis strategy for glucuronide-capped self-immolative prodrugs of DOX with 1-3 aromatic units (colored in yellow) in the spacer (DOX-AU1-3).

We developed a novel strategy to synthesize self-immolative DOX prodrugs which have increasing numbers of aromatic units to prolong the length of the spacer (Scheme 1). To this end, glucuronic acid methyl ester with 2,3,4-hydroxy groups protected with acetyl (**A**) was coupled to 4-(hydroxymethyl) benzoic acid with the hydroxy group protected by tert-butyldimethylsilyl chloride (TBDMSCl, **B**), via a carbamate bond (i). Subsequently, the TBDMS-protected hydroxy group was deprotected by CH_3COOH (ii) to yield the spacer (**C-1**) with 1 aromatic unit (colored in yellow) and a free hydroxy group. Step i and ii were repeated to prepare spacers with 2 or 3 aromatic units (in **C-2** and **C-3**, respectively). After incorporating the desired number of aromatic units in the spacer, the acetyl-protected glucuronide hydroxy groups of **C-1-3** were deprotected by LiOMe (iii). Afterwards, the hydroxy group linked to the aromatic unit was selectively activated by 4-nitrophenyl chloroformate ($\text{Cl-COOPh}\cdot\text{NO}_2$) to afford **E-1-3** (iv), which was coupled with the amine group

of DOX via a carbamate bond (v). Then, the methyl ester of the glucuronide moiety was removed by neutral hydrolysis in a mixture of phosphate-buffered saline at pH 7.4 and dimethyl sulfoxide (1/1, v/v) at 37°C (vi), yielding DOX prodrugs with 1-3 aromatic units in the self-immolative spacer (i.e. DOX-AU1-3; see Supporting Information).

We successfully synthesized DOX prodrugs containing self-immolative spacers with different lengths, using a new approach which is compatible with the base-labile drug DOX. It should be noted that the synthesis of self-immolative DOX prodrugs has been a long-standing challenge [15-18], because DOX is easily decomposed under the basic conditions needed for the final deprotection of sugar hydroxy and carboxyl ester groups. This led to the formation of multiple side products, difficulties in purification and low yields. Alternative solutions, such as replacing the acetyl protection groups with allyl groups for deprotection by palladium catalysts under weak basic conditions, were proposed [19-21]. However, also in this case, low yields were reported [21]. Our approach avoids DOX decomposition by bases and the use of palladium catalysts. Instead, we developed a relatively “green” approach, using a neutral aqueous solution at pH 7.4 for the final glucuronide ester deprotection, with easy purification and high yields (70-80%). The unique features of our approach also include the deprotection of the glucuronide hydroxy groups under basic conditions early on before DOX is conjugated (iii), followed by the site-specific activation of the hydroxy group of the aromatic unit by Cl-COOPh•NO₂ (iv) for DOX conjugation. Our protocol thus has fewer steps (i.e. no introduction and deprotection of allyl groups) and uses greener chemistry (i.e. no palladium catalysts), and it can also be adopted for synthesizing self-immolative prodrugs of other base-labile drugs, such as taxanes [22].

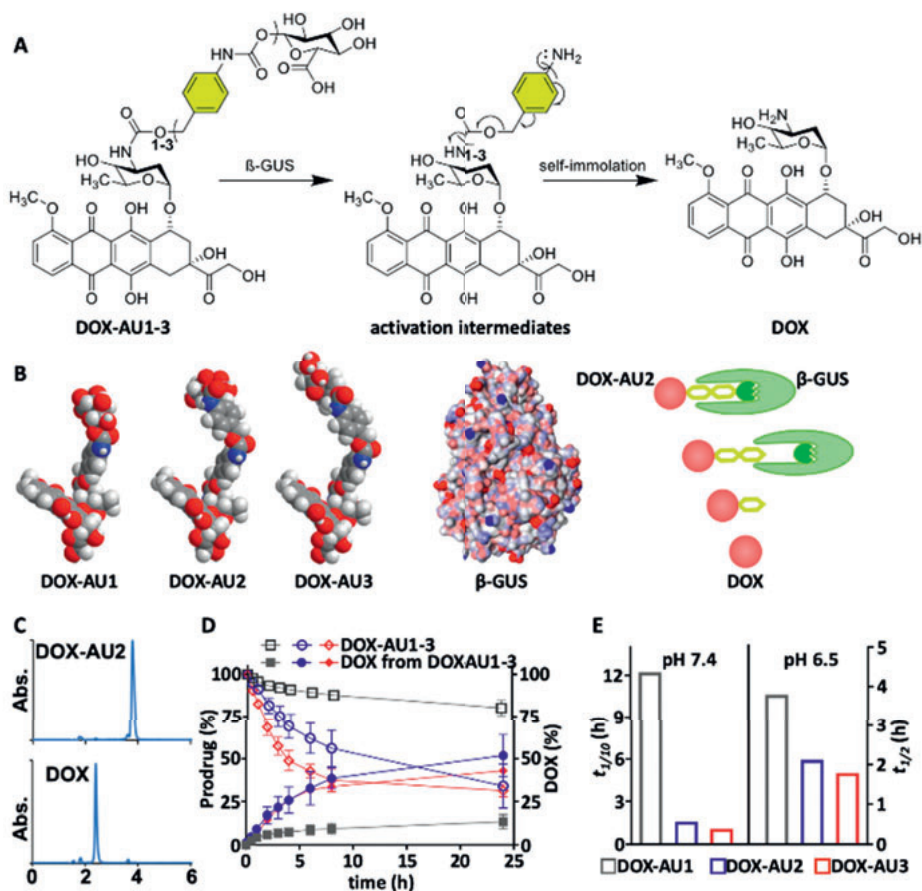


Figure 2. Enzymatic activation of the DOX prodrugs. (A) β -GUS-mediated conversion of DOX-AU1-3 to DOX. β -GUS digests the glucuronide moiety of the prodrugs, which is followed by self-immolation of the spacer via elimination of the aromatic units to release DOX. (B) By increasing the length of the spacer via adding more aromatic units, the glucuronide moiety (top) is better separated from DOX (bottom). This reduces steric hindrance and facilitates entry of the glucuronide moiety to the catalytic pocket of β -GUS. With a longer spacer, the prodrug is more easily activated by β -GUS. (C) HPLC chromatograms of DOX-AU2 and DOX generated after activation. (D) Kinetics of the degradation of DOX-AU1-3 and of DOX generation from the corresponding prodrugs upon β -GUS exposure at pH 7.4 and 37°C. The activation of the prodrugs was significantly faster when employing self-immolative spacers containing more than one aromatic unit. (E) The time needed to reach 10% ($t_{1/10}$) of DOX generation at pH 7.4 and 50% ($t_{1/2}$) of DOX generation at pH 6.5 for the prodrugs. Due to the very slow activation of DOX-AU1 at pH 7.4, the time needed for 10% DOX generation was used to compare the rate of prodrug activation.

The newly generated DOX prodrugs (i.e. DOX-AU1-3) have a glucuronide capping group, which can be specifically hydrolyzed by β -GUS [23, 24] to trigger the self-immolation of the spacer to release DOX (Figure 2A). Since the enzyme-mediated de-capping of the spacer is generally considered to be the rate-limiting step (NB: the self-immolation process is typically much faster), prolonging the spacer is hypothesized to promote prodrug activation, via reducing steric hindrance to facilitate the entrance of the glucuronide group into the catalytic pocket of β -GUS for hydrolysis [25] (Figure 2B). To verify this hypothesis, we assessed the activation kinetics of DOX-AU1-3 *in vitro* in the presence of β -GUS at 37°C and at two pH values (i.e. 7.4 and 6.5, representing relevant pH's in the tumor microenvironment). The degradation of the prodrugs and the generation of DOX were quantified by high-performance liquid chromatography (HPLC, Figure 2C). Intermediates of prodrug activation were not detected by HPLC, which suggests that the self-immolation of the spacer is a very rapid process and is highly unlikely to be the rate-limiting step in prodrug activation.

Quantitative HPLC analysis showed that the amount of prodrug activated by the enzyme at pH 7.4 correlated well to that of DOX generated (Figure 2D). Importantly, the activation of the prodrugs and the generation of DOX were significantly faster by prolonging the spacer from one aromatic unit (DOX-AU1) to two and three units (i.e. DOX-AU2 and DOX-AU3, Figure 2D). At pH 7.4, since the DOX-AU1 activation was extremely slow, we calculated the time to reach 10% DOX generation (i.e., $t_{1/10}$ instead of commonly used $t_{1/2}$) to compare the kinetics of enzymatic activation. The results show that DOX generation from both DOX-AU2 and DOX-AU3 in the presence of β -GUS was ~10 times faster than that of DOX-AU1 (1-1.5h versus ~12 h), and that the difference between DOX-AU2 and DOX-AU3 was marginal. A parallel study at pH 6.5 confirmed the much faster generation of DOX from DOX-AU2 and DOX-AU3 as compared to DOX-AU1 (Figure 2E). Overall, these observations confirm our hypothesis that the enzymatic activation of self-immolative prodrugs can be significantly accelerated by prolonging the spacer. This finding may be useful for the design of other enzyme-triggered prodrugs. For subsequent studies, DOX-AU2 was chosen, because of its faster activation than DOX-AU1 and the fewer steps of synthesis as compared to DOX-AU3.

We subsequently sought to demonstrate that the activation of DOX-AU2 can be enabled by ultrasound (US)-induced mechanical cell destruction, which is known to liberate β -GUS from cancer cells (Figure 3A). Since under homeostatic

conditions, β -GUS is almost exclusively located intracellularly in endosomes and lysosomes [26], its extracellular concentration in tissues, e.g., in tumors, is typically very low. To trigger β -GUS release, we exposed 4T1 triple negative breast cancer cells to HIFU. After 10 min of exposure to mechanically destructive US treatment at a peak-negative pressure 41 MPa, the cells were completely destroyed, as confirmed by microscopy (Figure 3B). Analysis of the release of bioactive β -GUS from the cells using the 4-methyl-umbelliferyl- β -D-glucuronide (MUG) assay showed that untreated cells did not present β -GUS activity extracellularly, while US exposure resulted in efficient release of β -GUS into the medium, reaching similar levels as observed for cells lysed by 3 cycles of freeze-thaw treatment (i.e. positive control; Figure 3C). Furthermore, US-mediated mechanical cell destruction occurred very rapidly and the maximal amount of β -GUS release was observed within 10 min (Figure 3D). It is important to note that the mechanical US treatment employed here, in contrast thermal US ablation used more commonly in clinics [27, 28], did not elevate the temperature. This is crucial for preserving enzymatic activity of β -GUS (supporting information, Supplementary Figure 1 and 2). Furthermore, mechanical US may also induce therapeutic synergism with prodrug chemotherapy by its ability to provoke immunoactivation against tumors [29, 30].

Finally, we studied the effect of US-induced β -GUS release and DOX-AU2 prodrug activation on cytotoxicity and on calreticulin translocation in 4T1 cells. Mechanical US destruction of 4T1 cells was performed at 41 MPa peak-negative pressure for 10 min. The obtained cell lysate was used to activate DOX-AU2 at 37°C. The activation of DOX-AU2 and the generation of parental DOX were monitored by HPLC, which confirmed the efficient conversion of the prodrug (Figure 3E). To assess the cytotoxicity of the prodrug in the presence of β -GUS, the US-treated cell lysate was mixed with the prodrug and the mixture was added to 4T1 cells cultured in well plates *in vitro*. As shown in Figure 3F, DOX-AU2 combined with US-disintegrated cells induced a comparable level of cytotoxicity in 4T1 cells as the native drug DOX (IC_{50} =0.94 and 1.07 μ M, respectively), and it was more potent than the prodrug without US-treated cell lysate (IC_{50} =3.04 μ M). This confirms efficient activation of the prodrug. Furthermore, since DOX is a potent inducer of immunogenic cell death (ICD, a mechanism which helps to induce anti-tumor immune responses [31]), we also examined the ability of activated DOX-AU2 to trigger calreticulin translocation in 4T1 cells, which is a key phenotype of ICD [32]. 4T1 cells treated with US-activated DOX-AU2 were shown to have significantly more calreticulin translocation as compared to controls (Figure 3H).

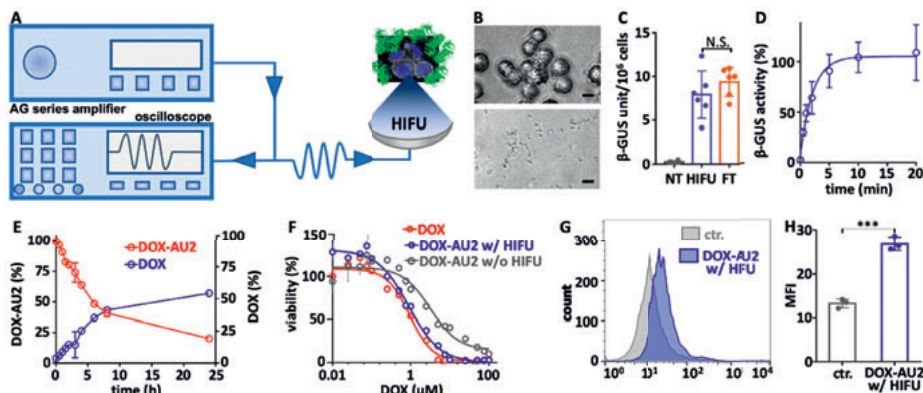


Figure 3. Ultrasound-induced mechanical cell destruction and β -GUS release for prodrug activation. (A) Schematic depiction of a HIFU setup composed of a series amplifier and an oscilloscope. The ultrasound (US) energy is spatially focused by a transducer, which can mechanically destroy tumor cells to release intracellular β -GUS for prodrug activation. (B) Microscopic images of 4T1 cells that underwent US treatment. The cells (upper image) were completely destroyed upon treatment (lower image) for 10 min at 41 MPa peak-negative pressure. (C) Bioactivity of β -GUS released from the cells by US as assessed by the MUG assay. Non-treated (NT) cells did not express significant extracellular β -GUS and the positive control with 3 cycles of freeze-thaw treatment released similar amounts of β -GUS as US treatment. (D) Release kinetics of β -GUS from 4T1 cells upon US treatment for up to 20 min, showing that maximal release of the enzyme was achieved in 10 min. (E) DOX-AU2 activation and DOX generation by β -GUS released from US-treated cells. (F) Cytotoxicity of DOX-AU2 in 4T1 cells with and without β -GUS released from US-treated cells. The prodrug with US-treated cells exhibited similar cytotoxicity as native DOX. (G-H) Flow cytometry analysis of calreticulin translocation in 4T1 cells treated with DOX-AU2 activated by US-released β -GUS, showing that significant amounts of calreticulin were translocated to outer surface of cell membrane, indicating the induction of immunogenic cell death.

Taken together, we established a modular and high-yield synthesis strategy for β -glucuronidase-activated self-immolative doxorubicin prodrugs. Our results demonstrated that increasing the spacer length in self-immolative prodrug designs can improve therapeutic performance, and they provide a proof-of-concept for the chemical engineering of prodrugs that can be activated by US-mediated mechanical cell destruction. Such strategies hold promise for assisting in improving the therapeutic index of traditional chemotherapy as well as for boosting the efficacy of (US-enhanced) chemo-immunotherapy regimens.

REFERENCES

1. Kratz F, Muller IA, Ryppa C, Warnecke A: **Prodrug strategies in anticancer chemotherapy.** *ChemMedChem* 2008, **3**:20-53.
2. Alouane A, Labruere R, Le Saux T, Schmidt F, Jullien L: **Self-immolative spacers: kinetic aspects, structure-property relationships, and applications.** *Angew Chem Int Ed Engl* 2015, **54**:7492-7509.
3. de Groot FM, Albrecht C, Koekkoek R, Beusker PH, Scheeren HW: **"Cascade-release dendrimers" liberate all end groups upon a single triggering event in the dendritic core.** *Angew Chem Int Ed Engl* 2003, **42**:4490-4494.
4. Shamis M, Lode HN, Shabat D: **Bioactivation of self-immolative dendritic prodrugs by catalytic antibody 38C2.** *J Am Chem Soc* 2004, **126**:1726-1731.
5. Legigan T, Clarhaut J, Tranoy-Opalinski I, Monvoisin A, Renoux B, Thomas M, Le Pape A, Lerondel S, Papot S: **The first generation of beta-galactosidase-responsive prodrugs designed for the selective treatment of solid tumors in prodrug monotherapy.** *Angew Chem Int Ed Engl* 2012, **51**:11606-11610.
6. Jarlstad Olesen MT, Walther R, Poier PP, Dagnaes-Hansen F, Zelikin AN: **Molecular, Macromolecular, and Supramolecular Glucuronide Prodrugs: Lead Identified for Anticancer Prodrug Monotherapy.** *Angew Chem Int Ed Engl* 2020, **59**:7390-7396.
7. Wang B, Van Herck S, Chen Y, Bai X, Zhong Z, Deswarte K, Lambrecht BN, Sanders NN, Lienenklaus S, Scheeren HW, et al: **Potent and Prolonged Innate Immune Activation by Enzyme-Responsive Imidazoquinoline TLR7/8 Agonist Prodrug Vesicles.** *J Am Chem Soc* 2020, **142**:12133-12139.
8. Dewit MA, Gillies ER: **A cascade biodegradable polymer based on alternating cyclization and elimination reactions.** *J Am Chem Soc* 2009, **131**:18327-18334.
9. Grether U, Waldmann H: **An Enzyme-Labile Safety Catch Linker for Combinatorial Synthesis on a Soluble Polymeric Support This work was supported by the Bundesministerium fur Bildung und Forschung and BASF AG.** *Angew Chem Int Ed Engl* 2000, **39**:1629-1632.
10. Robbins JS, Schmid KM, Phillips ST: **Effects of electronics, aromaticity, and solvent polarity on the rate of azaquinone-methide-mediated depolymerization of aromatic carbamate oligomers.** *J Org Chem* 2013, **78**:3159-3169.
11. Perry-Feigenbaum R, Baran PS, Shabat D: **The pyridinone-methide elimination.** *Org Biomol Chem* 2009, **7**:4825-4828.
12. Tranoy-Opalinski I, Legigan T, Barat R, Clarhaut J, Thomas M, Renoux B, Papot S: **beta-Glucuronidase-responsive prodrugs for selective cancer chemotherapy: an update.** *Eur J Med Chem* 2014, **74**:302-313.
13. Sharma SK, Bagshawe KD: **Antibody Directed Enzyme Prodrug Therapy (ADEPT): Trials and tribulations.** *Adv Drug Deliv Rev* 2017, **118**:2-7.
14. Xu G, McLeod HL: **Strategies for enzyme/prodrug cancer therapy.** *Clin Cancer Res* 2001, **7**:3314-3324.
15. Bakina E, Wu Z, Rosenblum M, Farquhar D: **Intensely cytotoxic anthracycline prodrugs: glucuronides.** *J Med Chem* 1997, **40**:4013-4018.

16. Florent JC, Dong X, Gaudel G, Mitaku S, Monneret C, Gesson JP, Jacquesy JC, Mondon M, Renoux B, Andrianomenjanahary S, et al: **Prodrugs of anthracyclines for use in antibody-directed enzyme prodrug therapy.** *J Med Chem* 1998, **41**:3572-3581.
17. Leenders RG, Damen EW, Bijsterveld EJ, Scheeren HW, Houba PH, van der Meulen-Muileman IH, Boven E, Haisma HJ: **Novel anthracycline-spacer-beta-glucuronide,-beta-glucoside, and -beta-galactoside prodrugs for application in selective chemotherapy.** *Bioorg Med Chem* 1999, **7**:1597-1610.
18. Papot S, Combaud D, Gesson JP: **A new spacer group derived from arylmalonaldehydes for glucuronylated prodrugs.** *Bioorg Med Chem Lett* 1998, **8**:2545-2548.
19. El Alaoui A, Schmidt F, Monneret C, Florent JC: **Protecting groups for glucuronic acid: application to the synthesis of new paclitaxel (taxol) derivatives.** *J Org Chem* 2006, **71**:9628-9636.
20. Legigan T, Clarhaut J, Renoux B, Tranoy-Opalinski I, Monvoisin A, Berjeaud JM, Guilhot F, Papot S: **Synthesis and antitumor efficacy of a beta-glucuronidase-responsive albumin-binding prodrug of doxorubicin.** *J Med Chem* 2012, **55**:4516-4520.
21. Niculescu-Duvaz I, Niculescu-Duvaz D, Friedlos F, Spooner R, Martin J, Marais R, Springer CJ: **Self-immolative anthracycline prodrugs for suicide gene therapy.** *J Med Chem* 1999, **42**:2485-2489.
22. Tian J, Stella VJ: **Degradation of paclitaxel and related compounds in aqueous solutions III: Degradation under acidic pH conditions and overall kinetics.** *J Pharm Sci* 2010, **99**:1288-1298.
23. de Graaf M, Nevalainen TJ, Scheeren HW, Pinedo HM, Haisma HJ, Boven E: **A methylester of the glucuronide prodrug DOX-GA3 for improvement of tumor-selective chemotherapy.** *Biochem Pharmacol* 2004, **68**:2273-2281.
24. Grinda M, Clarhaut J, Renoux B, Tranoy-Opalinski I, Papot S: **A self-immolative dendritic glucuronide prodrug of doxorubicin.** *MedChemComm* 2012:68-70.
25. Wu L, Jiang J, Jin Y, Kallemeijn WW, Kuo CL, Artola M, Dai W, van Elk C, van Eijk M, van der Marel GA, et al: **Activity-based probes for functional interrogation of retaining beta-glucuronidases.** *Nat Chem Biol* 2017, **13**:867-873.
26. Gonzalez-Noriega A, Michalak C, Antonio Sosa Melgarejo J: **Cation-independent mannose 6-phosphate and 78 kDa receptors for lysosomal enzyme targeting are located in different cell compartments.** *Biochim Biophys Acta* 2005, **1745**:7-19.
27. Kennedy JE: **High-intensity focused ultrasound in the treatment of solid tumours.** *Nat Rev Cancer* 2005, **5**:321-327.
28. Zhou YF: **High intensity focused ultrasound in clinical tumor ablation.** *World J Clin Oncol* 2011, **2**:8-27.
29. Eranki A, Srinivasan P, Ries M, Kim A, Lazarski CA, Rossi CT, Khokhlova TD, Wilson E, Knoblach SM, Sharma KV, et al: **High-Intensity Focused Ultrasound (HIFU) Triggers Immune Sensitization of Refractory Murine Neuroblastoma to Checkpoint Inhibitor Therapy.** *Clin Cancer Res* 2020, **26**:1152-1161.
30. Wang J, Huang C-H, Echeagaray OH, Amirfakhri S, Blair SL, Trogler WC, Kummel AC, Chen CC: **Immuno-Stimulatory Effects of Mechanical and Thermal High Intensity Focused Ultrasound.** *Neurosurgery* 2019, **66**.
31. Galluzzi L, Buque A, Kepp O, Zitvogel L, Kroemer G: **Reply: Immunosuppressive cell death in cancer.** *Nat Rev Immunol* 2017, **17**:402.

32. Galluzzi L, Humeau J, Buque A, Zitvogel L, Kroemer G: **Immunostimulation with chemotherapy in the era of immune checkpoint inhibitors.** *Nat Rev Clin Oncol* 2020.
33. Bosco M, Rat S, Dupre N, Hasenknopf B, Lacote E, Malacria M, Remy P, Kovensky J, Thorimbert S, Wadouachi A: **Lewis-acidic polyoxometalates as reusable catalysts for the synthesis of glucuronic acid esters under microwave irradiation.** *ChemSusChem* 2010, **3**:1249-1252.
34. Bollenback GN, Long JW, Benjamin DG, Lindquist JA: **The Synthesis of Aryl-D-glucopyranosiduronic Acids¹.** *Journal of the American Chemical Society* 1955, **77**:3310-3315.
35. de Groot FM, Loos WJ, Koekkoek R, van Berkom LW, Busscher GF, Seelen AE, Albrecht C, de Bruijn P, Scheeren HW: **Elongated multiple electronic cascade and cyclization spacer systems in activatable anticancer prodrugs for enhanced drug release.** *J Org Chem* 2001, **66**:8815-8830.
36. Jefferson RA, Kavanagh TA, Bevan MW: **GUS fusions: beta-glucuronidase as a sensitive and versatile gene fusion marker in higher plants.** *EMBO J* 1987, **6**:3901-3907.

SUPPLEMENTARY INFORMATION

1. Synthesis and characterization by $^1\text{H-NMR}$ and ESI-MS

Reagents: D-(+)-glucuronic acid γ -lactone, pyridine, methyl-(p-hydroxymethyl) benzoate, triethylamine (TEA), acetic acid, dichloromethane (DCM), acetonitrile (ACN), methanol (MeOH), heptane, ethyl acetate, toluene, tetrahydrofuran (THF), dimethylformamide (DMF) were ordered from Carl Roth. Tert-butyldimethylsilyl chloride (TBDMSCl), diphenylphosphoryl azide (DPPA), lithium methoxide solution (LiOMe), 4-nitrophenyl chloroformate (Cl-COOPh-NO₂) were ordered from Sigma. Doxorubicin hydrochloride salt (DOX·HCl) was ordered from Biomol.

$^1\text{H-NMR}$: $^1\text{H-NMR}$ spectra of the synthesized compounds were recorded using a Bruker 600 FT NMR spectrometer in CD₃OD, or CDCl₃ or DMSO-d₆ as indicated in the methods. Chemical shifts were reported as δ values (ppm) with tetramethylsilane (TMS) as the internal reference. Multiplicities were indicated as s (singlet), d (doublet), t (triplet), m (multiplet); coupling constants (J) were indicated in Hertz (Hz), rounded to the nearest 0.1 Hz.

ESI-MS: Full spectrometry was recorded with ThermoFisher LTQ-Orbitrap XL, positive ion mode, m/z (rel. intensity %).

Compound A

Compound A was synthesized according to a previously publication [33, 34]. $^1\text{H NMR}$ (600 MHz, DMSO-d₆) δ 7.61 – 7.37 (m, 1H, -OH), 5.53 – 5.12 (m, 2H, Glu 1,3-H), 5.12 – 4.86 (m, 1H, Glu 2-H), 4.86 – 4.58 (m, 1H, Glu 4-H), 4.41 (d, J = 10.2 Hz, 1H, Glu 5-H), 3.64 (s, 3H, COOCH₃), 2.03 – 1.88 (m, 9H, -OAc). Yield=17.3%.

Compound B

Compound B synthesis was performed using a previously established method [35].

$^1\text{H NMR}$ (600 MHz, DMSO-d₆) δ 12.85 (s, 1H, -COOH), 7.90 (d, J = 8.2 Hz, 2H, Ar), 7.38 (d, J = 8.0 Hz, 2H, Ar), 4.77 (s, 2H, Ar-CH₂), 0.91 (s, 9H, Si-tBut), 0.08 (s, 6H, Si-Me₂). Yield=57.5%.

Compound C-1, C-2 and C-3

Firstly, 6 g (1 equiv) compound B (HOOC-Ph-CH₂-OTBDMS) was dissolved in 120 mL dried toluene under argon atmosphere, to which solution, 1.2 equiv triethylamine (TEA) and 1.2 equiv diphenylphosphoryl azide (DPPA) were

added. After that, the reaction mixture was heated to 85°C for 3h with stirring. When this reaction mixture was cooled down to room temperature, 0.8 equiv compound A dissolved in 60 mL dried toluene was added and the mixture was stirred for overnight. After evaporation of the solvent, the residue was purified by column chromatography (heptane/ethyl acetate = 5/2) to get TBDMS protected single spacer moiety.

Afterwards, deprotection of the silyl group (TBDMS) was performed in THF/H₂O/acetic acid = 1/1/1 for 4 hours. The reaction mixture was concentrated by rotary evaporator, followed by purification by column chromatography (heptane/ethyl acetate = 2/3) to get C-1. Yield: 65.4%.

For the syntheses of C-2 and C-3, the above procedures were repeated for 1 and 2 more time, respectively. Yield of C-2, C-3: 38.3%; 23.7%.

Compound C-1

¹H NMR (600 MHz, Chloroform-d) δ 7.41 – 7.29 (m, 4H, Ar), 6.95 (s, 1H, NH), 5.78 (d, J = 8.0 Hz, 1H, Glu 1-H), 5.34 (t, J = 9.4 Hz, 1H, Glu 2-H), 5.24 (t, J = 9.7 Hz, 1H, Glu 3-H), 5.17 (dd, J = 9.3 Hz, 1H, Glu 4-H), 4.65 (s, 2H, Ar-CH₂), 4.20 (d, J = 9.8 Hz, 1H, Glu 5-H), 3.74 (s, 3H, COOCH₃), 2.08 – 2.01 (m, 9H, OAc).

Compound C-2

¹H NMR (600 MHz, Chloroform-d) δ 7.43 – 7.28 (m, 8H, Ar), 7.02 (s, 1H, NH), 6.70 (s, 1H, NH), 5.78 (d, J = 8.0 Hz, 1H, Glu 1-H), 5.35 (t, J = 9.4 Hz, 1H, Glu 2-H), 5.25 (t, J = 9.6 Hz, 1H, Glu 3-H), 5.19 (dd, J = 9.3 Hz, 1H, Glu 4-H), 5.14 (s, 2H, Ar-CH₂), 4.64 (s, 2H, Ar-CH₂), 4.21 (d, J = 9.8 Hz, 1H, Glu 5-H), 3.74 (s, 3H, COOCH₃), 2.08 – 2.02 (m, 9H, OAc).

Compound C-3

¹H NMR (600 MHz, Chloroform-d) δ 7.47 – 7.28 (m, 12H, Ar), 7.05 (s, 1H, NH), 6.77 (s, 1H, NH), 6.71 (s, 1H, NH), 5.78 (d, J = 8.1 Hz, 1H, Glu 1-H), 5.35 (t, J = 9.4 Hz, 1H, Glu 2-H), 5.25 (t, J = 9.6 Hz, 1H, Glu 3-H), 5.19 (dd, J = 9.3 Hz, 1H, Glu 4-H), 5.14 (s, 2H, Ar-CH₂), 5.13 (s, 2H, Ar-CH₂), 4.64 (s, 2H, Ar-CH₂), 4.20 (d, J = 9.9 Hz, 1H, Glu 5-H), 3.73 (s, 3H, COOCH₃), 2.08 – 2.02 (m, 9H, OAc).

Compound D-1, D-2 and D-3

A solution of 4.1 mmol of C-1, or C-2, or C-3 in 50 mL dried MeOH was cooled down to 0°C. To this solution, 4.6 mL 1 M LiOMe in 45 mL of MeOH was added dropwise. After 2 hours, the reaction mixture was neutralized by adding

silica. The purification was done by column chromatography (2% methanol/ethyl acetate followed by 4% methanol/ethyl acetate) after filtration and concentration. Yield of D-1, D-2, D-3: 53.6%; 58.0%; 25.1%.

Compound D-1

^1H NMR (600 MHz, Methanol- d_4) δ 7.49 – 7.24 (m, 4H, Ar), 5.49 (d, J = 8.0 Hz, 1H, Glu 1-H), 4.55 (s, 2H, Ar- CH_2), 3.97 (d, J = 9.7 Hz, 1H, Glu 5-H), 3.77 (s, 3H, COOCH_3), 3.56 (t, J = 9.3 Hz, 1H, Glu 2-H), 3.48 (t, J = 9.1 Hz, 1H, Glu 3-H), 3.42 (dd, J = 9.1 Hz, 1H, Glu 4-H).

Compound D-2

^1H NMR (600 MHz, Methanol- d_4) δ 7.52 – 7.21 (m, 8H, Ar), 5.50 (d, J = 8.0 Hz, 1H, Glu 1-H), 5.12 (s, 2H, Ar- CH_2), 4.53 (s, 2H, Ar- CH_2), 3.98 (d, J = 9.7 Hz, 1H, Glu 5-H), 3.77 (s, 3H, COOCH_3), 3.56 (t, J = 9.3 Hz, 1H, Glu 2-H), 3.49 (t, J = 9.0 Hz, 1H, Glu 3-H), 3.43 (dd, J = 9.1 Hz, 1H, Glu 4-H).

Compound D-3

^1H NMR (600 MHz, Methanol- d_4) δ 7.63 – 7.14 (m, 12H, Ar), 5.50 (d, J = 8.0 Hz, 1H, Glu 1-H), 5.12 (s, 2H, Ar- CH_2), 5.11 (s, 2H, Ar- CH_2), 4.53 (s, 2H, Ar- CH_2), 3.97 (d, J = 9.7 Hz, 1H, Glu 5-H), 3.77 (s, 3H, COOCH_3), 3.56 (t, J = 9.3 Hz, 1H, Glu 2-H), 3.48 (t, J = 9.0 Hz, 1H, Glu 3-H), 3.42 (dd, J = 9.1 Hz, 1H, Glu 4-H).

Compound E-1, E-2 and E-3

1 mmol of D-1, or D-2, or D-3 was dissolved in 32 mL ACN with 4.3 mL THF. When the mixture was cooled down to 0°C, 1.3 equiv pyridine and 1.2 equiv 4-nitrophenyl chloroformate (Cl-COOPh- NO_2) were added to the above solution. The mixture was stirred 2 hours. Afterwards, the crude product was purified by column chromatography (8% MeOH/DCM) to afford compound E-1, or E-2, or E-3. Yield of E-1, E-2, E-3: 71.1%; 78.4%; 52.0%.

Compound E-1

^1H NMR (600 MHz, Methanol- d_4) δ 8.39 – 8.23 (m, 2H, Ar- NO_2), 7.58 – 7.36 (m, 6H, Ar), 5.52 (d, J = 8.1 Hz, 1H, Glu 1-H), 5.25 (s, 2H, Ar- CH_2), 4.02 (d, J = 9.7 Hz, 1H, Glu 5-H), 3.76 (s, 3H, COOCH_3), 3.58 (t, J = 9.3 Hz, 1H, Glu 2-H), 3.50 (t, J = 9.0 Hz, 1H, Glu 3-H), 3.44 (dd, J = 9.1 Hz, 1H, Glu 4-H).

Compound E-2

^1H NMR (600 MHz, Methanol- d_4) δ 8.41 – 8.19 (m, 2H, Ar- NO_2), 7.58 – 7.28 (m, 10H, Ar), 5.50 (d, J = 7.8 Hz, 1H, Glu 1-H), 5.24 (s, 2H, Ar- CH_2), 5.13 (s, 2H, Ar-

CH₂), 3.98 (d, J = 9.6 Hz, 1H, Glu 5-H), 3.77 (s, 3H, COOCH₃), 3.56 (t, J = 9.1 Hz, 1H, Glu 2-H), 3.49 (t, J = 8.8 Hz, 1H, Glu 3-H), 3.43 (dd, J = 8.4 Hz, 1H, Glu 4-H).

Compound E-3

¹H NMR (600 MHz, Methanol-d₄) δ 8.42 – 8.23 (m, 2H, Ar-NO₂), 7.60 – 7.28 (m, 14H, Ar), 5.51 (d, J = 8.0 Hz, 1H, Glu 1-H), 5.24 (s, 2H, Ar-CH₂), 5.12 (s, 2H, Ar-CH₂), 5.11 (s, 2H, Ar-CH₂), 4.01 (d, J = 9.7 Hz, 1H, Glu 5-H), 3.77 (s, 3H, COOCH₃), 3.57 (t, J = 9.3 Hz, 1H, Glu 2-H), 3.49 (t, J = 9.0 Hz, 1H, Glu 3-H), 3.43 (dd, J = 9.1 Hz, 1H, Glu 4-H).

Compound F-1, F-2 and F-3

1.2 equiv compound E-1, or E-2, or E-3 was dissolved in dried DMF under N₂ environment. 1 equiv DOX·HCl and 1 equiv TEA were added to this solution. The reaction was kept on stirring overnight, and the DMF was removed by rotary evaporator. The crude product was purified by column chromatography (12% MeOH/ethyl acetate) to yield F-1, F-2 and F-3. Yield of F-1, F-2, F-3: 71.9%; 96.1%; 91.2%.

Compound F-1

¹H NMR (600 MHz, DMSO-d₆) δ 14.04 (s, 1H, 6-OH), 13.29 (s, 1H, 11-OH), 9.96 (s, 1H, Ar-NH), 7.95 – 7.90 (m, 2H, Ar), 7.72 – 7.61 (m, 1H, Ar), 7.52 – 7.15 (m, 4H, Ar), 6.83 (d, J = 8.0 Hz, 1H, 3'-NH), 5.48 – 5.39 (m, 4H, 2*Glu-OH, and Glu 1-H, and 9-OH), 5.32 (d, J = 4.9 Hz, 1H, Glu-OH), 5.23 – 5.19 (m, 1H, 1'-H), 4.98 – 4.92 (m, 1H, 7-H), 4.87 (s, 2H, Ar-CH₂), 4.83 (t, J = 5.9 Hz, 1H, 14-OH), 4.68 (d, J = 5.9 Hz, 1H, 4'-OH), 4.57 (d, J = 6.4 Hz, 2H, 14-CH₂), 4.15 (d, J = 6.7 Hz, 1H, 5'-H), 3.99 (s, 3H, 4-OMe), 3.90 (d, J = 9.0 Hz, 1H, Glu-5H), 3.79 – 3.68 (m, 1H, 3'-H), 3.66 (s, 3H, COOCH₃), 3.49 – 3.22 (m, 4H, Glu 2,3,4-H and 4'-H), 3.04 – 2.93 (m, 2H, 10_{eq} and 10_{ax}-H), 2.23 – 2.09 (m, 2H, 8_{ax} and 8_{eq}-H), 1.88 – 1.78 (m, 1H, 2'_{ax}-H), 1.52 – 1.41 (m, 1H, 2'_{eq}-H), 1.12 (d, J = 6.4 Hz, 3H, 5'-CH₃).

Compound F-2

¹H NMR (600 MHz, DMSO-d₆) δ 14.04 (s, 1H, 6-OH), 13.29 (s, 1H, 11-OH), 10.03 (s, 1H, Ar-NH), 9.72 (s, 1H, Ar-NH), 7.94 – 7.90 (m, 2H, Ar), 7.69 – 7.63 (m, 1H, Ar), 7.53 – 7.18 (m, 8H, Ar), 6.81 (d, J = 8.0 Hz, 1H, 3'-NH), 5.48 – 5.39 (m, 4H, 2*Glu-OH, and Glu 1-H, and 9-OH), 5.32 (d, J = 4.9 Hz, 1H, Glu-OH), 5.24 – 5.19 (m, 1H, 1'-H), 5.04 (s, 2H, Ar-CH₂), 4.99 – 4.9 (m, 1H, 7-H), 4.87 (s, 2H, Ar-CH₂), 4.83 (t, J = 5.9 Hz, 1H, 14-OH), 4.68 (d, J = 5.9 Hz, 1H, 4'-OH), 4.57 (d, J = 6.4 Hz, 2H, 14-CH₂), 4.15 (d, J = 6.7 Hz, 1H, 5'-H), 3.99 (s, 3H, 4-OMe), 3.90 (d, J = 9.0 Hz, 1H, Glu-5H), 3.79 – 3.68 (m, 1H, 3'-H), 3.66 (s, 3H, COOCH₃), 3.49 – 3.22 (m,

4H, Glu 2,3,4-H and 4'-H), 3.04 – 2.93 (m, 2H, 10_{eq} and 10_{ax} -H), 2.23 – 2.09 (m, 2H, 8_{ax} and 8_{eq} -H), 1.88 – 1.78 (m, 1H, $2'_{\text{ax}}$ -H), 1.53 – 1.39 (m, 1H, $2'_{\text{eq}}$ -H), 1.12 (d, $J = 6.4$ Hz, 3H, 5'-CH₃).

Compound F-3

¹H NMR (600 MHz, DMSO-d₆) δ 14.04 (s, 1H, 6-OH), 13.29 (s, 1H, 11-OH), 10.03 (s, 1H, Ar-NH), 9.83 (s, 1H, Ar-NH), 9.72 (s, 1H, Ar-NH), 7.93 – 7.90 (m, 2H, Ar), 7.68 – 7.63 (m, 1H, Ar), 7.54 – 7.17 (m, 12H, Ar), 6.81 (d, $J = 8.0$ Hz, 1H, 3'-NH), 5.48 – 5.39 (m, 4H, 2*Glu-OH, and Glu 1-H, and 9-OH), 5.32 (d, $J = 4.9$ Hz, 1H, Glu-OH), 5.24 – 5.17 (m, 1H, 1'-H), 5.06 (s, 2H, Ar-CH₂), 5.02 (s, 2H, Ar-CH₂), 4.95 – 4.90 (m, 1H, 7-H), 4.87 (s, 2H, Ar-CH₂), 4.77 (t, $J = 5.9$ Hz, 1H, 14-OH), 4.68 (d, $J = 5.9$ Hz, 1H, 4'-OH), 4.57 (d, $J = 6.4$ Hz, 2H, 14-CH₂), 4.15 (d, $J = 6.7$ Hz, 1H, 5'-H), 3.99 (s, 3H, 4-OMe), 3.90 (d, $J = 9.0$ Hz, 1H, Glu-5H), 3.79 – 3.68 (m, 1H, 3'-H), 3.66 (s, 3H, COOCH₃), 3.49 – 3.22 (m, 4H, Glu 2,3,4-H and 4'-H), 3.04 – 2.93 (m, 2H, 10_{eq} and 10_{ax} -H), 2.23 – 2.09 (m, 2H, 8_{ax} and 8_{eq} -H), 1.88 – 1.78 (m, 1H, $2'_{\text{ax}}$ -H), 1.51 – 1.44 (m, 1H, $2'_{\text{eq}}$ -H), 1.12 (d, $J = 6.4$ Hz, 3H, 5'-CH₃).

Compound DOX-AU1, DOX-AU2 and DOX-AU3

1 mmol of F-1, or F-2, or F-3 was dissolved in DMSO and PBS ($v/v=1/1$) and incubated at 37°C for 20 hours. The solutions were lyophilized and the products were purified by column chromatography to obtain DOX-AU1-3. Yield of DOX-AU1-3: 71.6%; 78.3%; 72.5%.

DOX-AU1

¹H NMR (600 MHz, DMSO-d₆) δ 14.04 (s, 1H, 6-OH), 13.29 (s, 1H, 11-OH), 9.96 (s, 1H, Ar-NH), 7.95 – 7.90 (m, 2H, Ar), 7.72 – 7.61 (m, 1H, Ar), 7.52 – 7.15 (m, 4H, Ar), 6.83 (d, $J = 8.0$ Hz, 1H, 3'-NH), 5.49 – 5.32 (m, 4H, 2*Glu-OH, and Glu 1-H, and 9-OH), 5.27 (d, $J = 5.2$ Hz, 1H, Glu-OH), 5.23 – 5.19 (m, 1H, 1'-H), 4.98 – 4.92 (m, 1H, 7-H), 4.88 (s, 2H, Ar-CH₂), 4.83 (t, $J = 5.9$ Hz, 1H, 14-OH), 4.68 (d, $J = 5.7$ Hz, 1H, 4'-OH), 4.57 (d, $J = 6.4$ Hz, 2H, 14-CH₂), 4.15 (d, $J = 6.9$ Hz, 1H, 5'-H), 3.99 (s, 3H, 4-OMe), 3.72 (d, $J = 9.1$ Hz, 1H, Glu-5H), 3.64 – 3.57 (m, 1H, 3'-H), 3.49 – 3.22 (m, 4H, Glu 2,3,4-H and 4'-H), 3.09 – 2.88 (m, 2H, 10_{eq} and 10_{ax} -H), 2.23 – 2.09 (m, 2H, 8_{ax} and 8_{eq} -H), 1.87 – 1.77 (m, 1H, $2'_{\text{ax}}$ -H), 1.52 – 1.41 (m, 1H, $2'_{\text{eq}}$ -H), 1.12 (d, $J = 6.5$ Hz, 3H, 5'-CH₃).

ESI-MS: $(M+Na)_{\text{cal}} = 935.8$; $(M+Na)_{\text{find}} = 935.2$.

DOX-AU2

^1H NMR (600 MHz, DMSO- d_6) δ 14.04 (s, 1H, 6-OH), 13.29 (s, 1H, 11-OH), 10.02 (s, 1H, Ar-NH), 9.72 (s, 1H, Ar-NH), 7.95 – 7.89 (m, 2H, Ar), 7.69 – 7.63 (m, 1H, Ar), 7.53 – 7.18 (m, 8H, Ar), 6.81 (d, J = 8.1 Hz, 1H, 3'-NH), 5.54 – 5.35 (m, 4H, 2*Glu-OH, and Glu 1-H, and 9-OH), 5.28 (d, J = 5.0 Hz, 1H, Glu-OH), 5.24 – 5.19 (m, 1H, 1'-H), 5.04 (s, 2H, Ar-CH $_2$), 4.99 – 4.9 (m, 1H, 7-H), 4.87 (s, 2H, Ar-CH $_2$), 4.84 (t, J = 5.9 Hz, 1H, 14-OH), 4.68 (d, J = 5.6 Hz, 1H, 4'-OH), 4.57 (d, J = 6.4 Hz, 2H, 14-CH $_2$), 4.15 (d, J = 6.9 Hz, 1H, 5'-H), 3.99 (s, 3H, 4-OMe), 3.75 (d, J = 9.3 Hz, 1H, Glu 5-H), 3.73 – 3.66 (m, 1H, 3'-H), 3.49 – 3.22 (m, 4H, Glu 2,3,4-H and 4'-H), 3.09 – 2.88 (m, 2H, 10 $_{\text{eq}}$ and 10 $_{\text{ax}}$ -H), 2.24 – 2.09 (m, 2H, 8 $_{\text{ax}}$ and 8 $_{\text{eq}}$ -H), 1.88 – 1.77 (m, 1H, 2' $_{\text{ax}}$ -H), 1.53 – 1.39 (m, 1H, 2' $_{\text{eq}}$ -H), 1.12 (d, J = 6.5 Hz, 3H, 5'-CH $_3$).

ESI-MS: (M+Na) $_{\text{cal}}$ = 1084.9; (M+Na) $_{\text{find}}$ = 1084.3.

DOX-AU3

^1H NMR (600 MHz, DMSO- d_6) δ 14.02 (s, 1H, 6-OH), 13.28 (s, 1H, 11-OH), 10.04 (s, 1H, Ar-NH), 9.83 (s, 1H, Ar-NH), 9.75 (s, 1H, Ar-NH), 7.93 – 7.90 (m, 2H, Ar), 7.68 – 7.63 (m, 1H, Ar), 7.54 – 7.17 (m, 12H, Ar), 6.86 (d, J = 8.1 Hz, 1H, 3'-NH), 5.66 – 5.40 (m, 4H, 2*Glu-OH, and Glu 1-H and 9-OH), 5.36 (d, J = 5.2 Hz, 1H, Glu-OH), 5.24 – 5.17 (m, 1H, 1'-H), 5.06 (s, 2H, Ar-CH $_2$), 5.02 (s, 2H, Ar-CH $_2$), 4.95 – 4.90 (m, 1H, 7-H), 4.86 (s, 2H, Ar-CH $_2$), 4.77 (t, J = 5.9 Hz, 1H, 14-OH), 4.75 (d, J = 5.6 Hz, 1H, 4'-OH), 4.58 (d, J = 6.4 Hz, 2H, 14-CH $_2$), 4.14 (d, J = 6.8 Hz, 1H, 5'-H), 3.98 (s, 3H, 4-OMe), 3.70 (d, J = 9.1 Hz, 1H, Glu 5-H), 3.64 – 3.57 (m, 1H, 3'-H), 3.49 – 3.22 (m, 4H, Glu 2,3,4-H and 4'-H), 3.04 – 2.94 (m, 2H, 10 $_{\text{eq}}$ and 10 $_{\text{ax}}$ -H), 2.22 – 2.09 (m, 2H, 8 $_{\text{ax}}$ and 8 $_{\text{eq}}$ -H), 1.87 – 1.78 (m, 1H, 2' $_{\text{ax}}$ -H), 1.51 – 1.44 (m, 1H, 2' $_{\text{eq}}$ -H), 1.11 (d, J = 6.5 Hz, 3H, 5'-CH $_3$).

ESI-MS: (M+Na) $_{\text{cal}}$ = 1234.1; (M+Na) $_{\text{find}}$ = 1233.3.

2. Activation of DOX-AU1-3 by β -GUS.

DOX-AU1-3 were dissolved in DMSO to prepare 1 mM stock solutions, which were diluted in PBS (pH 7.4 or 6.5) containing β -GUS (activity $\geq 1,000$ units/mg, ordered from Sigma) to yield mixtures of 50 μM DOX-AU1-3 and 50 $\mu\text{g/mL}$ β -GUS in the solutions. Afterwards, the mixtures were kept at 37°C and 200 μL of samples were taken out from the solutions at scheduled time points. The samples were analyzed by HPLC to detect the concentrations of DOX-AU1-3 and DOX. All the experiments were performed in triplicates. HPLC conditions: C18 column; gradient elution method (40% ACN / 60% H $_2$ O + 0.1% TFA to 95%

ACN / 5% H₂O + 0.1% TFA in 11 minutes). The flow rate was 1 mL/min and the detection wavelength was 486 nm.

3. Cell culture

Mouse mamma carcinoma (4T1, ATCC CRL-2539) cells were obtained from ATCC (Rockville, MD, USA) and cultured in RPMI 1640 (Sigma). The medium was supplemented with 10% Fetal Bovine Serum (Sigma F7524) and 1% penicillin-streptomycin-amphotericin B (Sigma). Cells were cultured at 37°C in 5% CO₂ in an air humidified incubator and regularly tested negative for mycoplasma contamination.

4. HIFU setup

High-intensity focused ultrasound (HIFU) exposure was performed by an in-house-build system consisted of a transducer, oscilloscope, combined amplifier and wave generator and sample holder. The single element focused ultrasound transducer (Imasonic, Besançon, France) had a focal length of 8 cm, external radius of aperture of 14 cm and focal point of 1x1x3 mm³ (at -3dB). Sine shaped waves were generated by an AG Series Amplifier (AG 1006, T&C Power Conversion Inc.) operated at a frequency of 1.3 MHz, duty cycle of 1% and pulse repetition time of 50 ms. The input voltage of the transducer was measured by the oscilloscope. These input voltages were used to determine acoustic pressures that were calibrated in the focal points as a function of input voltage using a fiber optic probe hydrophone (FOPH 2000, RP Acoustics, Leutenbach, Germany) in a tank filled with degassed water.

5. HIFU treatment of 4T1 cells

4T1 cells dissolved in 170 µL PBS were added in a PCR tube (Bio rad, California USA) (2*10⁶ cells for microscopy (Section 8); 8.5*10⁶ cells for prodrug activation, cytotoxicity and calreticulin translocation study (Section 10, 11 and 12)). The PCR tube was positioned in the sample holder in the focus of the ultrasound beam for 10 minutes and exposed to HIFU at a peak-negative pressure of 41 MPa. After HIFU exposure, samples containing cells were immediately placed on ice. Subsequently, the sample was analyzed by microscopy, or centrifuged at 16,000 g for 15 minutes and supernatant was used in prodrug activation and cell studies.

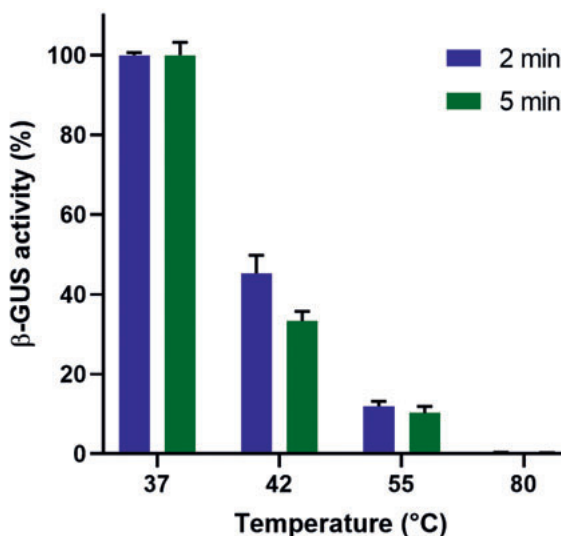
6. *β*-GUS activity by MUG assay

The *β*-GUS activity was investigated by 4-methyl-umbelliferyl-*β*-D-glucuronide (MUG) assay adapted from Jefferson et al. [36]. Briefly, 20 µL sample was

added to 180 μL 4-MUG (1 mg/mL in 0.1 M sodium acetate (pH 4.5)) and incubated for 1 hour in a water bath of 37°C. Subsequently, 950 μL of 0.2 M sodium carbonate (i.e. stopping buffer) was added to 50 μL of all samples. Finally, fluorescence intensity was measured using a spectrofluorometer (Jasco FP8300) with excitation of 380 nm and emission of 454 ± 5 nm.

7. Activity of β -GUS exposed to different temperatures

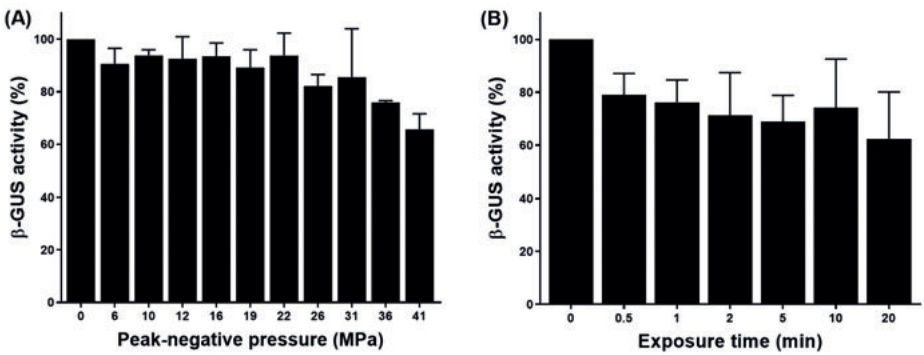
Bovine β -GUS (50 $\mu\text{g/mL}$ in PBS corresponding to 112 units/mL) was incubated for 2 or 5 minutes at 37, 42, 55 or 80°C. Subsequently, β -GUS activity was determined by a MUG assay and normalized to the bovine β -GUS activity incubated at 37°C for 2 minutes. All experiments were performed in triplicate and error bars represent standard deviations.



Supplementary Figure 1: Influence of temperature on bovine β -GUS activity.

8. Activity of β -GUS exposed to HIFU

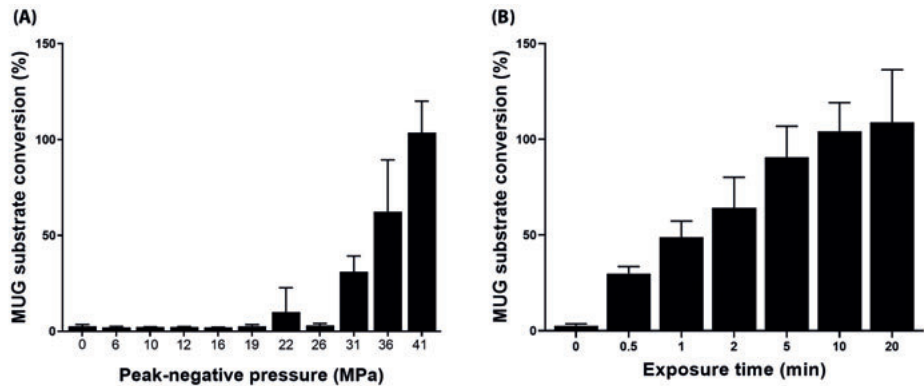
Bovine β -GUS (8.5 μg in 170 μL PBS corresponding to 19 units in 170 μL) exposed to HIFU with A) different peak-negative pressures in the range of 0 to 41 MPa for 10 minutes and B) a peak-negative pressure of 41 MPa for exposure durations up to 20 minutes. β -GUS activity was measured by a MUG assay. The β -GUS activity was normalized to untreated enzymes. All experiments were performed in triplicate and error bars represent standard deviations.



Supplementary Figure 2: Influence of HIFU treatment on the bioactivity of β -GUS.

9. Activity of released β -GUS after cells exposed to HIFU

MUG substrate conversion by β -GUS released from cells (2×10^6 cells in 170 μ L PBS) after exposure to HIFU with A) different peak-negative pressures in the range of 0 to 41 MPa for 10 minutes and B) a peak-negative pressure of 41 MPa for exposure durations up to 20 minutes. MUG substrate conversion was measured by a MUG assay. The MUG substrate conversion was normalized to the MUG substrate conversion by β -GUS released from cells after 3 freeze-thaw cycles, which was set at 100%. All experiments were performed in triplicate and error bars represent standard deviations.



Supplementary Figure 3: Influence of HIFU treatment to cells on β -GUS liberation.

10. Bright field microscopy

After exposure of 4T1 cells to HIFU treatment a peak-negative pressure of 41 MPa and upto 20 minutes, 10 μ L sample and 240 μ L cell culture medium were placed in an ibidi chamber of 1 μ -Slide 8 Well ibiTreat (Ibidi GmbH, Munich,

Germany) and incubated for 60 minutes under normal cell culture conditions. Finally, cells were imaged by inverted bright field microscopy (Olympus CK2, ULWCD 0.30, Japan) with a Moticam 5-5.0 MP camera using a 20x objective.

11. Activation of DOX-AU2 in the presence of HIFU-treated cell lysate

The experimental procedure of DOX-AU2 activation by HIFU-treated 4T1 cell supernatant was similar as that by commercial β -GUS. Firstly, 4T1 triple negative breast cancer cells were treated by HIFU as described in Section 5 to release intracellular β -GUS, which was mixed with 1 mM DOX-AU2 in DMSO. The mixture was diluted with PBS to reach DOX-AU2 at 50 μ M. The activation study was performed at 37°C and the drug concentrations were analyzed by HPLC.

12. Cytotoxicity of DOX-AU2 in the presence of HIFU-treated cell lysate

4T1 cells were cultured in a 96 well plate (5,000 cells/well) overnight and then incubated with DOX-AU2 or DOX in 200 μ L culture medium at concentrations between 5 and 100 μ M. The medium was supplemented with either 20 μ L of HIFU-treated cell lysate supernatant or PBS at a pH of 7.4. After incubation for 72 hours at standard culturing conditions, cell survival was measured by (2,3-bis-(2-methoxy-4-nitro-5-sulfophenyl)-2H-tetrazolium-5-carboxanilide) (XTT) assay according to the manufacturer protocol. Finally, cell viability was calculated as percentage of viable cells compared to the untreated control cells and IC₅₀ values were calculated using GraphPad Prism 5.

13. Calreticulin translocation analysis by flow cytometry

4T1 cells were treated as described in Section 11. After the treatment, the cells were collected (detached by trypsin) and washed 3 times with cold PBS, and then stained with anti-calreticulin primary antibody (Calreticulin (D3E6) XP® Rabbit mAb, #12238 from Cell Signaling Technology) and Alexa647 secondary antibody (Anti-rabbit IgG (H+L), F(ab')₂ Fragment (Alexa Fluor® 647 Conjugate), #4414 from Cell Signaling Technology). After that, the cells were washed with cold PBS and stained with Hoechst 33342 (for detecting dead cells) for 5 minutes before analysis by flow cytometry (BD FACSCanto II).

CHAPTER 5

A Doxorubicin-Glucuronide Prodrug Released from Nanogels Activated by High-Intensity Focused Ultrasound Liberated β -Glucuronidase

Helena C. Besse*

Yinan Chen*

Hans W. Scheeren

Josbert M. Metselaar

Twan Lammers

Chrit T.W. Moonen

Wim E. Hennink

Roel Deckers

* These authors contributed equally to this work

Based on: **Pharmaceutics** (2020); 12(6)

ABSTRACT

The poor pharmacokinetics and selectivity of low-molecular-weight anticancer drugs contribute to the relatively low effectiveness of chemotherapy treatments. To improve the pharmacokinetics and selectivity of these treatments, the combination of a doxorubicin-glucuronide prodrug (DOX-propGA3) nanogel formulation and the liberation of endogenous β -glucuronidase from cells exposed to high-intensity focused ultrasound (HIFU) were investigated *in vitro*. First, a DOX-propGA3-polymer was synthesized. Subsequently, DOX-propGA3-nanogels were formed from this polymer dissolved in water using inverse mini-emulsion photopolymerization. In the presence of bovine β -glucuronidase, the DOX-propGA3 in the nanogels was quantitatively converted into the chemotherapeutic drug doxorubicin. Exposure of cells to HIFU efficiently induced liberation of endogenous β -glucuronidase, which in turn converted the prodrug released from the DOX-propGA3-nanogels into doxorubicin. β -glucuronidase liberated from cells exposed to HIFU increased the cytotoxicity of DOX-propGA3-nanogels to a similar extent as bovine β -glucuronidase, whereas in the absence of either bovine β -glucuronidase or β -glucuronidase liberated from cells exposed to HIFU, the DOX-propGA3-nanogels hardly showed cytotoxicity. Overall, DOX-propGA3-nanogels systems might help to further improve the outcome of HIFU-related anticancer therapy.

1. INTRODUCTION

Chemotherapy is one of the most commonly used treatment modalities in cancer, either as a monotherapy or in combination with another treatment modalities, such as radiotherapy and surgery [1]. The agents used in chemotherapy treatment are often not tumor-cell-specific. Hence, these agents also cause damage to normal tissue, which could ultimately cause severe dose-limiting side effects and reduce the efficacy of chemotherapy treatment [2-4].

These chemotherapy-related side effects can potentially be reduced by using prodrug therapy. Prodrugs are non-cytotoxic drug precursors that ideally are only activated in the tumor microenvironment into the pharmacologically active cytotoxic drug [5, 6]. The activation of the prodrug can be caused by many triggers, like hypoxia, radiation, pH, tumor-specific antigens, and enzymes [6].

In cancer treatment most prodrugs are activated by enzymes, i.e., enzyme prodrug therapy [7, 8]. A previously synthesized prodrug for enzyme prodrug therapy is DOX-GA3 [9], which is converted into the cytotoxic agent doxorubicin (DOX) by the enzyme β -glucuronidase (β -GUS) [9, 10]. β -GUS is a lysosomal enzyme that is limitedly present in the blood [11] and is only extracellularly present in necrotic tumor microenvironment [12, 13]. Therefore, there is only conversion of DOX-GA3 into DOX in the necrotic tumor [9]. As a single treatment, DOX-GA3 is 12 times less cytotoxic than DOX, *in vitro* [10]. The low cytotoxicity of DOX-GA3 is mainly caused by the fact that DOX-GA3 is hydrophilic and therefore not able to cross the cell membrane [14], whereas treatment with DOX-GA3 in combination with β -GUS results *in vitro* in similar efficacy to DOX treatment [9, 10]. In addition, *in vivo* the efficacy of DOX-GA3 is higher than DOX, since DOX-GA3 has a larger maximum tolerated injected dose [9, 10]. The therapeutic effectiveness of DOX-GA3, however, can be further increased by increasing its circulation half-life [15].

To improve the pharmacokinetics of DOX-GA3, this prodrug can be loaded into a drug delivery system such as liposomes and nanogels [16-21]. Nanogels are nano-sized hydrogel particles consisting of crosslinked hydrophilic polymer chains that can be physically loaded with drugs and biotherapeutics or chemically conjugated with pharmacologically active agents [22]. As shown before, nanogels are able to improve the half-life of small drugs in the circulation [23-25]. In addition, nanogels passively target the tumor by the loosely vascular aligning and the lack of lymphatic drainage in tumors,

also known as the enhanced permeability and retention (EPR) effect [26, 27]. Therefore, nanogels are promising delivery systems for small molecular prodrugs.

Besides the pharmacokinetics, the site selective activation of the prodrug is also an important factor for effective prodrug therapy [28, 29]. To achieve effective prodrug therapy treatment, the enzymes that are able to convert the inactive prodrug into its active constituent should be highly expressed in the tumor [30]. Since the β -GUS concentrations are only sufficient in large necrotic tumors, in small tumors the efficacy of doxorubicin-glucuronide prodrugs is hampered [31]. Many strategies have been investigated to increase the β -GUS concentration available for prodrug conversion in the tumor, like transfecting tumor cells with the gene encoding for β -GUS (gene-directed enzyme prodrug therapy (GDEPT)) [32, 33] and administration of antibody-enzyme conjugates (antibody-directed enzyme prodrug therapy (ADEPT)) [34]. Currently, these therapies are not used in the clinic, due to insertional mutagenesis in GDEPT, and costs and immunogenicity of ADEPT constructs [30, 33, 35]. Recently, the concept of ultrasound-directed enzyme prodrug therapy (UDEPT) was introduced by Besse et al. (Chapter 4 of this thesis). In this concept, endogenous β -GUS is liberated from tumor cells by exposing them to high-intensity focused ultrasound (HIFU). Subsequently, the liberated β -GUS from the cells is able to convert the prodrug into the cytotoxic agent. Since HIFU is a local and noninvasive technique [36], this enables the possibility of increasing the β -GUS concentration available for prodrug conversion locally in the tumor by a noninvasive treatment, without damaging the normal tissue.

As mentioned, both the pharmacokinetics and tumor side selective activation of the prodrug are important factors for effective prodrug therapy treatment [28, 29]. Here, we investigated the combination of prodrug-nanogel formulation and UDEPT to address the shortcomings of small molecular prodrugs and increase the enzyme concentration available for prodrug conversion, *in vitro*. To this end, doxorubicin-glucuronide prodrug (DOX-propGA3) (structure shown in Figure 1A) was coupled to the polymer hydroxyethyl methacrylamide-oligoglycolates-derivatized poly(hydroxyethyl methacrylamide-co- N-(2-azidoethyl)methacrylamide (p(HEMAm-co-AzEMAm)-Gly-HEMAm) via click chemistry (DOX-propGA3-polymer). The formed conjugate was further used for the preparation of nanogels (DOX-propGA3-nanogels), Figure 1B. Subsequently, the conversion of DOX from the DOX-propGA3-nanogel in the presence of bovine β -GUS was investigated. Finally, it was confirmed *in vitro*

that β -GUS liberated from cells exposed to HIFU was able to increase the cytotoxicity of DOX-propGA3-nanogels.

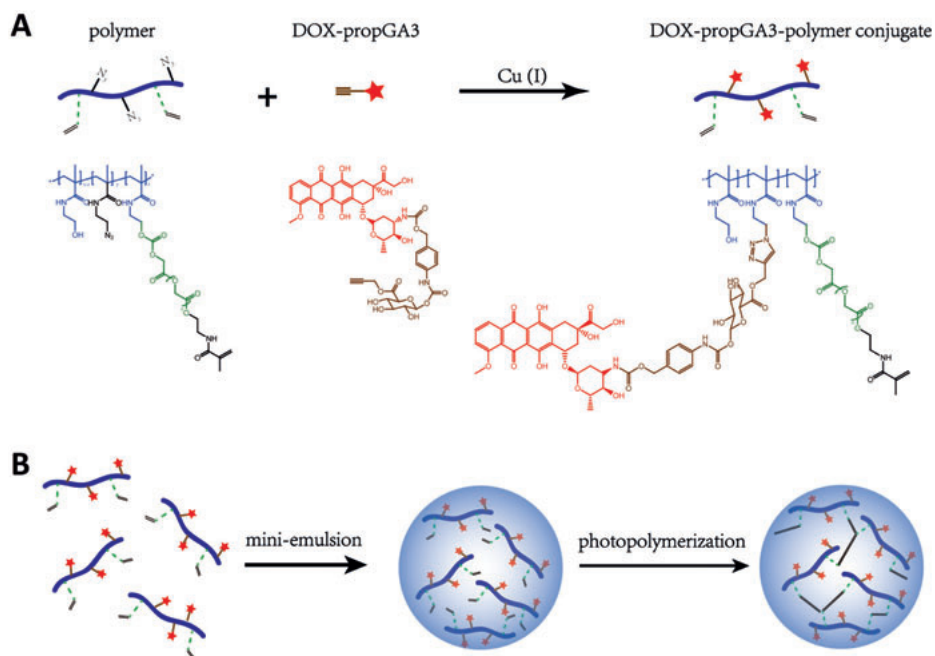


Figure 1: Schematic representation of the synthesis of the doxorubicin-glucuronide prodrug (DOX-propGA3)-polymer and DOX-propGA3-nanogels. (A) Synthesis of DOX-propGA3-polymer conjugate using click-chemistry and (B) preparation of prodrug-loaded nanogels from DOX-propGA3-polymer conjugates using inverse mini-emulsion photopolymerization.

2. MATERIALS AND METHODS

2.1. Materials

DOX-HCl was purchased from Guanyu bio-technology Co., LTD (Xi'an, China). Bovine β -GUS (G0376, Type B-3, 2,000 units/mg solid) and 4-methylumbelliferyl β -D-glucuronide (M9130, 4-MUG) were purchased from Sigma-Aldrich (Zwijndrecht, The Netherlands). Irgacure 2959 was obtained from Ciba Specialty Chemicals Inc. (Bazel, Switzerland). ABIL EM 90 was provided from Evonik Industries AG (Essen, Germany). Acetonitrile (ACN), dichloromethane (DCM), dimethylformamide (DMF), ethyl acetate, methanol, hexane, and dimethyl sulfoxide (DMSO) were obtained from Biosolve (Valkenswaard, The Netherlands). RPMI 1640 (R8758) and fetal bovine serum (FBS) were purchased

from ThermoFisher (Bleiswijk, The Netherlands). CellTiter 96® AQueous One Solution Cell Proliferation Assay (G3580, MTS reagent) was obtained by Promega (Leiden, The Netherlands). All other chemicals and reagents were obtained from Sigma-Aldrich (Zwijndrecht, The Netherlands).

2.2. Cell Culture

Mouse mamma carcinoma 4T1 cells (ATCC, ATCC CRL-2539, Rockville, MD, USA) were cultured in RPMI 1640 supplemented with 10% FBS at a temperature of 37°C in a humidified atmosphere containing 5% CO₂. Cells were regularly tested mycoplasma negative.

2.3. Synthesis of DOX-propGA3-Polymer

DOX-propGA3-polymer conjugate was synthesized as shown in Figure 1A. First, the synthesis of the polymer p(HEMAm-co-AzEMA)-Gly-HEMAm (further referred to as ‘polymer’) (20 mol% AzEMA, degree of substitution 10, Mn 15 kDa, PDI 3.0) [37] and DOX-propGA3 [38] was performed as previously described. The polymer (100 mg) and DOX-propGA3 (8.9 mg, 0.1 mol prodrug/mol azide) were dissolved in 1.8 mL DMF. Then, a mixture of 1.45 mg CuSO₄ (1 eq to DOX-propGA3) and 1.8 mg sodium ascorbate (1 eq to DOX-propGA3) dissolved in 200 µL ammonium acetate buffer (100 mM, pH 5) was added. The resulting solution was stirred at room temperature for 24h under a nitrogen atmosphere. Next, the obtained product was purified by three times precipitation in diethyl ether and dissolving in methanol. Subsequently, the precipitate was dissolved in water and dialyzed (membrane cut-off 3.5 kDa) against ammonium acetate buffer (20 mM, pH 5, containing 10 mM EDTA) for 2 days, followed by dialysis against water for 24h. The ammonium acetate buffer and water were changed at least six times. Ratios between ammonium acetate buffer and sample and between water and sample were larger than 500. Finally, DOX-propGA3-polymer conjugate was recovered by freeze drying.

2.4. Characterization of the DOX-propGA3-Polymer Conjugate

The synthesized DOX-propGA3-polymer conjugate was analyzed by gel permeation chromatography (GPC) using a Waters System (Waters Associates Inc., Milford, MA, USA) with refractive index (RI) and UV detection using two PLgel 5 µm MIXED-D columns (Agilent, Pal Alto, CA, city, state abbreviation, USA) and DMF containing 10 mM LiCl as eluent, with an injection volume of 100 µL, and flow rate of 1 mL/min at a temperature of 60°C. UV detection of DOX was performed at 480 nm.

The conjugation efficacy of DOX-propGA3-polymer conjugate was determined at a concentration of 0.5 mg/mL in phosphate-buffered saline (PBS). Calibration was done using DOX (10 to 100 μ g/mL in PBS). DOX concentration was determined by ultraviolet-visible (UV-vis) spectrophotometry (BMG Labtech, Offenburgcity, Germany) at an absorbance of 480 nm. The conjugation efficiency and loading capacity were calculated according to Equations (1) and (2), respectively.

$$\text{conjugation efficiency} = \frac{\text{amount of DOX - propGA3 conjugated to polymer}}{\text{amount of DOX - propGA3 feed}} \times 100\% \quad (1)$$

$$\text{loading capacity} = \frac{\text{amount of DOX - propGA3 conjugated to polymer}}{\text{amount of DOX - propGA3 - polymer conjugate}} \times 100\% \quad (2)$$

2.5. Preparation of DOX-propGA3-Nanogels

DOX-propGA3-nanogels were prepared by inverse mini-emulsion photo polymerization as previously described [39], Figure 1B. Briefly, 37.5 mg DOX-propGA3-polymer was dissolved in 412.5 μ L DMSO, and subsequently 150 μ L Irgacure 2959 (10 mg/mL in water) was added. This mixture was added to 5 mL mineral oil (containing 10% v/v ABIL EM 90) and thoroughly vortexed. The primary emulsion was ultra-sonicated (Bandelin Sonopuls, pulse on/off 0.5 s, and amplitude 10%) for 15 min and irradiated under UV (60% amplitude, 940 mW/cm², 300–650 nm, Bluepoint UVC source, Höonle UV technology, Gräfelfing, Germany) for 15 min. Subsequently, the mineral oil, surfactant, and DMSO were removed by washing the formed DOX-propGA3-nanogels once with acetone (40 mL) and four times with acetone/hexane (40 mL, 1:1, v/v). Finally, the DOX-propGA3-nanogels were recovered by re-dispersion in water and freeze drying.

The size of DOX-propGA3-nanogels was measured by dynamic light scattering (DLS) on an ALV CGS-3 system (Malvern Instruments, Malvern, UK) with a JDS Uniphase 22 mW He-Ne laser operating at 632.8 nm, an optical fiber-based detector, digital LV/LSE-5003 correlator at 25°C, expressed on intensity. The ζ potential of DOX-propGA3-nanogels was measured with Malvern Zetasizer Nano-Z (Malvern, UK) at 25°C. Measurements were performed in 20 mM HEPES buffer (pH 7.4) at a DOX-propGA3-nanogel concentration of 0.5 mg/mL.

2.6. Prodrug Conversion

Both DOX-propGA3-polymer and DOX-propGA3-nanogels were dispersed in phosphate buffered saline (PBS, pH 7.4, containing 0.049 M NaH₂PO₄, 0.099 M

Na_2HPO_4 and 0.006 M NaCl) containing 0.1% (w/v) bovine serum albumin (BSA) [39] to a final concentration of 100 $\mu\text{g}/\text{mL}$. This corresponds to a concentration of 7 $\mu\text{g}/\text{mL}$ DOX. Next, 50 μL of a stock solution of bovine β -GUS (2 mg/mL in PBS) was added to yield a final enzyme activity of 100 units/mL in a total volume of 2 mL. As a negative control, the DOX-propGA3-polymer and DOX-propGA3-nanogels were dispersed in the same buffer without bovine β -GUS. Samples were incubated in a water bath at 37°C. After incubation times ranging from 0 to 48h, 200 μL samples were taken at different time points and centrifuged (20,000 \times g for 60 min) at 4°C. Subsequently, DOX concentration in the supernatant was determined using UPLC analysis (Waters ACQUITY UPLC system (Waters Associates Inc., Milford, MA, USA)) using an Acquity BEH C18 column 1.7 μm (2.1 \times 50 mm); eluent A and B were potassium phosphate buffer (20 mM, pH 3)/acetonitrile (95/5, v/v) and 100% ACN, respectively. The injection volume was 5 μL , and fluorescence was detected at a wavelength of 560 nm (excitation wavelength of 480 nm). After an isocratic flow of 75% eluent A for 1 min, a gradient was run from 75 to 60% eluent A in 3 min with a flow rate of 0.5 mL/min. The retention time of DOX was 0.78 min. The calibration curve of DOX was linear between 0.01 and 10 $\mu\text{g}/\text{mL}$. Finally, chromatograms were analyzed by Empower Software, Version 1154.

2.7. Induction of β -GUS Liberated from 4T1 Cells by HIFU

Endogenous β -GUS was liberated from cells by exposing them to HIFU by an in-house developed HIFU system. HIFU was performed by a single-element transducer (external radius of aperture 120 mm, focal length 80 mm and focal point 1 \times 1 \times 3 mm³ (at -3dB)). Sine-shaped waves were generated by an AG Series Amplifier (AG 1006, T&C Power Conversion Inc. Rochester, NY, USA) at a frequency of 1.3 MHz, a pulse repetition time of 50 ms, a duty cycle of 1% (corresponding to 650 cycles per pulse), and a peak-negative pressure of 41 MPa; a schematic representation of the setup is present in Supplementary Figure 1. Acoustic pressures in the focal point were measured as a function of input voltage using a fiber optic hydrophone in a tank filled with degassed water, see [40] for details. Cells (2 \times 10⁶ cells in 170 μL PBS) in a PCR tube (200 μL , Bio rad, California, CA, USA) were exposed to HIFU by positioning this tube in the focus of the HIFU beam for 10 min. Immediately after exposure of the cells to HIFU, samples were placed on ice and either analyzed by microscopy or centrifuged at 16,000 \times g for 15 min at 4°C. The supernatant after centrifugation was further used to measure the β -GUS activity, conversion of DOX-propGA3-nanogels into DOX, and cytotoxicity in combination with DOX-propGA3-polymer and DOX-propGA3-nanogels, as described below.

2.8. Microscopy of Cells Exposed to HIFU

Samples of 10 μ L from cells exposed to HIFU and untreated cells (negative control) were taken and added to 240 μ L cell culture medium in an ibidi chamber of 1 μ -Slide 8 Well ibiTreat (Ibidi GmbH, Munich, Germany). Subsequently, samples were 1h incubated under normal culturing conditions, to allow attachment of the cells to the plate. Finally, samples were imaged by inverted microscopy (ULWCD 0.30, Olympus CK2, Tokyo city, Japan) with a digital camera (Moticam 5-5.0 MP, Hong Kongcity, China) using a 10 \times objective.

2.9. Determination of the β -GUS Activity

β -GUS activity in the supernatant of cells exposed to HIFU and untreated cells (negative control) was measured by a MUG assay adapted from Jefferson et al. [41]. Briefly, 20 μ l sample was added to 180 μ L 4-methylumbelliferyl β -D-glucuronide solution (1 mg/mL in 0.1 M sodium acetate (pH 4.5)) and incubated for 1h in a water bath of 37°C. Subsequently, 950 μ L of 0.2 M sodium carbonate (i.e., stopping buffer) was added to 50 μ L of all samples. Finally, the fluorescence intensity was measured using a spectrofluorometer (Jasco FP8300, Tokyo, Japan), excitation of 380 nm, and emission of 454 ± 5 nm. The enzyme activity was calculated based on the enzyme activity of commercial bovine β -GUS.

2.10. Conversion of DOX-propGA3-Nanogels into DOX by β -GUS Liberated from HIFU Treated Cells

Freeze-dried DOX-propGA3-nanogels were dispersed in 0.95 mL PBS containing 0.1% (w/v) BSA at a DOX concentration of 5 μ g/mL. Next, 50 μ L of the supernatant of cells exposed to HIFU was added and mixed carefully. After incubation in a water bath at 37°C for 48h, the solution was analyzed for DOX concentration by UPLC as described in section “prodrug conversion”.

2.11. In Vitro Cytotoxicity

In a 96 well plate, 4T1 cells were seeded at a density of 2,500 cells/well. After 24h, the cell culture medium was removed and 200 μ L of DOX, DOX-propGA3, DOX-propGA3-polymer, and DOX-propGA3-nanogels, in cell culture medium with PBS (10 μ L in 190 μ L cell culture medium); bovine β -GUS (50 μ g/mL, enzyme activity of 100 units/mL in cell culture medium); or supernatant of 4T1 cells exposed to HIFU (10 μ L in 190 μ L cell culture medium) was added to the wells at equivalent DOX concentrations ranging from 2 to 100,000 nM. After 24h incubation, cells were washed three times with 200 μ L PBS and 100 μ L fresh cell culture medium was added. Subsequently, MTS assay was performed

according to manufacturer's protocol. Briefly, 20 μL of MTS reagent was added to each well and incubated for 3h under normal culturing conditions. Finally, the optical density of the different samples was recorded by an EZ Read 400 microplate reader (Biochrom Ltd., Cambridge, UK) at an absorbance of 492 nm; an absorbance of 690 nm was used as background.

2.12. Statistical Analysis

All data is presented as mean, with error bars representing the standard deviation of at least three independent experiments. To determine differences in cytotoxicity, a two-tailed student's t-test was used to determine significance between the IC_{50} value of the different groups. Significant differences were considered as $p < 0.05$.

3. RESULTS AND DISCUSSION

3.1. Synthesis of DOX-propGA3-Polymer Conjugate and DOX-propGA3-Nanogels

P(HEMAm-co-AzEMAm) was synthesized by free radical polymerization using HEMAm and AzEMAm as monomers and ABCPA as initiator as described in detail in our previous publication [37]. The characteristics and $^1\text{H-NMR}$ spectrum of the obtained polymer are given in [37]. In the next step, the obtained p(HEMAm-co-AzEMAm) was further modified with HEMAm-Gly (a polymerizable group) to yield p(HEMAm-co-AzEMAm)-Gly-HEMAm [37].

The DOX-propGA3-polymer was synthesized from DOX-propGA3 prodrug, as shown in Figure 1A. The conjugation of DOX-propGA3 to the p(HEMAm-co-AzEMAm)-Gly-HEMAm was performed by Cu(I)-catalyzed azide-alkyne cycloaddition (CuAAC). In this conjugation, step sodium ascorbate was added as reducing agent to generate Cu(I) from the Cu(II) salt (CuSO_4) instead of directly adding active Cu(I) to the reaction since conjugation does not occur by using active Cu(I) in the reaction of this sterically hindered doxorubicin molecule with the bulky polymer [38]. After the reaction, the sample was dialyzed against an EDTA solution to remove Cu-ions and to avoid possible toxicity caused by this heavy metal, as mentioned before [42, 43]. The conjugation efficiency was rather high, 80.4%, as reported before by Hein and Fokin [44]. The synthesized DOX-propGA3-polymer conjugate contained 7 wt% DOX.

The DOX-propGA3-polymer conjugate was further characterized using GPC with dual UV (480 nm to detect DOX) and RI detection (Figure 2). The chromatogram of the physical mixture of p(HEMAm-co-AzEMAm)-Gly-HEMAm and DOX-propGA3 displayed a RI peak of the polymer with retention time of 12.4 min and a UV peak of the prodrug with retention time of 16.5 min (Figure 2A). After the click chemistry reaction, the obtained product eluted at 12.4 min (RI detection) and the UV peak shifted from 16.5 min to 12.4 min (Figure 2B), which demonstrates that DOX was indeed successfully conjugated to the polymer. A small peak was observed at the retention time of free DOX-propGA3. Calculation of the area under the curve of conjugated and free DOX-propGA3 prodrug shows that there was approximately 5% of free prodrug DOX-propGA3 present in the final product. This trace amount of free propGA3-DOX was most likely washed away during the nanogel preparation procedure and therefore not present in the final formulation added to the cells.

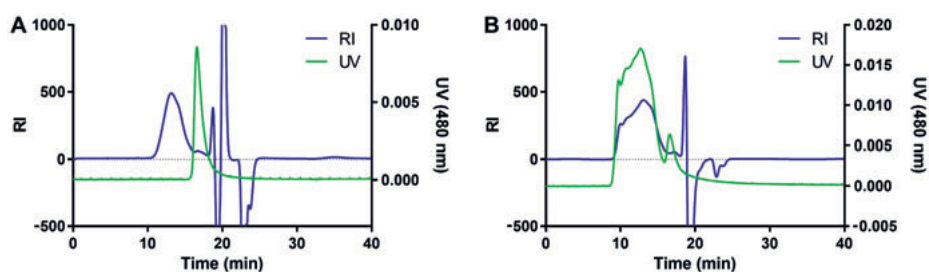


Figure 2. GPC analysis with dual refractive index (RI) and ultraviolet (UV) (480 nm) detection of (A) physical mixture of p(HEMAm-co-AzEMAm)-Gly-HEMAm and DOX-propGA3, and (B) DOX-propGA3-polymer conjugate.

The DOX-propGA3-polymer was subsequently used in the preparation of nanogels via mini-emulsion photopolymerization, Figure 1B. The methacrylamide groups at the side chain of the conjugate were crosslinked under UV. The size and ζ -potential of DOX-propGA3-nanogels were 164 nm (PDI 0.14) and -2.7 ± 0.1 mV, respectively, which was similar to empty nanogels (size 172 nm, PDI 0.16 and ζ -potential -2.5 ± 0.2 mV). This indicated that conjugation of DOX-propGA3 to the polymer did not affect the size and ζ -potential of the formed nanogels.

3.2. Conversion of Prodrug into DOX by Bovine β -GUS

Figure 3A shows the percentage converted DOX from the DOX-propGA3-polymers and DOX-propGA3-nanogels in the presence and absence of bovine β -GUS over time, in PBS supplemented with 0.1% BSA. Only in the presence of

bovine β -GUS were the DOX-propGA3-polymer and DOX-propGA3-nanogel converted into DOX. This indicates that there was no chemical conversion of DOX-propGA3 into DOX, which is in line with other prodrugs with similar structures [10, 14]. Complete conversion of DOX-propGA3-polymer and DOX-propGA3-nanogel into DOX was obtained after 24 and 48h, respectively. The complete conversion of DOX-propGA3-nanogel into DOX was slower than DOX-propGA3-polymer. This difference was most likely related to the difference in structure between DOX-propGA3-polymer and DOX-propGA3-nanogels. Since β -GUS has a rather high molecular weight (>300 kDa) [45], the β -GUS is not able to enter the nanogels. Therefore, the DOX-GA3 (a substrate of β -GUS) first needs to be released from the nanogels. The release of DOX-GA3 from the nanogel most likely takes place by either diffusion of DOX-GA3 out of the nanogels after hydrolysis of the ester between the triazole and DOX-GA3 or by nanogel degradation leading to (free) polymer chains, Figure 3B. Subsequently, the β -GUS is able to convert the DOX-GA3 into DOX, whereas for the DOX-propGA3-polymer only the ester group between the triazole and prodrug needs to be hydrolyzed before DOX-GA3 is released, that is, subsequently quickly converted into DOX by β -GUS. As a consequence, DOX formation from the nanogels was slower than from the polymer conjugate. In contrast, the conversion rate of DOX-propGA3-nanogel into DOX is much faster than previously designed micelles containing DOX-propGA3, viz. 100% conversion after 2 days incubation compared to 25–35% conversion after 4 days incubation [32, 38], respectively. This could be due to the lower water activity in the hydrophobic core of micelles, compared to the nanogels, resulting in a slower hydrolysis of the ester bond connecting the prodrug and the polymer backbone.

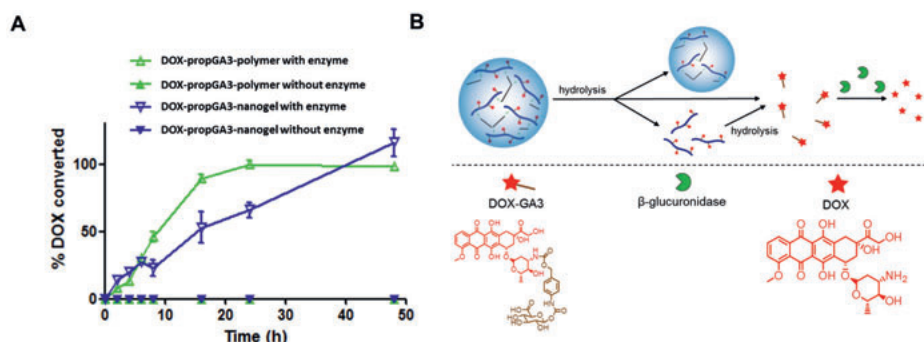


Figure 3: Conversion of DOX-propGA3-nanogels and DOX-propGA3-polymer into DOX. (A) Conversion profile of DOX from DOX-propGA3-polymer and DOX-propGA3-nanogels with or without bovine β -GUS at a concentration of 100 units/mL ($n = 3$). (B) Schematic representation of prodrug conversion from the nanogel into DOX.

3.3. Exposure of 4T1 Cells to HIFU and Conversion of Prodrug by HIFU Treated Cells

Figure 4 shows the microscopic images of untreated cells (A) and cells exposed to HIFU (B) at a magnification of 10 \times . Untreated cells were round and had a smooth surface, representing normal physiology of the cells 1h after plating. In the sample of cells exposed to HIFU, only cell debris was present and no viable cells were observed. The supernatant of cells exposed to HIFU contained a β -GUS enzyme activity of 7.3 ± 0.7 units/ 1×10^6 cells, whereas the supernatant of untreated cells contained a β -GUS enzyme activity of only 0.31 ± 0.1 units/ 1×10^6 cells. The supernatant of cells exposed to HIFU was able to convert the DOX-propGA3-nanogels completely into DOX within 48h. These results were in line with the DOX release results from DOX-propGA3-nanogels with bovine β -GUS.

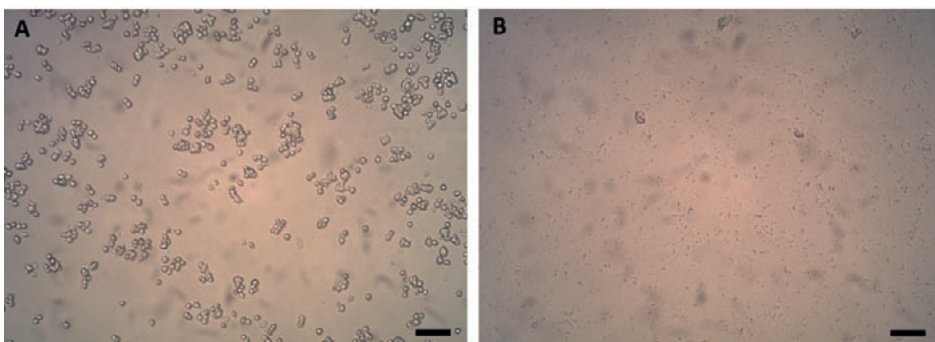


Figure 4. Bright field microscopy images with a magnification of 10 \times of (A) untreated cells and (B) cells after exposure to HIFU for 10 min with a peak negative pressure of 41 MPa; bar represents 500 μ m.

3.4. In Vitro Cytotoxicity

Figure 5 shows cell viability of cells treated with different concentrations of DOX, DOX-propGA3, DOX-propGA3-polymer, and DOX-propGA3-nanogels, in complete cell culture medium, supplemented with (A) PBS (negative control), (B) bovine β -GUS, and (C) supernatant of 4T1 cells exposed to HIFU. Treatment of cells with DOX-propGA3, DOX-propGA3-polymer, and DOX-propGA3-nanogels in complete cell culture medium supplemented with 5% PBS (Figure 5A) did not result in cytotoxicity, except for cells treated with DOX-propGA3-nanogels at a concentration of 1 mM, the highest concentration investigated. These results are in line with previous studies with comparable prodrugs [15, 38]. Cells treated with DOX-propGA3, DOX-propGA3-polymer, and DOX-propGA3-nanogel, in combination with bovine β -GUS at a concentration

of 50 $\mu\text{g/mL}$ (Figure 5B) and supernatant of cells exposed to HIFU (Figure 5C), experienced at an increase in concentration, resulting in a decrease in cell viability. Both bovine β -GUS and supernatant of cells exposed to HIFU significantly increased the cytotoxicity of the different prodrug formulations to a similar extent. In all conditions, cells treated with DOX showed the largest cytotoxicity (IC_{50} of 2,000 nM), Table 1. Lysate of cells exposed to HIFU caused limited cytotoxicity, and cell viability of $93.6 \pm 3.9\%$. In addition, empty nanogels have good cytocompatibility at the used concentrations [40]. This indicates that the cytotoxicity of the nanogels in combination with liberated β -GUS from cells exposed to HIFU was caused by the converted prodrug, released from the nanogels. The cytotoxicity of DOX was not influenced by the β -GUS or supernatant of cells exposed to HIFU. Therefore, DOX-propGA3-nanogel is a promising formulation since it only converts into DOX in the presence of β -GUS and it does not result in cytotoxicity in the absence of this enzyme.

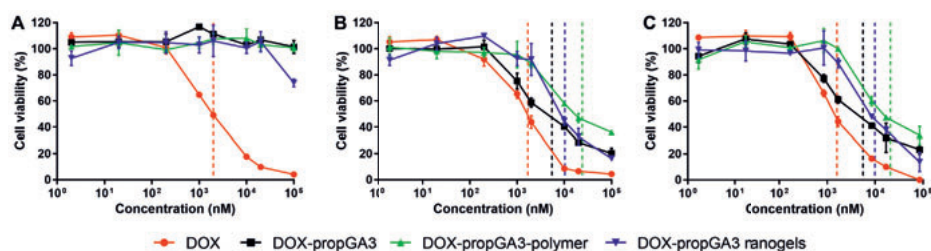


Figure 5. Viability of 4T1 cells incubated with doxorubicin (DOX), DOX-propGA3, DOX-propGA3-polymer, and DOX-propGA3-nanogels with PBS (A), bovine β -GUS (B), and supernatant of HIFU-treated cells (C) cells ($n = 3$). Dashed lines represent the IC_{50} of each treatment.

Table 1. IC_{50} (nM) of 4T1 cells incubated with DOX, DOX-propGA3, DOX-propGA3-polymer, and DOX-propGA3-nanogels, with PBS, bovine β -GUS, and supernatant of cells, exposed to HIFU. * $p < 0.05$ between PBS and bovine β -GUS or supernatant of cells exposed to HIFU.

	IC_{50} with PBS (nM)	IC_{50} with bovine β -GUS (nM)	IC_{50} with Supernatant of Cells Exposed to HIFU (nM)
DOX	$2,000 \pm 300$	$1,700 \pm 200$	$1,600 \pm 300$
DOX-propGA3	$>100,000$	$5,500 \pm 1,100^*$	$5,600 \pm 1,400^*$
DOX-propGA3-polymer	$>100,000$	$24,100 \pm 4,700^*$	$21,00 \pm 1,800^*$
DOX-propGA3 nanogels	$>100,000$	$10,300 \pm 1,800^*$	$9,900 \pm 1,100^*$

It has been observed before that nanogels can be internalized by cells by endocytosis and end in endosomes and lysosomes [25]. These lysosomes contain the β -GUS enzyme [46]. Therefore, specific activation of the prodrug into the cytotoxic drug could occur. However, the pH in these lysosomes is rather low (pH between 4.5 and 5 [47]). Since the hydrolysis rate of ester bonds is at a low pH [48], the hydrolysis of DOX-propGA3 into DOX-GA3 is hampered in these lysosomes. Therefore, DOX-propGA3-nanogels will not cause cytotoxicity in the normal cells when DOX-propGA3-nanogels are endocytosed in these cells.

These results motivate further *in vivo* testing of this proof of principle. *In vivo* experiments are required to optimize the tumor volume that is exposed to HIFU in order to liberate their β -GUS for prodrug conversion, released from nanogels, into the chemotherapeutic agent doxorubicin in order to kill the remaining tumor cells in the tumor margin.

4. CONCLUSIONS

A DOX-glucuronide prodrug (DOX-propGA3) was conjugated to the polymer p(HEMAm-co-AzEMAm)-Gly-HEMAm by click chemistry (to yield DOX-propGA3-polymer). Subsequently, this DOX-propGA3-polymer was used to prepare DOX-propGA3-nanogels. The glucuronide spacer was selectively cleaved by liberated β -GUS from cells exposed to HIFU. Furthermore, the supernatant of cells exposed to HIFU increased the cytotoxicity of DOX-propGA3-polymer and DOX-propGA3-nanogels due to liberated β -GUS from 4T1 cells. Therefore, DOX-propGA3-nanogels in combination with HIFU treatment of the tumor could be a novel and attractive therapeutic modality for anticancer therapy.

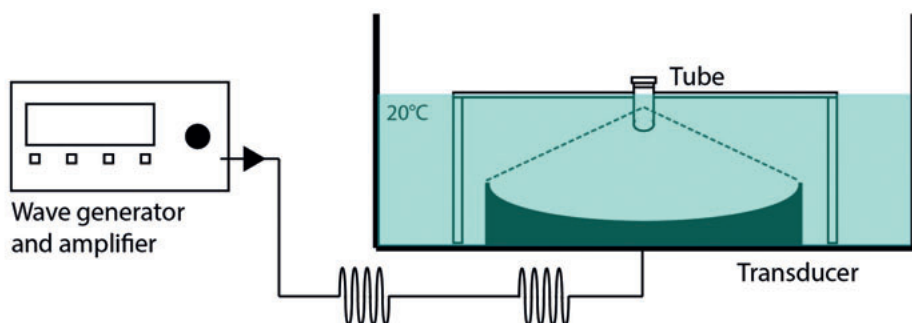
REFERENCES

1. Siegel RL, Miller KD, Jemal A: **Cancer statistics, 2019.** *CA Cancer J Clin* 2019, **69**:7-34.
2. Beijers AJ, Jongen JL, Vreugdenhil G: **Chemotherapy-induced neurotoxicity: the value of neuroprotective strategies.** *Neth J Med* 2012, **70**:18-25.
3. Riddell E, Lenihan D: **The role of cardiac biomarkers in cardio-oncology.** *Curr Probl Cancer* 2018, **42**:375-385.
4. Speth PA, van Hoesel QG, Haanen C: **Clinical pharmacokinetics of doxorubicin.** *Clin Pharmacokinet* 1988, **15**:15-31.
5. Delahousse J, Skarbek C, Paci A: **Prodrugs as drug delivery system in oncology.** *Cancer Chemother Pharmacol* 2019, **84**:937-958.
6. Denny WA: **Prodrug strategies in cancer therapy.** *Eur J Med Chem* 2001, **36**:577-595.
7. Kratz F, Muller IA, Rypa C, Warnecke A: **Prodrug strategies in anticancer chemotherapy.** *ChemMedChem* 2008, **3**:20-53.
8. Tietze LF, Krewer B: **Antibody-directed enzyme prodrug therapy: a promising approach for a selective treatment of cancer based on prodrugs and monoclonal antibodies.** *Chem Biol Drug Des* 2009, **74**:205-211.
9. Houba PH, Boven E, van der Meulen-Muileman IH, Leenders RG, Scheeren JW, Pinedo HM, Haisma HJ: **A novel doxorubicin-glucuronide prodrug DOX-GA3 for tumour-selective chemotherapy: distribution and efficacy in experimental human ovarian cancer.** *Br J Cancer* 2001, **84**:550-557.
10. Houba PH, Boven E, van der Meulen-Muileman IH, Leenders RG, Scheeren JW, Pinedo HM, Haisma HJ: **Pronounced antitumor efficacy of doxorubicin when given as the prodrug DOX-GA3 in combination with a monoclonal antibody beta-glucuronidase conjugate.** *Int J Cancer* 2001, **91**:550-554.
11. Wang SM, Chern JW, Yeh MY, Ng JC, Tung E, Roffler SR: **Specific activation of glucuronide prodrugs by antibody-targeted enzyme conjugates for cancer therapy.** *Cancer Res* 1992, **52**:4484-4491.
12. Bosslet K, Straub R, Blumrich M, Czech J, Gerken M, Sperker B, Kroemer HK, Gesson JP, Koch M, Monneret C: **Elucidation of the mechanism enabling tumor selective prodrug monotherapy.** *Cancer Res* 1998, **58**:1195-1201.
13. Sperker B, Werner U, Mordt TE, Tekkaya C, Fritz P, Wacke R, Adam U, Gerken M, Drewelow B, Kroemer HK: **Expression and function of beta-glucuronidase in pancreatic cancer: potential role in drug targeting.** *Naunyn Schmiedebergs Arch Pharmacol* 2000, **362**:110-115.
14. de Graaf M, Boven E, Scheeren HW, Haisma HJ, Pinedo HM: **Beta-glucuronidase-mediated drug release.** *Curr Pharm Des* 2002, **8**:1391-1403.
15. de Graaf M, Nevalainen TJ, Scheeren HW, Pinedo HM, Haisma HJ, Boven E: **A methylester of the glucuronide prodrug DOX-GA3 for improvement of tumor-selective chemotherapy.** *Biochem Pharmacol* 2004, **68**:2273-2281.
16. Gentile E, Cilurzo F, Di Marzio L, Carafa M, Ventura CA, Wolfram J, Paolino D, Celia C: **Liposomal chemotherapeutics.** *Future Oncol* 2013, **9**:1849-1859.
17. Shimanovich U, Bernardes GJ, Knowles TP, Cavaco-Paulo A: **Protein micro- and nano-capsules for biomedical applications.** *Chem Soc Rev* 2014, **43**:1361-1371.

18. Siepmann J, Faham A, Clas SD, Boyd BJ, Jannin V, Bernkop-Schnurch A, Zhao H, Lecommandoux S, Evans JC, Allen C, et al: **Lipids and polymers in pharmaceutical technology: Lifelong companions.** *Int J Pharm* 2019, **558**:128-142.
19. van der Meel R, Sulheim E, Shi Y, Kiessling F, Mulder WJM, Lammers T: **Smart cancer nanomedicine.** *Nat Nanotechnol* 2019, **14**:1007-1017.
20. Yallapu MM, Jaggi M, Chauhan SC: **Design and engineering of nanogels for cancer treatment.** *Drug Discov Today* 2011, **16**:457-463.
21. Zhou H, Ichikawa A, Ikeuchi-Takahashi Y, Hattori Y, Onishi H: **Nanogels of Succinylated Glycol Chitosan-Succinyl Prednisolone Conjugate: Preparation, In Vitro Characteristics and Therapeutic Potential.** *Pharmaceutics* 2019, **11**.
22. Yin Y, Hu B, Yuan X, Cai L, Gao H, Yang Q: **Nanogel: A Versatile Nano-Delivery System for Biomedical Applications.** *Pharmaceutics* 2020, **12**.
23. Chacko RT, Ventura J, Zhuang J, Thayumanavan S: **Polymer nanogels: a versatile nanoscopic drug delivery platform.** *Adv Drug Deliv Rev* 2012, **64**:836-851.
24. Hamidi M, Azadi A, Rafiei P: **Hydrogel nanoparticles in drug delivery.** *Adv Drug Deliv Rev* 2008, **60**:1638-1649.
25. Li D, van Nostrum CF, Mastrobattista E, Vermonden T, Hennink WE: **Nanogels for intracellular delivery of biotherapeutics.** *J Control Release* 2017, **259**:16-28.
26. Fang J, Nakamura H, Maeda H: **The EPR effect: Unique features of tumor blood vessels for drug delivery, factors involved, and limitations and augmentation of the effect.** *Adv Drug Deliv Rev* 2011, **63**:136-151.
27. Soni KS, Desale SS, Bronich TK: **Nanogels: An overview of properties, biomedical applications and obstacles to clinical translation.** *J Control Release* 2016, **240**:109-126.
28. Denny WA: **Tumor-activated prodrugs--a new approach to cancer therapy.** *Cancer Invest* 2004, **22**:604-619.
29. Han HK, Amidon GL: **Targeted prodrug design to optimize drug delivery.** *AAPS PharmSci* 2000, **2**:E6.
30. Xu G, McLeod HL: **Strategies for enzyme/prodrug cancer therapy.** *Clin Cancer Res* 2001, **7**:3314-3324.
31. Antunes IF, Haisma HJ, Elsinga PH, Di Gialleonardo V, van Waarde A, Willemsen AT, Dierckx RA, de Vries EF: **Induction of beta-glucuronidase release by cytostatic agents in small tumors.** *Mol Pharm* 2012, **9**:3277-3285.
32. Ruiz-Hernandez E, Hess M, Melen GJ, Theek B, Talelli M, Shi Y, Ozbakir B, Teunissen EA, Ramirez M, Moeckel D, et al: **PEG-pHPMAm-based polymeric micelles loaded with doxorubicin-prodrugs in combination antitumor therapy with oncolytic vaccinia viruses.** *Polym Chem* 2014:1674-1681.
33. Zhang J, Kale V, Chen M: **Gene-directed enzyme prodrug therapy.** *AAPS J* 2015, **17**:102-110.
34. Bagshawe KD, Sharma SK, Springer CJ, Rogers GT: **Antibody directed enzyme prodrug therapy (ADEPT). A review of some theoretical, experimental and clinical aspects.** *Ann Oncol* 1994, **5**:879-891.
35. Sharma SK, Bagshawe KD: **Antibody Directed Enzyme Prodrug Therapy (ADEPT): Trials and tribulations.** *Adv Drug Deliv Rev* 2017, **118**:2-7.
36. Hill CR, ter Haar GR: **Review article: high intensity focused ultrasound--potential for cancer treatment.** *Br J Radiol* 1995, **68**:1296-1303.

37. Chen Y, Tezcan O, Li D, Beztsinna N, Lou B, Etrych T, Ulbrich K, Metselaar JM, Lammers T, Hennink WE: **Overcoming multidrug resistance using folate receptor-targeted and pH-responsive polymeric nanogels containing covalently entrapped doxorubicin.** *Nanoscale* 2017, **9**:10404-10419.
38. Talelli M, Morita K, Rijcken CJ, Aben RW, Lammers T, Scheeren HW, van Nostrum CF, Storm G, Hennink WE: **Synthesis and characterization of biodegradable and thermosensitive polymeric micelles with covalently bound doxorubicin-glucuronide prodrug via click chemistry.** *Bioconjug Chem* 2011, **22**:2519-2530.
39. Chen Y, van Steenberg MJ, Li D, van de Dikkenberg JB, Lammers T, van Nostrum CF, Metselaar JM, Hennink WE: **Polymeric Nanogels with Tailorable Degradation Behavior.** *Macromol Biosci* 2016, **16**:1122-1137.
40. Ramaekers P, de Greef M, van Breugel JM, Moonen CT, Ries M: **Increasing the HIFU ablation rate through an MRI-guided sonication strategy using shock waves: feasibility in the in vivo porcine liver.** *Phys Med Biol* 2016, **61**:1057-1077.
41. Jefferson RA, Kavanagh TA, Bevan MW: **GUS fusions: beta-glucuronidase as a sensitive and versatile gene fusion marker in higher plants.** *EMBO J* 1987, **6**:3901-3907.
42. Hein CD, Liu XM, Wang D: **Click chemistry, a powerful tool for pharmaceutical sciences.** *Pharm Res* 2008, **25**:2216-2230.
43. Presolski SI, Hong VP, Finn MG: **Copper-Catalyzed Azide-Alkyne Click Chemistry for Bioconjugation.** *Curr Protoc Chem Biol* 2011, **3**:153-162.
44. Hein JE, Fokin VV: **Copper-catalyzed azide-alkyne cycloaddition (CuAAC) and beyond: new reactivity of copper(I) acetylides.** *Chem Soc Rev* 2010, **39**:1302-1315.
45. Jain S, Drendel WB, Chen ZW, Mathews FS, Sly WS, Grubb JH: **Structure of human beta-glucuronidase reveals candidate lysosomal targeting and active-site motifs.** *Nat Struct Biol* 1996, **3**:375-381.
46. Naz H, Islam A, Waheed A, Sly WS, Ahmad F, Hassan I: **Human beta-glucuronidase: structure, function, and application in enzyme replacement therapy.** *Rejuvenation Res* 2013, **16**:352-363.
47. Mindell JA: **Lysosomal acidification mechanisms.** *Annu Rev Physiol* 2012, **74**:69-86.
48. Deshmukh M, Chao P, Kutscher HL, Gao D, Sinko PJ: **A series of alpha-amino acid ester prodrugs of camptothecin: in vitro hydrolysis and A549 human lung carcinoma cell cytotoxicity.** *J Med Chem* 2010, **53**:1038-1047.

SUPPLEMENTARY INFORMATION



Supplementary Figure 1: Schematic representation of the in-house-build HIFU setup, consisting of a transducer, an amplifier, an oscilloscope, a wave generator, a hydrophone, and a sample holder. HIFU was performed by a single element focused ultrasound transducer (Imasonic, Besançon, France). During HIFU treatment, a PCR tube (Bio rad, California, USA), containing the sample, was positioned in the sample holder in the focus of the ultrasound beam

CHAPTER 6

Summary and general discussion

CHAPTER 6.1 SUMMARY

The goal of this thesis was to improve local drug deposition in the primary tumor by physical activation of temperature sensitive liposomes (TSL) and prodrugs. Chemotherapy is, along with radiotherapy and surgery, one of the cornerstones in cancer therapy. It is often systemically administered to the patient, hence it exposes the primary tumor, but also the metastases. Since local control of the primary tumor is of utmost importance to restrict metastatic disease [1-3], it is of utmost importance to effectively treat the primary tumor. To achieve this, drug exposure in the tumor should be sufficient, *i.e.* high enough drug concentration for a sufficient exposure duration. Due to the systemic drug administration and the non-specific tumor targeting of these drugs, normal tissues are also exposed to them, adding constraints in the drug dosing. This limitation stresses the clear clinical need for local drug delivery in the primary tumor.

In chapter 2 and 3 temperature sensitive liposomes in combination with hyperthermia were investigated as a means to introduce triggered radiosensitization and enhance drug delivery in the primary tumor.

In the clinic, chemotherapy and radiotherapy are in some specific cases combined to improve the efficacy of radiotherapy in the primary tumor, so called chemoradiation. Since the chemotherapeutic agent does not specifically target tumor tissue, the normal tissue located in the radiation beam path is also sensitized to the radiation, causing unwanted toxicities in these tissues. To address this limitation, in **chapter 2** the concept of triggered radiosensitizer delivery by TSLs was introduced and investigated *in vitro*. The aim of triggered radiosensitizer delivery is to increase the intratumoral radiosensitizer concentration, while reducing its concentration in the normal tissue, in particular normal tissues located in the beam path. To do so, ThermoDox was used, a TSL containing doxorubicin (DOX), a chemotherapeutic agent with radiosensitizing properties. Only upon concurrent treatment of ThermoDox and hyperthermia, ThermoDox sensitized the cells to radiotherapy. This observation indicates that radiosensitization only occurred upon triggered release of DOX from ThermoDox by hyperthermia. Since the mechanism of action of DOX, hyperthermia and radiotherapy influence each other when applied simultaneously or in short succession, *i.e.* I) DOX is a radiosensitizer, II) hyperthermia has a radiosensitization effect and III) hyperthermia enhanced DOX cytotoxicity; the order of the different treatment modalities was expected

to be important to achieve the highest radiosensitization. Though, in this study concurrent DOX administration and hyperthermia before or after radiotherapy resulted in a comparable radiosensitization effect. Whereas these results demonstrate the potential of the concept of triggered radiosensitizer delivery by TSLs *in vitro*, future research will confirm whether similar results can be obtained *in vivo*.

The efficacy of chemotherapy treatment depends, among others, on the intratumoral drug concentration and spatial drug distribution [4-6]. In **chapter 3** intratumoral DOX concentration and spatial distribution obtained upon different doses of I) ThermoDox (TSL) in combination with hyperthermia treatment and II) DOXIL (non-temperature sensitive liposome) were compared with those collected after free DOX administration *in vivo* in a subcutaneous humane fibrosarcoma model. An increase in injected dose was found to result in an increase in overall survival, for all formulations. Importantly, ThermoDox treatment led to the largest survival at low and medium doses, whereas at the highest dose DOXIL treatment resulted in the largest survival. Intratumoral DOX concentrations and spatial DOX distributions were determined by fluorescence confocal microscopy of the tumor tissue *ex vivo*. Intratumoral DOX concentrations were increased with an increase in administered dose, for all drug formulations. For all dosages, the intratumoral DOX concentration was always the highest after ThermoDox treatment, compared to DOXIL and free DOX treatment. With respect to the spatial drug distribution, an increase in injected dose resulted in a more homogeneous intratumoral DOX distribution, for all formulations. Interestingly, no correlation could be established between the survival after treatment with the different encapsulation formulations and intratumoral drug concentration and spatial drug distribution. Nonetheless, this study indicates that the intratumoral drug concentration and distribution are key factors for effective treatment, although the link between the use of specific DOX-encapsulation formulations and the resulting intratumoral drug distribution remains to be further established.

Besides exogenous triggers, like hyperthermia, local drug delivery could also be achieved by endogenous triggers, such as enzymes in enzyme prodrug therapy, as described in chapter 4 and 5. For effective enzyme prodrug therapy there should be I) a quick conversion of prodrug into the cytotoxic drug, II) a high enzyme concentration available for prodrug conversion in the tumor and III) a low bioavailable enzyme concentration in the normal tissue. Glucuronide-prodrugs are widely investigated for enzyme prodrug therapy.

They are converted by the enzyme β -glucuronidase (β -GUS) into the cytotoxic drug and consist of a glucuronic acid, a spacer and a cytotoxic drug, of which the glucuronic acid is cleaved by the β -GUS, followed by hydrolysis of the spacer and finally releasing the cytotoxic drug.

Since a rather short size of the spacer hinders a fast cleaving of the glucuronic acid by the β -GUS, in **chapter 4** two glucuronide-prodrugs were synthesized with a double and triple elongation of the spacer (DOX-AU2 and DOX-AU3). The conversion rate of DOX-AU2 and DOX-AU3 into DOX was increased compared to DOX-GA3 (DOX-AU1), as expected. To increase the bioavailable β -GUS concentration in the tumor, the concept of ultrasound directed enzyme prodrug therapy (UDEPT) was introduced and investigated *in vitro*. In this concept cells are exposed to high-intensity focused ultrasound (HIFU) to liberate their β -GUS content. The mechanical bio-effects of HIFU were able to liberate β -GUS from cells, in a peak-negative pressure and time dependent manner, upon a threshold peak-negative pressure. The liberated β -GUS was able to convert DOX-AU2 into DOX and increased the cytotoxicity of DOX-AU2 to a similar extend as DOX. Although these results indicate the potential of spacer elongation in the prodrug formulation and UDEPT *in vitro*, further research should confirm if similar results can be obtained *in vivo*.

Prodrugs are often rather small molecular drugs, hence they are quickly excreted from the body. To solve this problem, in **chapter 5** the prodrug DOX-GA3 (DOX-AU1) was conjugated to a polymer (prodrug-polymer conjugate) and subsequently encapsulated into a nanogel formulation. The conversion rate of the newly synthesized nanogel into DOX was slightly decreased compared to conversion of un-encapsulated DOX-GA3 into DOX. Most likely since β -GUS was not able to penetrate into the nanogel, therefore the prodrug first had to be released from the nanogel before it was converted into the cytotoxic agent. This nanogel was finally investigated *in vitro* in combination with the UDEPT concept. The liberated β -GUS from the cells after exposed to HIFU were able to convert the prodrug from the nanogel into DOX and increased the cytotoxicity of the prodrug. This concept should be further investigated *in vivo* with the DOX-AU2 prodrug.

CHAPTER 6.2 GENERAL DISCUSSION

The goal of this thesis was to improve local drug deposition in the primary tumor by the local drug delivery approaches: I) temperature sensitive liposomes (TSLs) in combination with hyperthermia and II) prodrugs in combination with the mechanical bio-effects of high-intensity focused ultrasound (HIFU). Both topics are discussed below.

Temperature sensitive liposomes in combination with hyperthermia

In the clinic, chemotherapy is in some specific cases combined with radiotherapy to improve the efficacy of the radiotherapy treatment on the primary tumor, so called chemoradiation. Since most chemotherapeutic agents with radiosensitizing properties are not tumor cell specific, also normal tissue is sensitized to the radiotherapy treatment. This leads to unwanted toxicities, especially in normal tissue located in the beam path of radiotherapy. Chapter 2 shows the potential of the concept of triggered radiosensitizer delivery by TSL containing the radiosensitizer doxorubicin (DOX) in combination with hyperthermia to only cause radiosensitization of cells upon triggered release of the liposomes by hyperthermia. Incubation of cells with ThermoDox (TSL) at 37°C did not result in any cytotoxicity, whereas at 43°C ThermoDox resulted in equal cytotoxicity compared to DOX. In addition, ThermoDox at 37°C did not result in any radiosensitization. However, at 43°C, ThermoDox and DOX resulted in comparable radiosensitization of the cells. Hence, for a radiosensitizing of the tumor cells *in vitro* TSL and hyperthermia treatment need to be concurrently combined, which requires further investigation *in vivo*. Although the mechanism of action of DOX, hyperthermia and radiotherapy influence each other when applied simultaneously or in short succession, the degree of sensitization of the cells to radiotherapy by exposing them to DOX at 43°C was similar when triggered radiosensitizer delivery was applied before or after radiotherapy treatment.

For effective chemotherapy treatment, the drug concentration should be high and homogeneously distributed in the tumor [4-6], among others. These requirements are in line with chapter 3 within the use of different concentration of one DOX encapsulation formulation, i.e. un-encapsulated (free) DOX, DOXIL and ThermoDox. Though, in a head-to-head comparison between the different formulations, survival was not correlated with drug concentration and spatial drug distribution in the tumor. Animals bearing a subcutaneous human fibrosarcoma were treated with different concentrations of free DOX,

DOXIL (non-temperature sensitive liposome (NTSL)) and ThermoDox (TSL). Only tumors of animals treated with ThermoDox were after drug administration treated with hyperthermia for 1 hour by placing the tumor in a water bath of 42°C. For each formulation, an increase in injected dose resulted in an increase in survival, an increased intratumoral drug concentration and a more homogeneous drug distribution in the tumor. In addition, tumor areas with high drug concentrations were correlated with a low amount of proliferating cells, indicating an early tumor response. In comparison of different formulations at low and intermediate doses, ThermoDox treatment resulted in the largest increase in survival, whereas at the highest dose DOXIL treatment resulted in the largest survival increase. In this head-to-head comparison no correlation was observed between survival, intratumoral drug concentration and spatial drug distribution.

More potent radiosensitizer for triggered radiosensitizer delivery

In the triggered radiosensitizer delivery study the TSL formulation ThermoDox was used, containing DOX, a chemotherapeutic agent with radiosensitizing properties. Although DOX is known for its radiosensitizing properties [7-11], in clinical practice it is not used as such, due to its severe toxicities in normal tissue located in the radiation beam path [9-11]. In clinical practice, there are other chemotherapeutic agents available that are more frequently used for its radiosensitizing properties, like cisplatin [12] and gemcitabine [13], which can be encapsulated in a TSL [14,15]. In addition, the cytotoxicity of both cisplatin and gemcitabine is increased by hyperthermia treatment [16,17], making chemoradiation treatment with these radiosensitizers possibly even more effective. Though, the synthesized TSLs containing cisplatin and gemcitabine have a rather low loading efficiency, 10% [18] and 1.5 to 2.5% [19] respectively, compared to ThermoDox, which has a loading efficiency of almost 100%. Since the loading efficiency of the TSLs containing cisplatin and gemcitabine is rather low, a high concentration of lipids needs to be injected in the patient to achieve an effective drug concentration in the tumor, which could lead to systemic toxicity of the lipids [19]. For effective triggered radiosensitizer delivery it is important that liposomes have a high loading efficiency to avoid unwanted toxicities by the lipids.

Besides chemotherapeutic agents that have radiosensitization properties, there are also drugs available that only sensitize the tumor cells to radiotherapy and have no cytotoxic effect on their own, so called 'true' radiosensitizer, like nitroimidazoles [20]. Though, nitroimidazoles induce severe neurotoxicity [21],

limiting the administration dose to the patient. Therefore, they could be a good candidate for the concept of local triggered radiosensitizer delivery. By encapsulating these nitroimidazoles in TSLs the neurotoxicity will likely be reduced, whereas upon triggering of the TSLs in the tumor the radiosensitizer is released from the TSLs and they will subsequently sensitize the tumor to radiotherapy. Encapsulation of the nitroimidazole pimonidazole in a TSL has been proven feasible. In addition, only upon triggered release pimonidazole sensitizes the tumor to radiotherapy, *in vitro* [22]. This study indicates that 'true' radiosensitizers might benefit from the local triggered radiosensitizer delivery to increase their efficacy.

From in vitro to in vivo

Based on *in vitro* results presented in this thesis, the concept of local triggered radiosensitizer delivery might be very promising *in vivo*, since I) cells were only sensitized to radiotherapy treatment by DOX released from the TSLs when heated to 43°C, chapter 2, that will likely result in only radiosensitizer delivery in the heated tumor and II) the tumor drug concentration is higher after treatment with TSL treatment compared to free drug, chapter 3, which likely indicates that the radiosensitizer concentration is increased in the tumor upon treatment with TSL compared to free radiosensitizer administration. As shown before for TSLs *in vivo*, its payload is only released upon triggering by local hyperthermia [23,24], which likely indicates that in the treatment with TSL containing a radiosensitizer the normal tissue is not sensitized to radiotherapy. Local drug release from TSLs increase the drug concentration in the tumor, compared to free drug treatment as observed in chapter 3 and by others [25-27]. Since an increase in radiosensitizer concentration results in increased radiosensitization, as observed in chapter 2, *in vitro*, and by others [28,29], the increased radiosensitizer concentration in the tumor by the concept of local triggered radiosensitizer delivery might lead to increased radiosensitization of the tumor. Hence, these *in vitro* results in the triggered radiosensitizer delivery study are encouraging to further investigate the concept of local triggered radiosensitizer delivery *in vivo*.

Intratumoral drug distribution

As mentioned before, the efficacy of the chemotherapeutic agent depends, among others, on intratumoral drug concentration and spatial drug distribution [4-6]. An increase in injected dose was correlated with an increase in survival, increase in intratumoral drug concentration and a more homogeneous drug distribution in the tumor within the treatment of one encapsulation formulation,

i.e. free DOX, DOXIL (NTSL) and ThermoDox (TSL). Interestingly, no correlation could be established between the survival after treatment with the different encapsulation formulation and intratumoral drug concentration and spatial drug distribution. It is known that the intratumoral DOX concentration changes over time, and that these changes are formulation dependent [30]. Whereas after free DOX [30] and ThermoDox treatment [24] the peak bioavailable DOX concentration in the tumor is quickly reached after injection and triggering, respectively, after DOXIL treatment the peak bioavailable DOX concentration in the tumor is reached after 24 hours [30]. In addition, the intratumoral spatial free DOX distribution changes over time, as observed by Uster and colleagues for DOXIL [31], in a small part within the tumor. Therefore, the efficacy of the chemotherapeutic agent might not only depend on the intratumoral drug concentration and spatial distribution at one moment in time, but on its variation over time. This concept should be further investigated *in vivo*, in order to fundamentally understand the relationship between efficacy of a chemotherapeutic agent and its intratumoral concentration and spatial distribution over time. One of the possibilities to investigate the intratumoral drug concentration and spatial distribution over time *in vivo* is by synthesizing a radioactively labeled drug, with a long radioactive half-life, in combination with SPECT imaging to enable mini-invasive measurements of the drug concentration and spatial distribution within one animal in the whole tumor over time [32-34].

Towards clinical approval

In pre-clinical studies, local chemotherapy treatment of the primary tumor by TSLs in combination with hyperthermia has shown promising results to increase the efficacy of chemotherapy treatment [24,27]. To evaluate TSLs and local hyperthermia in clinical studies, the following suggestions are proposed for a smooth translation towards clinical approval.

Many pre-clinical TSL studies use their own synthesized TSLs. This leads to small differences between the TSL formulations, like differences in phase transition temperature (T_m), release kinetics and liposomal stability [23,35-37]. It is of utmost importance to synthesize and investigate these different TSLs to develop a most favorable TSL formulation for the local drug delivery concept. Though, for clinical translatability of TSLs, it is also important to investigate standardized TSLs in pre-clinical studies as well. ThermoDox by Celision and ThermoSome by ThermoSome GmbH are good examples of these temperature sensitive liposomes that are patented. Pre-clinical studies with ThermoDox

have led to the clinical ThermoDox studies in liver and breast cancer and in pediatric refractory solid tumors [38].

For local radiosensitizer and drug delivery by TSLs, it is important that only the tumor is heated to temperatures in the range of 41 to 42°C, *i.e.* hyperthermia treatment, and maintained for 1 hour [39], for effective treatment of the tumor and avoiding toxicities in the normal tissue. There are already many strategies available for hyperthermia treatment in the clinic, among them radiofrequency, capacitive heating, water-filtered infrared-A, microwave and focused ultrasound [40,41]. Currently, hyperthermia treatment by microwaves [42] and focused ultrasound are under clinical evaluation in combination with ThermoDox [38,43]. Since temperature monitoring is important for effective treatment, thermocouples are often inserted in or near the tumor [42], which is invasive. A non-invasive method to monitor the tumor temperature is by MR thermometry. Currently, hyperthermia by high-intensity focused ultrasound has been integrated in a MRI, MRgHIFU, for tumor temperature monitoring, which is under clinical investigation in combination with TSL treatment [38].

Prodrugs in combination with mechanical HIFU

In order to achieve effective enzyme prodrug therapy treatment, the following requirements are of major importance; I) quick enzymatic conversion of the prodrug into the cytotoxic drug, II) high concentration of the enzyme in the tumor and III) absence of the enzyme in the normal tissue [44,45]. Chapter 4 shows the potential of improving the activation of a glucuronide-prodrug by A) increasing the length of the spacer to reduce steric hindrance, increasing its conversion rate, and B) increasing the amount of bioavailable enzymes for prodrug conversion in the tumor by the concept ultrasound directed enzyme prodrug therapy (UDEPT). The conversion rate of the glucuronide-prodrug into its cytotoxic agent DOX was increased by the newly synthesized prodrugs DOX-AU2 and DOX-AU3 with a double and triple spacer, respectively, compared to the prodrug DOX-AU1 (DOX-GA3) with a single spacer. The conversion rates of DOX-AU2 and DOX-AU3 were comparable. The activation of the glucuronide-prodrug depends also highly on the bioavailable β -glucuronidase (β -GUS) concentration. Cells exposed to high-intensity focused ultrasound (HIFU) liberated their endogenous β -GUS content, in a peak-negative pressure and exposure time dependent manner. Exposure of β -GUS to HIFU had limited effect on its activity. The liberated β -GUS from HIFU-exposed cells was able to convert DOX-AU2 into DOX and increased the cytotoxicity of DOX-AU2 to a similar extent as DOX.

Prodrugs are often small molecules that are quickly excreted from the body [46]. To address this issue, in chapter 5 a nanogel containing the prodrug DOX-GA3 (DOX-AU1) was successfully synthesized and characterized. The prodrug DOX-propGA3 was successfully coupled to a polymer (DOX-propGA3-polymer). Subsequently, the DOX-propGA3-polymer was encapsulated in a nanogel formulation. The encapsulation of the DOX-propGA3-polymer did not affect the size and ζ -potential of the nanogel. The prodrugs encapsulated in the nanogels were only in the presence of β -GUS converted into DOX, though the conversion rate was slower compared to conversion of DOX-propGA3-polymer into DOX. This is most likely related to the rather large molecular weight of the β -GUS, hampering diffusion of the β -GUS into the nanogels. The nanogels did not cause cytotoxicity on their own, whereas in combination with bovine β -GUS or liberated β -GUS from HIFU-exposed cells, nanogels were able to cause cytotoxicity, that was similar for nanogels in combination with bovine β -GUS and liberated β -GUS from HIFU-exposed cells. Though this cytotoxicity was 5 to 10 times lower compared to free DOX, *in vitro*.

Choice of the chemotherapeutic agent

In the prodrug studies, the glucuronide-prodrugs contained the chemotherapeutic agent DOX, a frequently used chemotherapeutic agent in the clinic. In order to obtain a self-sustaining system for enzyme prodrug therapy, as proposed by Antunes et al. [47], the cytotoxic drug should induce cell death by necrosis, in order to liberate their endogenous β -GUS content [48]. Since DOX induces cell death mainly by apoptosis [49], endogenous β -GUS is not liberated upon DOX exposure. Other chemotherapeutic agents, like carmustine [50], TNF- α [51], cisplatin [52] and taxol [53], do induce cell death by necrosis, and will therefore cause β -GUS liberation upon cell death. From these chemotherapeutic agents only taxol has previously been synthesized into a glucuronide-prodrug formulation [54]. In addition, there is some evidence that synthesizing a platinum complex into a glucuronide-prodrug is feasible [55]. Using these drugs in the concept of UDEPT, a self-sustaining system could be obtained. In this self-sustaining system, HIFU might be used to induce destruction of the tumor cells, in order to non-invasively initiate the first β -GUS liberation from the tumor cells, subsequently the β -GUS concentration will be maintained by β -GUS liberation from cells that die by necrosis upon drug exposure.

Optimization of HIFU parameters to move from in vitro towards in vivo

In chapter 4 and 5 of this thesis, β -GUS liberation from cells was investigated by exposing a cell suspension to HIFU. Subsequently, the liberated β -GUS was combined with the prodrug to investigate conversion of the prodrug or the prodrug was added to fresh cells, to investigate the cytotoxicity of the combination. This is an important first step to investigate the potency of β -GUS liberation from HIFU-exposed cells for enzyme prodrug therapy treatment, however, further studies are required to determine the efficacy of UDEPT *in vivo*.

Currently, the exact underlying mechanism of β -GUS liberation from HIFU-exposed cells in the UDEPT concept is unknown. The β -GUS liberation from these cells most likely occurs by cavitation, since I) the minimum required peak-negative pressure for β -GUS liberation is in line with the cavitation threshold of water [56] and II) an increase in peak-negative pressure, above the threshold pressure, causes both an increase in β -GUS liberation, chapter 4, and an increase in cavitation probability [56,57]. In case β -GUS liberation from cells is indeed caused by cavitation, the required pressures and exposure times for β -GUS liberation from tumor cells *in vivo* needs to be further investigated.

As indicated in chapter 3 and before by others [4-6], for effective chemotherapy treatment, the drug concentration needs to be high and homogeneously distributed in the tumor tissue. Upon liquefaction of the tissue by HIFU *in vivo*, besides the tumor cells also the tumor vessels might be destroyed [58], this will highly likely hamper drug delivery in the tumor. Therefore, the prodrug most likely needs to be administrated before cells are destructed by HIFU in order to achieve a high prodrug concentration in the tumor as soon as β -GUS is liberated from the HIFU-exposed cells. To achieve high concentrations of the prodrug over a prolonged period of time in the tumor, required for effective tumor treatment, these prodrugs could be encapsulated in nanogels, as synthesized in chapter 4 of this thesis, that release their drug payload over a prolonged period of time [59,60]. Before investigating the efficacy of prodrugs combined with liberated β -GUS *in vivo*, the prodrug distribution in the tumor should be thoroughly investigated when administrated before or after exposing the tumor to HIFU to maximize the intratumoral prodrug concentration that is homogeneously distributed.

UDEPT in combination with histotripsy

The technique of mechanically destroying tissue by mechanical tissue ablation due to the bio-effects of HIFU, i.e. histotripsy [61,62], is relatively new. This technique uses, like UDEPT, very high peak-negative pressures (>10 MPa) and short pulses with a low duty cycle in order to liquefy tissues [63]. Currently, histotripsy is under clinical investigation in order to liquefy the complete tumor [38]. The first clinical study confirms liquefaction of the prostate tumor by histotripsy, which was well tolerated by the patients [64]. It is currently unknown if this liquefied core contains bioavailable active proteins and enzymes. As observed in our studies *in vitro*, chapter 4, cells were quickly, in tens of seconds, destroyed by exposing them to HIFU at microscopic level, whereas a longer exposure time was required, between 5 and 10 minutes, for endogenous β -GUS liberation from these cells. Hence, possibly only limited bioavailable β -GUS concentration is present in the liquefied regions after histotripsy treatment, that could be increased by increasing the exposure time of histotripsy for each focus point. If β -GUS liberation is indeed achieved by histotripsy, the UDEPT concept might be used as an addition to histotripsy, since complete liquefaction of the tumor tissue upon histotripsy is not yet possible [64]. Incorporating prodrug therapy to the treatment protocol of histotripsy treatment might lead to the eradication of non-liquefied cells after histotripsy.

Whereas for the HIFU settings used in UDEPT treatment it is unknown if vessels will be destroyed *in vivo*, there is evidence that after histotripsy treatment the large vessels are still intact [62,65]. This is most likely caused by the rather high resistance of large vessels to histotripsy compared to the surrounding tissue [62,65]. Though, small vessels (<50 μ m) were destroyed upon histotripsy treatment [65]. In addition, tumor vessels might be destroyed by histotripsy treatment, since they have a lower mechanical strength [66]. In order to use UDEPT as an addition to histotripsy treatment, it is important to investigate the correlation between the intratumoral spatial prodrug distribution and the areas in the tumor that are liquefied. In order to achieve effective treatment of histotripsy and UDEPT, the prodrug needs to be delivered in areas that are not completely liquefied. In these areas the prodrug can be converted into the cytotoxic drug and kill the remaining tumors cells.

Towards a clinical application

To avoid suboptimal tumor treatment and normal tissue toxicity, the tumor needs to be correctly targeted for local drug delivery by UDEPT. It has been shown before that T2 weighted magnetic resonance imaging (MRI) is able to

visualize liquefied regions after mechanical HIFU treatment [67]. In addition, cavitation bubbles, likely the mechanism behind β -GUS liberation from HIFU-exposed cells, appear as bright spots in ultrasound B-mode imaging [68], indicating destruction of the tumor. Though, these measurements are performed during or after treatment. Most likely as soon as these changes are visible on imaging modalities, the damage to the tissue has already occurred. Upon UDEPT treatment this could lead to severe side effects, since the prodrug highly likely needs to be injected before the tissue is exposed to HIFU, as indicated above. Incorrect targeting of the tissue will cause toxicity in these normal tissues by I) HIFU destruction of the cells and II) the activated chemotherapeutic agent. Therefore, correct localization and targeting of the tumor is of major importance in UDEPT. This could be achieved by slightly adjusting the ultrasound settings, decreasing peak-negative pressure and increasing duty cycle, in order to heat the tissue in the ultrasound focus to temperatures in the range of 40 to 43°C. It is possible to observe these increases in temperature by MR thermometry [69], while it will have limited effect on the cells and β -GUS activity [70].

Upon mechanical cell destruction by HIFU, besides β -GUS also other endogenous enzymes and proteins will be liberated from the cells. These liberated proteins could be immune stimulator factors, that recruit antigen presenting cells, like dendritic cells and macrophages, to the liquefied tumor microenvironment. These antigen presenting cells can subsequently be activated by the tumor antigens [71] and activate T-cells to finally kill micrometastases [72]. This could lead to the creation of an *in situ* cancer vaccine in order to treat micrometastases while performing UDEPT on the primary tumor.

CONCLUSION

The work in this thesis aimed to improve local drug deposition in the primary tumor by temperature sensitive liposomes in combination with hyperthermia and prodrugs in combination with mechanical bio-effects of high-intensity focused ultrasound. These strategies showed only in the presence of physical activation, i.e. hyperthermia or HIFU, effective treatment by TSL, *in vitro* and *in vivo*, and prodrugs, *in vitro*. The encouraging results obtained in these studies show a first promising step towards implementation of these techniques into the clinic to increase effective chemotherapy treatment of the primary tumor and reduce undesired toxicities in the normal tissue.

REFERENCES

1. McAllister, S.S.; Gifford, A.M.; Greiner, A.L.; Kelleher, S.P.; Saelzler, M.P.; Ince, T.A.; Reinhardt, F.; Harris, L.N.; Hylander, B.L.; Repasky, E.A., et al. **Systemic endocrine instigation of indolent tumor growth requires osteopontin.** *Cell* **2008**, *133*, 994-1005, doi:10.1016/j.cell.2008.04.045.
2. Rusthoven, C.G.; Jones, B.L.; Flaig, T.W.; Crawford, E.D.; Koshy, M.; Sher, D.J.; Mahmood, U.; Chen, R.C.; Chapin, B.F.; Kavanagh, B.D., et al. **Improved Survival With Prostate Radiation in Addition to Androgen Deprivation Therapy for Men With Newly Diagnosed Metastatic Prostate Cancer.** *Journal of clinical oncology : official journal of the American Society of Clinical Oncology* **2016**, *34*, 2835-2842, doi:10.1200/JCO.2016.67.4788.
3. Xu, H.; Xia, Z.; Jia, X.; Chen, K.; Li, D.; Dai, Y.; Tao, M.; Mao, Y. **Primary Tumor Resection Is Associated with Improved Survival in Stage IV Colorectal Cancer: An Instrumental Variable Analysis.** *Scientific Reports* **2015**, *5*.
4. Minchinton, A.I.; Tannock, I.F. **Drug penetration in solid tumours.** *Nature reviews. Cancer* **2006**, *6*, 583-592, doi:10.1038/nrc1893.
5. Torok, S.; Rezeli, M.; Kelemen, O.; Vegvari, A.; Watanabe, K.; Sugihara, Y.; Tisza, A.; Marton, T.; Kovacs, I.; Tovari, J., et al. **Limited Tumor Tissue Drug Penetration Contributes to Primary Resistance against Angiogenesis Inhibitors.** *Theranostics* **2017**, *7*, 400-412, doi:10.7150/thno.16767.
6. Tredan, O.; Galmarini, C.M.; Patel, K.; Tannock, I.F. **Drug resistance and the solid tumor microenvironment.** *Journal of the National Cancer Institute* **2007**, *99*, 1441-1454, doi:10.1093/jnci/djm135.
7. Bonner, J.A.; Lawrence, T.S. **Doxorubicin decreases the repair of radiation-induced DNA damage.** *International journal of radiation biology* **1990**, *57*, 55-64, doi:10.1080/09553009014550341.
8. Durand, R.E.; LePard, N.E. **Tumour blood flow influences combined radiation and doxorubicin treatments.** *Radiotherapy and oncology : journal of the European Society for Therapeutic Radiology and Oncology* **1997**, *42*, 171-179, doi:10.1016/s0167-8140(96)01878-6.
9. Myrehaug, S.; Pintilie, M.; Tsang, R.; Mackenzie, R.; Crump, M.; Chen, Z.; Sun, A.; Hodgson, D.C. **Cardiac morbidity following modern treatment for Hodgkin lymphoma: supra-additive cardiotoxicity of doxorubicin and radiation therapy.** *Leukemia & lymphoma* **2008**, *49*, 1486-1493, doi:10.1080/10428190802140873.
10. Haas, R.L.; de Klerk, G. **An illustrated case of doxorubicin-induced radiation recall dermatitis and a review of the literature.** *The Netherlands journal of medicine* **2011**, *69*, 72-75.
11. Adams, M.J.; Hardenbergh, P.H.; Constine, L.S.; Lipshultz, S.E. **Radiation-associated cardiovascular disease.** *Critical reviews in oncology/hematology* **2003**, *45*, 55-75, doi:10.1016/s1040-8428(01)00227-x.
12. Candelaria, M.; Garcia-Arias, A.; Cetina, L.; Duenas-Gonzalez, A. **Radiosensitizers in cervical cancer. Cisplatin and beyond.** *Radiation oncology* **2006**, *1*, 15, doi:10.1186/1748-717X-1-15.

13. Lawrence, T.S.; Eisbruch, A.; McGinn, C.J.; Fields, M.T.; Shewach, D.S. Radiosensitization by gemcitabine. *Oncology (Williston Park)* **1999**, *13*, 55-60.
14. Nishimura, Y.; Ono, K.; Hiraoka, M.; Masunaga, S.; Jo, S.; Shibamoto, Y.; Sasai, K.; Abe, M.; Iga, K.; Ogawa, Y. **Treatment of murine SCC VII tumors with localized hyperthermia and temperature-sensitive liposomes containing cisplatin.** *Radiation research* **1990**, *122*, 161-167.
15. Lim, S.K.; Shin, D.H.; Choi, M.H.; Kim, J.S. **Enhanced antitumor efficacy of gemcitabine-loaded temperature-sensitive liposome by hyperthermia in tumor-bearing mice.** *Drug development and industrial pharmacy* **2014**, *40*, 470-476, doi: 10.3109/03639045.2013.768631.
16. Hettinga, J.V.; Konings, A.W.; Kampinga, H.H. **Reduction of cellular cisplatin resistance by hyperthermia--a review.** *International journal of hyperthermia : the official journal of European Society for Hyperthermic Oncology, North American Hyperthermia Group* **1997**, *13*, 439-457.
17. Issels, R.D. **Hyperthermia adds to chemotherapy.** *Eur J Cancer* **2008**, *44*, 2546-2554, doi:10.1016/j.ejca.2008.07.038.
18. Woo, J.; Chiu, G.N.; Karlsson, G.; Wasan, E.; Ickenstein, L.; Edwards, K.; Bally, M.B. **Use of a passive equilibration methodology to encapsulate cisplatin into preformed thermosensitive liposomes.** *Int J Pharm* **2008**, *349*, 38-46, doi:10.1016/j.ijpharm.2007.07.020.
19. Tucci, S.T.; Kheirloomoom, A.; Ingham, E.S.; Mahakian, L.M.; Tam, S.M.; Foiret, J.; Hubbard, N.E.; Borowsky, A.D.; Baikoghli, M.; Cheng, R.H., et al. **Tumor-specific delivery of gemcitabine with activatable liposomes.** *Journal of controlled release : official journal of the Controlled Release Society* **2019**, *309*, 277-288, doi:10.1016/j.jconrel.2019.07.014.
20. Seiwert, T.Y.; Salama, J.K.; Vokes, E.E. **The concurrent chemoradiation paradigm--general principles.** *Nature clinical practice. Oncology* **2007**, *4*, 86-100, doi:10.1038/ncponc0714.
21. Dische, S.; Saunders, M.I.; Lee, M.E.; Adams, G.E.; Flockhart, I.R. **Clinical testing of the radiosensitizer Ro 07-0582: experience with multiple doses.** *British journal of cancer* **1977**, *35*, 567-579, doi:10.1038/bjc.1977.90.
22. Sadeghi, N.; Kok, R.J.; Bos, C.; Zandvliet, M.; Geerts, W.J.C.; Storm, G.; Moonen, C.T.W.; Lammers, T.; Deckers, R. **Hyperthermia-triggered release of hypoxic cell radiosensitizers from temperature-sensitive liposomes improves radiotherapy efficacy in vitro.** *Nanotechnology* **2019**, *30*, 264001, doi:10.1088/1361-6528/ab0ce6.
23. Li, L.; ten Hagen, T.L.; Hossann, M.; Suss, R.; van Rhoon, G.C.; Eggermont, A.M.; Haemmerich, D.; Koning, G.A. **Mild hyperthermia triggered doxorubicin release from optimized stealth thermosensitive liposomes improves intratumoral drug delivery and efficacy.** *Journal of controlled release : official journal of the Controlled Release Society* **2013**, *168*, 142-150, doi:10.1016/j.jconrel.2013.03.011.
24. Manzoor, A.A.; Lindner, L.H.; Landon, C.D.; Park, J.Y.; Simnick, A.J.; Dreher, M.R.; Das, S.; Hanna, G.; Park, W.; Chilkoti, A., et al. **Overcoming limitations in nanoparticle drug delivery: triggered, intravascular release to improve drug penetration into tumors.** *Cancer research* **2012**, *72*, 5566-5575, doi:10.1158/0008-5472.CAN-12-1683.

25. Ranjan, A.; Jacobs, G.C.; Woods, D.L.; Negussie, A.H.; Partanen, A.; Yarmolenko, P.S.; Gacchina, C.E.; Sharma, K.V.; Frenkel, V.; Wood, B.J., et al. **Image-guided drug delivery with magnetic resonance guided high intensity focused ultrasound and temperature sensitive liposomes in a rabbit Vx2 tumor model.** *Journal of controlled release : official journal of the Controlled Release Society* **2012**, *158*, 487-494, doi:10.1016/j.jconrel.2011.12.011.
26. Staruch, R.M.; Hynynen, K.; Chopra, R. **Hyperthermia-mediated doxorubicin release from thermosensitive liposomes using MR-HIFU: therapeutic effect in rabbit Vx2 tumours.** *International journal of hyperthermia : the official journal of European Society for Hyperthermic Oncology, North American Hyperthermia Group* **2015**, *31*, 118-133, doi:10.3109/02656736.2014.992483.
27. Kong, G.; Anyarambhatla, G.; Petros, W.P.; Braun, R.D.; Colvin, O.M.; Needham, D.; Dewhurst, M.W. **Efficacy of liposomes and hyperthermia in a human tumor xenograft model: importance of triggered drug release.** *Cancer research* **2000**, *60*, 6950-6957.
28. Miyanaga, S.; Ninomiya, I.; Tsukada, T.; Okamoto, K.; Harada, S.; Nakanuma, S.; Sakai, S.; Makino, I.; Kinoshita, J.; Hayashi, H., et al. **Concentration-dependent radiosensitizing effect of docetaxel in esophageal squamous cell carcinoma cells.** *International journal of oncology* **2016**, *48*, 517-524, doi:10.3892/ijo.2015.3291.
29. van de Vaart, P.J.; Klaren, H.M.; Hofland, I.; Begg, A.C. **Oral platinum analogue JM216, a radiosensitizer in oxyc murine cells.** *International journal of radiation biology* **1997**, *72*, 675-683.
30. Laginha, K.M.; Verwoert, S.; Charrois, G.J.; Allen, T.M. **Determination of doxorubicin levels in whole tumor and tumor nuclei in murine breast cancer tumors.** *Clinical cancer research : an official journal of the American Association for Cancer Research* **2005**, *11*, 6944-6949, doi:10.1158/1078-0432.CCR-05-0343.
31. Uster, P.S.; Working, P.K.; Vaage, J. **Pegylated liposomal doxorubicin (DOXIL®, CAELYX®) distribution in tumour models observed with confocal laser scanning microscopy.** *International Journal of Pharmaceutics* **1998**, *162*, 77-86.
32. Chakravarty, R.; Hong, H.; Cai, W. **Image-Guided Drug Delivery with Single-Photon Emission Computed Tomography: A Review of Literature.** *Current drug targets* **2015**, *16*, 592-609, doi:10.2174/1389450115666140902125657.
33. Gomes, C.M.; Abrunhosa, A.J.; Ramos, P.; Pauwels, E.K. **Molecular imaging with SPECT as a tool for drug development.** *Advanced drug delivery reviews* **2011**, *63*, 547-554, doi:10.1016/j.addr.2010.09.015.
34. Cook, G.J. **Oncological molecular imaging: nuclear medicine techniques.** *The British journal of radiology* **2003**, *76 Spec No 2*, S152-158, doi:10.1259/bjr/16098061.
35. Lindner, L.H.; Eichhorn, M.E.; Eibl, H.; Teichert, N.; Schmitt-Sody, M.; Issels, R.D.; Dellian, M. **Novel temperature-sensitive liposomes with prolonged circulation time.** *Clinical cancer research : an official journal of the American Association for Cancer Research* **2004**, *10*, 2168-2178, doi:10.1158/1078-0432.ccr-03-0035.
36. Anyarambhatla, G.R.; Needham, D. **Enhancement of the Phase Transition Permeability of DPPC Liposomes by Incorporation of MPPC: A New Temperature-Sensitive Liposome for use with Mild Hyperthermia.** *Journal of Liposome Research* **2008**, *9*, 491-506.

37. Sadeghi, N.; Deckers, R.; Ozbakir, B.; Akthar, S.; Kok, R.J.; Lammers, T.; Storm, G. **Influence of cholesterol inclusion on the doxorubicin release characteristics of lysolipid-based thermosensitive liposomes.** *Int J Pharm* **2018**, *548*, 778-782, doi:10.1016/j.ijpharm.2017.11.002.
38. **ClinicalTrials.org.** Available online: <https://clinicaltrials.gov/ct2/show/NCT03749850> [Accessed: 08/Nov/2020]
39. Peeken, J.C.; Vaupel, P.; Combs, S.E. **Integrating Hyperthermia into Modern Radiation Oncology: What Evidence Is Necessary?** *Frontiers in oncology* **2017**, *7*, 132, doi:10.3389/fonc.2017.00132.
40. Kok, H.P.; Kotte, A.; Crezee, J. **Planning, optimisation and evaluation of hyperthermia treatments.** *International journal of hyperthermia : the official journal of European Society for Hyperthermic Oncology, North American Hyperthermia Group* **2017**, *33*, 593-607, doi:10.1080/02656736.2017.1295323.
41. Behrouzkhia, Z.; Joveini, Z.; Keshavarzi, B.; Eyvazzadeh, N.; Aghdam, R.Z. **Hyperthermia: How Can It Be Used?** *Oman medical journal* **2016**, *31*, 89-97, doi:10.5001/omj.2016.19.
42. Zagar, T.M.; Vujaskovic, Z.; Formenti, S.; Rugo, H.; Muggia, F.; O'Connor, B.; Myerson, R.; Stauffer, P.; Hsu, I.C.; Diederich, C., et al. **Two phase I dose-escalation/ pharmacokinetics studies of low temperature liposomal doxorubicin (LTLTD) and mild local hyperthermia in heavily pretreated patients with local regionally recurrent breast cancer.** *International journal of hyperthermia : the official journal of European Society for Hyperthermic Oncology, North American Hyperthermia Group* **2014**, *30*, 285-294, doi:10.3109/02656736.2014.936049.
43. Gray, M.D.; Lyon, P.C.; Mannaris, C.; Folkes, L.K.; Stratford, M.; Campo, L.; Chung, D.Y.F.; Scott, S.; Anderson, M.; Goldin, R., et al. **Focused Ultrasound Hyperthermia for Targeted Drug Release from Thermosensitive Liposomes: Results from a Phase I Trial.** *Radiology* **2019**, *291*, 232-238, doi:10.1148/radiol.2018181445.
44. Rooseboom, M.; Commandeur, J.N.; Vermeulen, N.P. **Enzyme-catalyzed activation of anticancer prodrugs.** *Pharmacological reviews* **2004**, *56*, 53-102, doi:10.1124/pr.56.1.3.
45. Sherwood, R.F. **Advanced drug delivery reviews: Enzyme prodrug therapy.** *Advanced drug delivery reviews* **1996**, *22*, 269-288, doi:10.1016/S0169-409x(96)00450-4.
46. de Graaf, M.; Nevalainen, T.J.; Scheeren, H.W.; Pinedo, H.M.; Haisma, H.J.; Boven, E. **A methylester of the glucuronide prodrug DOX-GA3 for improvement of tumor-selective chemotherapy.** *Biochemical pharmacology* **2004**, *68*, 2273-2281, doi:10.1016/j.bcp.2004.08.004.
47. Antunes, I.F.; Haisma, H.J.; Elsinga, P.H.; Di Galleonardo, V.; van Waarde, A.; Willemsen, A.T.; Dierckx, R.A.; de Vries, E.F. **Induction of beta-glucuronidase release by cytostatic agents in small tumors.** *Molecular pharmaceutics* **2012**, *9*, 3277-3285, doi:10.1021/mp300327w.
48. Schumacher, U.; Adam, E.; Zangemeister-Wittke, U.; Gossrau, R. **Histochemistry of therapeutically relevant enzymes in human tumours transplanted into severe combined immunodeficient (SCID) mice: nitric oxide synthase-associated diaphorase, beta-D-glucuronidase and non-specific alkaline phosphatase.** *Acta histochemica* **1996**, *98*, 381-387, doi:10.1016/s0065-1281(96)80004-3.

49. Wang, S.; Konorev, E.A.; Kotamraju, S.; Joseph, J.; Kalivendi, S.; Kalyanaraman, B. **Doxorubicin induces apoptosis in normal and tumor cells via distinctly different mechanisms. intermediacy of H(2)O(2)- and p53-dependent pathways.** *The Journal of biological chemistry* **2004**, *279*, 25535-25543, doi:10.1074/jbc.M400944200.
50. Ueda-Kawamitsu, H.; Lawson, T.A.; Gwilt, P.R. **In vitro pharmacokinetics and pharmacodynamics of 1,3-bis(2-chloroethyl)-1-nitrosourea (BCNU).** *Biochemical pharmacology* **2002**, *63*, 1209-1218, doi:10.1016/s0006-2952(02)00878-x.
51. Li, M.; Beg, A.A. **Induction of necrotic-like cell death by tumor necrosis factor alpha and caspase inhibitors: novel mechanism for killing virus-infected cells.** *Journal of virology* **2000**, *74*, 7470-7477, doi:10.1128/jvi.74.16.7470-7477.2000.
52. Lieberthal, W.; Triaca, V.; Levine, J. **Mechanisms of death induced by cisplatin in proximal tubular epithelial cells: apoptosis vs. necrosis.** *The American journal of physiology* **1996**, *270*, F700-F708, doi:10.1152/ajprenal.1996.270.4.F700.
53. Yeung, T.K.; Germond, C.; Chen, X.; Wang, Z. **The mode of action of taxol: apoptosis at low concentration and necrosis at high concentration.** *Biochemical and biophysical research communications* **1999**, *263*, 398-404, doi:10.1006/bbrc.1999.1375.
54. Alaoui, A.E.; Saha, N.; Schmidt, F.; Monneret, C.; Florent, J.C. **New Taxol (paclitaxel) prodrugs designed for ADEPT and PMT strategies in cancer chemotherapy.** *Bioorganic & medicinal chemistry* **2006**, *14*, 5012-5019, doi:10.1016/j.bmc.2006.03.002.
55. Tromp, R.A.; van Boom, S.S.; Marco Timmers, C.; van Zutphen, S.; van der Marel, G.A.; Overkleeft, H.S.; van Boom, J.H.; Reedijk, J. **The beta-glucuronyl-based prodrug strategy allows for its application on beta-glucuronyl-platinum conjugates.** *Bioorganic & medicinal chemistry letters* **2004**, *14*, 4273-4276, doi:10.1016/j.bmcl.2004.06.015.
56. Maxwell, A.D.; Cain, C.A.; Hall, T.L.; Fowlkes, J.B.; Xu, Z. **Probability of cavitation for single ultrasound pulses applied to tissues and tissue-mimicking materials.** *Ultrasound in medicine & biology* **2013**, *39*, 449-465, doi:10.1016/j.ultrasmedbio.2012.09.004.
57. Davitt, K.; Rolley, E.; Caupin, F.; Arvengas, A.; Balibar, S. **Equation of state of water under negative pressure.** *The Journal of chemical physics* **2010**, *133*, 174507, doi:10.1063/1.3495971.
58. Daoudi, K.; Hoogenboom, M.; den Brok, M.; Eikelenboom, D.; Adema, G.J.; Futterer, J.J.; de Korte, C.L. **In vivo photoacoustics and high frequency ultrasound imaging of mechanical high intensity focused ultrasound (HIFU) ablation.** *Biomedical optics express* **2017**, *8*, 2235-2244, doi:10.1364/BOE.8.002235.
59. Maya, S.; Sarmiento, B.; Nair, A.; Rejinold, N.S.; Nair, S.V.; Jayakumar, R. **Smart stimuli sensitive nanogels in cancer drug delivery and imaging: a review.** *Current pharmaceutical design* **2013**, *19*, 7203-7218.
60. Tahara, Y.; Mukai, S.A.; Sawada, S.; Sasaki, Y.; Akiyoshi, K. **Nanocarrier-Integrated Microspheres: Nanogel Tectonic Engineering for Advanced Drug-Delivery Systems.** *Adv Mater* **2015**, *27*, 5080-5088, doi:10.1002/adma.201501557.

61. Hoogenboom, M.; Eikelenboom, D.; den Brok, M.H.; Heerschap, A.; Futterer, J.J.; Adema, G.J. **Mechanical high-intensity focused ultrasound destruction of soft tissue: working mechanisms and physiologic effects.** *Ultrasound in medicine & biology* **2015**, *41*, 1500-1517, doi:10.1016/j.ultrasmedbio.2015.02.006.
62. Khokhlova, V.A.; Fowlkes, J.B.; Roberts, W.W.; Schade, G.R.; Xu, Z.; Khokhlova, T.D.; Hall, T.L.; Maxwell, A.D.; Wang, Y.N.; Cain, C.A. **Histotripsy methods in mechanical disintegration of tissue: towards clinical applications.** *International journal of hyperthermia : the official journal of European Society for Hyperthermic Oncology, North American Hyperthermia Group* **2015**, *31*, 145-162, doi:10.3109/02656736.2015.1007538.
63. Dubinsky, T.J.; Khokhlova, T.D.; Khokhlova, V.; Schade, G.R. **Histotripsy: The Next Generation of High-Intensity Focused Ultrasound for Focal Prostate Cancer Therapy.** *Journal of ultrasound in medicine : official journal of the American Institute of Ultrasound in Medicine* **2020**, *39*, 1057-1067, doi:10.1002/jum.15191.
64. Schuster, T.G.; Wei, J.T.; Hendlin, K.; Jahnke, R.; Roberts, W.W. **Histotripsy Treatment of Benign Prostatic Enlargement Using the Vortx Rx System: Initial Human Safety and Efficacy Outcomes.** *Urology* **2018**, *114*, 184-187, doi:10.1016/j.urology.2017.12.033.
65. Vlaisavljevich, E.; Kim, Y.; Allen, S.; Owens, G.; Pelletier, S.; Cain, C.; Ives, K.; Xu, Z. **Image-guided non-invasive ultrasound liver ablation using histotripsy: feasibility study in an in vivo porcine model.** *Ultrasound in medicine & biology* **2013**, *39*, 1398-1409, doi:10.1016/j.ultrasmedbio.2013.02.005.
66. Jain, R.K. **Determinants of tumor blood flow: a review.** *Cancer research* **1988**, *48*, 2641-2658.
67. Hoogenboom, M.; Eikelenboom, D.C.; van den Bijgaart, R.J.E.; Heerschap, A.; Wesseling, P.; den Brok, M.H.; Futterer, J.J.; Adema, G.J. **Impact of MR-guided boiling histotripsy in distinct murine tumor models.** *Ultrasonics sonochemistry* **2017**, *38*, 1-8, doi:10.1016/j.ultsonch.2017.02.035.
68. Roberts, W.W. **Development and translation of histotripsy: current status and future directions.** *Current opinion in urology* **2014**, *24*, 104-110, doi:10.1097/MOU.0000000000000001.
69. Quesson, B.; de Zwart, J.A.; Moonen, C.T. **Magnetic resonance temperature imaging for guidance of thermotherapy.** *Journal of magnetic resonance imaging : JMIR* **2000**, *12*, 525-533.
70. Hildebrandt, B.; Wust, P.; Ahlers, O.; Dieing, A.; Sreenivasa, G.; Kerner, T.; Felix, R.; Riess, H. **The cellular and molecular basis of hyperthermia.** *Critical reviews in oncology/hematology* **2002**, *43*, 33-56.
71. van den Bijgaart, R.J.; Eikelenboom, D.C.; Hoogenboom, M.; Futterer, J.J.; den Brok, M.H.; Adema, G.J. **Thermal and mechanical high-intensity focused ultrasound: perspectives on tumor ablation, immune effects and combination strategies.** *Cancer immunology, immunotherapy : CII* **2017**, *66*, 247-258, doi:10.1007/s00262-016-1891-9.
72. Prise, K.M.; O'Sullivan, J.M. **Radiation-induced bystander signalling in cancer therapy.** *Nature reviews. Cancer* **2009**, *9*, 351-360, doi:10.1038/nrc2603.

APPENDIX

NEDERLANDSE SAMENVATTING

Het doel van dit proefschrift was het verbeteren van lokale medicijn afgifte in de primaire tumor door middel van fysische activatie van temperatuur gevoelige liposomen (TSL) en prodrugs. Chemotherapie is, naast radiotherapie en chirurgie, een van de meest gebruikte behandelingen tegen kanker. Tijdens chemotherapie behandeling worden de meeste medicijnen systemisch aan de patiënt toegediend, waardoor deze medicijnen zowel in de primaire tumor als de in metastases terechtkomen. In de behandeling van kanker is het van belang dat de primaire tumor zo effectief mogelijk behandeld wordt, zodat het aantal metastases beperkt blijft en daarmee de prognose en overlevingskans van de patiënt zo optimaal mogelijk is. Dit kan met chemotherapie worden bereikt door de primaire tumor voor een lange periode bloot te stellen aan een hoge medicijn concentratie. Doordat de meeste chemotherapeutica I) systemisch worden toegediend en II) niet alleen specifiek werken op de tumor, hebben deze medicijnen ook een effect op het gezonde weefsel en kunnen bijwerkingen in deze gezonde weefsels ontstaan. Deze bijwerkingen kunnen er uiteindelijk voor zorgen dat de dosering van de medicijnen verlaagd moet worden, waardoor de effectiviteit van de behandeling mogelijk afneemt. Door het werkende medicijn alleen in de tumor af te geven, zo genaamde lokale medicijnafgifte, worden de bijwerkingen in het normale weefsel verminderd en kan de primaire tumor effectiever worden behandeld. Dit benadrukt de duidelijke klinische behoefte aan lokale medicijnafgifte in de primaire tumor.

In hoofdstuk 2 en 3 zijn temperatuur gevoelige liposomen in combinatie met hyperthermie behandeling onderzocht om I) het concept getriggerde radiosensitizer afgifte te introduceren en II) de medicijn afgifte in de primair tumor te verbeteren.

In de kliniek worden in sommige specifieke gevallen chemotherapie en radiotherapie gecombineerd om de effectiviteit van de radiotherapie behandeling in de primaire tumor te verhogen, zogenoemde chemoradiotherapie. Een nadeel van de chemoradiotherapie behandeling is dat het gezonde weefsel dat in de radiotherapie straal ligt ook gevoeliger wordt voor de straling, waardoor ernstige bijwerkingen in deze weefsels kunnen ontstaan. Om dit te overkomen werd in **Hoofdstuk 2** het concept getriggerde radiosensitizer afgifte door TSLs geïntroduceerd en vervolgens onderzocht *in vitro*. Het doel van dit concept is om de radiosensitizer concentratie in de tumor te verhogen, terwijl zijn concentratie in het gezonde weefsel verminderd

wordt. In deze studie werd ThermoDox gebruikt, een TSL dat doxorubicine (DOX) bevat, een chemotherapeuticum dat ook het effect van de radiotherapie versterkt, een zogenoemde radiosensitizer. Alleen bij gelijktijdige blootstelling van cellen aan ThermoDox en hyperthermie, werden de cellen gevoeliger voor de radiotherapie behandeling. Dit geeft aan dat radiosensitizatie door ThermoDox alleen plaatsvindt wanneer de DOX vrijgezet wordt uit de ThermoDox liposomen door hyperthermie. Doordat de werkingsmechanismes van DOX, hyperthermie en radiotherapie elkaar kunnen beïnvloeden wanneer ze gelijktijdig of kort na elkaar worden gegeven, I) DOX versterkt het effect van radiotherapie, II) hyperthermie maakt cellen gevoeliger voor radiotherapie en III) hyperthermie verhoogt de effectiviteit van DOX; werd verwacht dat de volgorde van de behandeling invloed zou hebben op de uiteindelijke radiosensitizatie. Echter, in deze studie werd eenzelfde radiosensitizatie effect waargenomen wanneer cellen werden blootgesteld aan gelijktijdige DOX en hyperthermie behandeling voor of na radiotherapie behandeling. Hoewel de resultaten in deze studie de potentie van het concept van getriggerde radiosensitizer afgifte door TSLs *in vitro* aantonen, moet toekomstig onderzoek uitwijzen of deze resultaten vertaald kunnen worden *in vivo*.

De effectiviteit van de chemotherapie behandeling hangt onder andere af van de medicijn concentratie en de ruimtelijke verdeling van het medicijn in de tumor. In **Hoofdstuk 3** werden de intratumorale DOX concentratie en ruimtelijke DOX verdeling onderzocht in een humaan fibrosarcoom muismodel na behandeling met verschillende doses van de DOX-formuleringen ThermoDox (TSL), DOXIL (niet-temperatuur gevoelig liposoom) en vrije DOX. Alleen de behandeling met ThermoDox werd gecombineerd met lokale hyperthermie behandeling van de tumor. Een toename in geïnjecteerde dosis zorgde voor een toename in algehele overleving, onafhankelijk van de gebruikte medicijn formulering. De ThermoDox behandeling zorgde voor de langste overleving bij lage en gemiddelde dosis, terwijl bij de hoogste dosis DOXIL behandeling zorgde voor de langste overleving. Intratumorale DOX concentraties en ruimtelijke DOX verdeling werden bepaald met behulp van confocale fluorescentie microscopie van het tumor weefsel *ex vivo*. Een toename in geïnjecteerde dosis zorgde voor een toename in intratumorale DOX concentratie, voor alle DOX-formuleringen. Voor elke geïnjecteerde dosis was de intratumorale DOX concentratie altijd het hoogst na ThermoDox behandeling, ten opzichte van DOXIL en vrije DOX behandeling. Met betrekking tot de ruimtelijke DOX verdeling resulteerde een toename in geïnjecteerde doses in een homogener intratumorale DOX verdeling, voor alle formuleringen. Echter kon er geen correlatie worden

waargenomen tussen de overleving na behandeling met de verschillende DOX-formuleringen en intratumorale DOX concentratie en ruimtelijke DOX verdeling. Desalniettemin geeft deze studie aan dat de intratumorale DOX concentratie en ruimtelijke DOX verdeling belangrijke factoren zijn voor een effectieve chemotherapie behandeling. De link tussen de verschillende gebruikte DOX-formuleringen en de resulterende overleving, intratumorale DOX concentratie en intratumorale ruimtelijke DOX verdeling moet verder worden onderzocht.

Naast triggers van buitenaf, zoals hyperthermie, kan lokale medicijn afgifte ook verkregen worden door triggers vanuit het lichaam zelf, zoals enzymen in enzym prodrug-therapie, beschreven in hoofdstuk 4 en 5. Voor effectieve enzym prodrug-therapie moet aan de volgende eisen worden voldaan; I) een snelle omzetting van de prodrug in het cytotoxische medicijn, II) een hoge biologisch beschikbare enzym concentratie voor prodrug omzetting in de tumor en III) een lage biologisch beschikbare enzym concentratie voor prodrug omzetting in het gezonde weefsel. Een veel onderzochte groep prodrugs voor enzym prodrug-therapie zijn de glucuronide-prodrugs. Deze glucuronide-prodrugs worden omgezet door het enzym β -glucuronidase (β -GUS) in het cytotoxische medicijn, en bestaan uit een glucuronzuur, een spacer en het cytotoxische medicijn. Bij de omzetting wordt het glucuronzuur gespleten door de β -GUS, waardoor vervolgens de spacer verwijderd wordt door hydrolyse en uiteindelijk het cytotoxisch medicijn vrijkomt.

Een vrij korte lengte van de spacer hindert een snelle splijting van het glucuronzuur door de β -GUS. Om dit te overkomen werden in **Hoofdstuk 4** twee glucuronide-prodrugs gesynthetiseerd met een verdubbeling en een verdrievoudiging van de lengte van de spacer (DOX-AU2 en DOX-AU3), ten opzichte van de eerder gesynthetiseerde prodrug DOX-AU1 (DOX-GA3). Zoals verwacht was de omzettingssnelheid van DOX-AU2 en DOX-AU3 in DOX verhoogd in vergelijking met DOX-AU1. Om de biologische beschikbaarheid van β -GUS in de tumor te verhogen, werd het concept 'ultrageluid directed enzym prodrug-therapie' (UDEPT) geïntroduceerd en vervolgens onderzocht *in vitro*. In dit concept werden cellen blootgesteld aan high-intensity focused ultrasound (HIFU) om β -GUS vrij te zetten. Alleen wanneer cellen werden blootgesteld aan HIFU bij drukken boven een minimale piek-negatieve druk waren de mechanische bio-effecten van de HIFU in staat om de β -GUS vrij te zetten uit de cellen. Blootstelling van cellen aan HIFU bij drukken onder deze minimale piek-negatieve druk zorgde niet voor het vrijzetten van β -GUS uit de cellen. De hoeveelheid vrijgezette β -GUS, vanaf de minimale piek-negatieve

druk, was afhankelijk van de piek-negatieve druk en de blootstellingstijd. De vrijgezette β -GUS was vervolgens in staat om DOX-AU2 om te zetten in DOX en om de cytotoxiciteit van DOX-AU2 te verhogen naar eenzelfde cytotoxiciteit als DOX. Hoewel deze resultaten de potentie van het verlengen van de spacer in de prodrug formulering en het concept UDEPT *in vitro* aantonen, is verder onderzoek nodig om aan te tonen of deze resultaten vertaald kunnen worden *in vivo*.

Prodrugs zijn meestal kleine moleculen, waardoor ze na systemische toediening in de patiënt vaak snel uit het lichaam worden uitgescheiden. Om dit probleem aan te pakken werd in **Hoofdstuk 5** de prodrug DOX-AU1 (DOX-GA3) geconjugeerd aan een polymeer (prodrug-polymeer conjugatie) en vervolgens ingekapseld in een nanogel formulering. De omzettingssnelheid van deze nieuwe gesynthetiseerde nanogel in DOX was iets langzamer in vergelijking met de omzetting van vrije DOX-AU1 in DOX. Dit komt waarschijnlijk doordat de β -GUS niet in staat was om in de nanogel door te dringen, waardoor de prodrug eerst vrijgezet moest worden uit de nanogel voordat deze omgezet kon worden in DOX. De nanogel formulering werd tenslotte *in vitro* onderzocht in combinatie met het UDEPT concept, beschreven in hoofdstuk 4. De vrijgezette β -GUS van de cellen die blootgesteld werden aan HIFU was in staat om de prodrug uit de nanogel formulering om te zetten in DOX en om de cytotoxiciteit van de prodrug te verhogen. Dit concept moet verder worden onderzocht *in vivo* in combinatie met de DOX-AU2 prodrug.

LIST OF PUBLICATIONS

Full papers in peer-reviewed journals

Helena C. Besse , Clemens Bos, Maurice M. J. M. Zandvliet, Kim van der Wurff-Jacobs, Chrit T. W. Moonen, Roel Deckers. *Triggered radiosensitizer delivery using thermosensitive liposomes and hyperthermia improves efficacy of radiotherapy: An in vitro proof of concept study*. PlosOne. E 13(9): e0204063. <https://doi.org/10.1371/journal.pone.0204063>

Helena C. Besse , Angelique D. Barten-van Rijbroek, Kim M.G. van der Wurff-Jacobs, Clemens Bos, Chrit T.W. Moonen and Roel Deckers. *Tumor drug distribution after local drug delivery by hyperthermia, in vivo*. Cancers. 2019, 11, 1512; doi:10.3390/cancers11101512

Helena C. Besse *, Yinan Chen *, Hans W. Scheeren, Josbert M. Metselaar, Twan Lammers, Chrit T. W. Moonen, Wim E. Hennink and Roel Deckers. *A Doxorubicin-Glucuronide Prodrug Released from Nanogels Activated by High-Intensity Focused Ultrasound Liberated β -Glucuronidase*. Pharmaceutics 2020, 12, 536; doi:10.3390/pharmaceutics12060536 [* These authors contributed equally to this work]

Oral presentations

Helena C. Besse, Clemens Bos, Chrit T.W. Moonen, Roel Deckers. *Tri-modality treatment with chemotherapy, radiotherapy and mild-hyperthermia, in vitro*. International Conference of Hyperthermic Oncology, New Orleans, United States of America. April 2016

Helena C. Besse, Clemens Bos, Maurice M.J.M. Zandvliet, Chrit T.W. Moonen, Roel Deckers. *Combination of hyperthermia and radiosensitizer-loaded thermosensitive liposomes improves efficacy of radiotherapy: an in vitro proof of concept study*. European Society for Hyperthermic Oncology. Athens, Greece. June 2017

Poster presentations

Helena C. Besse, Clemens Bos, Chrit T. W. Moonen, Roel Deckers. *Chemoradiation with hyperthermia; influence of timing in vitro*. European Radiation Research Society. Amsterdam, The Netherlands. September 2016

Helena C. Besse, Clemens Bos, Maurice M.J.M. Zandvliet, Chrit T.W. Moonen, Roel Deckers. *Combination of chemotherapy, radiotherapy and hyperthermia in vitro*, Synergy Forum, Bonn, Germany, March 2018

Published as short communication:

Helena C. Besse, Clemens Bos, Maurice M.J.M. Zandvliet, Chrit T.W. Moonen, Roel Deckers. *Combination of chemotherapy, radiotherapy and hyperthermia in vitro*. Synergy, 2019, 9, 100052 <http://dx.doi.org/10.1016/j.synres.2019.100052>

Helena C. Besse, Clemens Bos, Maurice M.J.M. Zandvliet, Chrit Moonen and Roel Deckers. *Triggered radiosensitizer release by radiosensitizer-loaded thermosensitive liposomes and hyperthermia improves efficacy of radiotherapy: an in vitro proof of concept study*. European Molecular Imaging Meeting. San Sebastián, Spain. March 2018

Helena C. Besse, Angeliqué D. Barten-van Rijbroek, Kim M.G. van der Wurff-Jacobs, Clemens Bos, Chrit T.W. Moonen, Roel Deckers. *Imaging the effect of local drug delivery on the tumor drug distribution*. European Molecular Imaging Meeting. Glasgow, United Kingdom, March 2019

CURRICULUM VITAE

Helen Besse was born on June 17th 1990 in Haarlem, The Netherlands. She graduated from high school at the Kennemer College in Beverwijk in 2007. This same year she started studying 'Medisch Ingenieur' at the Inholland University of Applied Science in Haarlem. After her graduation in 2011, she decided to continue studying and enrolled in the premaster program of 'Biomedical Engineering' at the Eindhoven University of Technology in Eindhoven. After successful finishing the premaster she started the master 'Medical Engineering' at the Eindhoven University of Technology in Eindhoven. Her final internship took place at the University Medical Center Utrecht in Utrecht where she met her current PhD supervisors. Her internship revolved around the triggered radiosensitizer delivery concept. She was asked to continue and extend her research during a PhD supervised by prof. dr. C.T.W. Moonen, dr. R. Deckers and dr. C. Bos. The results of this work are described in this thesis. Since 2019 Helen works as a junior researcher in the UMC Utrecht in collaboration with the Van Vuurden group in The Maxima in Utrecht.

ACKNOWLEDGEMENTS

En dan is het proefschrift klaar en is het dankwoord het enige dat nog geschreven dient te worden. Dit proefschrift had niet tot stand kunnen komen zonder alle mensen om mij heen, zowel in het UMC Utrecht, de Universiteit Utrecht als daar buiten. Graag wil ik een aantal mensen persoonlijk bedanken.

Prof. dr. C.T.W. Moonen, beste Chrit, als eerste wil ik u bedanken. Zonder u lag er nu geen proefschrift. Bedankt dat u mij de kans heeft gegeven om in uw groep mijn promotieonderzoek te kunnen uitvoeren. Dank voor de begeleiding, de discussies en het kritisch lezen van mijn manuscripten. Ik bewonder uw kwaliteit om op de hoogte te zijn van de grote lijnen van alle onderzoeken van uw PhD-studenten en postdocs, vooral doordat de groep zo breed georiënteerd is.

Dr. R. Deckers, beste Roel, als eerste co-promotor heb jij enorm bijgedragen aan dit werk. Bedankt dat jij, na mijn stage in de groep, mijn eerste co-promotor wilde zijn. Dank voor de vele discussies over de projecten en experimenten en voor het kritisch lezen van mijn manuscripten. Ik zal proberen in de toekomst om mijn ABA schrijfvorm alleen nog in sinterklaas gedichten te verwerken.

Dr. C. Bos, beste Clemens, als tweede co-promotor heb jij, naast Roel, ook een grote bijdragen in dit werk gehad. Ondanks dat celbiologie niet jou vakgebied is, heb ik veel geleerd van de discussies die we gehad hebben, misschien juist wel doordat je niet volledig in het vakgebied zit en daardoor er beter van een afstand naar kon kijken. Bedankt voor je bijdrage.

Leden van de beoordelingscommissie, bedankt dat jullie mijn proefschrift kritische wilden lezen en beoordelen.

De HIFU groep, with a special thanks to Marc, Jean-Michel, Bart, Cyril, Noboru, Yuana, Josanne, Charis, Negar, Ilya, Daiki and Bucin thanks for your discussions, suggestions, help and all the lunches.

Karolin, Bi, Qingxue, Yinan, Hans, Gert, Fabian, Bart, Twan, Yang and Wim, thank you all for your help with the prodrug studies. Without your help it would not have been possible to have such nice chapters about the improvement in prodrug conversion and improvement of the pharmacokinetics of the prodrug. Hopefully we are able to publish the improvement in prodrug conversion for enzyme prodrug therapy soon in a nice journal.

De afdeling Biofarmacie van de Universiteit Utrecht, met in het bijzonder Joep, Louis, Roel en Mies. Bedankt dat ik bij jullie mijn experimenten heb mogen uitvoeren. Ondanks dat ik een gast was, heb ik mij nooit zo gevoeld. Als ik vragen had kon ik bij jullie allemaal langs lopen en werd ik direct geholpen. Dank voor jullie luisterend oor en meedenkend vermogen.

Maurice Zandvliet, dankzij jou kon ik de cellen en de muizen bestralen. Ondanks dat jij niet altijd direct bij de projecten betrokken was, was je wel altijd geïnteresseerd in de voortgang van de projecten en de resultaten. Ook als de resultaten tegen vielen, wist jij er een positieve draai aan te geven.

De ‘meiden van radiotherapie’, Ingrid, Kim, Masha en Marjolijn ontzettend bedankt dat ik (‘Helen van de cellen’) altijd langs kon komen om mijn cellen en ook een aantal muizen te bestralen. Het was altijd gezellig bij jullie, waardoor ik altijd graag bij jullie langs kwam.

De medewerkers van het GDL, zonder jullie hulp was het niet mogelijk geweest om mijn dierexperimenten uit te voeren. Anja een speciaal woord voor jou, wat vond ik het fijn dat jij altijd tijd probeerde vrij te maken om mijn muizen te injecteren.

De secretaresses, met in het bijzonder Judith, dank voor al jullie hulp met bestellingen. Zonder jullie hadden de projecten een hoop vertraging gehad. Ook was het altijd gezellig om even bij jullie langs te komen om te buurten.

De collega's in het Prinses Maxima Centrum. Graag wil ik jullie bedanken voor al jullie steun en goede en wijze woorden. Ondanks dat jullie niet direct betrokken zijn geweest bij mijn PhD onderzoek, was er altijd wel een luisterend oor als ik dat nodig had. Ik hoop nog heel lang met jullie samen te mogen werken.

Marjolein, bedankt voor de gezellige lunches. Het was fijn om soms even te sparren over het onderzoek met iemand die er niet direct bij betrokken was. Dit bracht mij vaak weer tot nieuwe inzichten.

Annelies, bedankt voor de gezellige tijd dat jij stagiaire was in onze groep. Wat hebben we gelachen, maar ook kei hard gewerkt. Bedankt voor de brainstorm sessie over de voorkant van deze thesis.

Angelique, ontzettend bedankt dat je mij de fijne kneepjes uit het vak hebt geleerd met het werken met muizen. Ontzettend bedankt voor een luisterend oor als ik die nodig had. De vele cappuccino's zal ik niet snel vergeten.

Kim, paranimf, ontzettend bedankt dat jij mijn extra paar handen (en af en toe ook mijn extra hersens) was op het lab. Zonder jouw hulp had ik een hele hoop dingen niet kunnen doen. Ook ontzettend veel dank voor je luisterend oor als ik die nodig had, niet oordelen, maar gewoon even luisteren was soms voldoende voor mij.

Oom Wim bedankt voor je steun. Als ik het over mijn onderzoek had was je altijd geïnteresseerd en vroeg je altijd door.

Henk, ukkie, broerie, bedankt dat je mijn paranimf wilt zijn. Bedankt dat je altijd naar mijn verhaal wilde luisteren, al was er waarschijnlijk vaak geen touw aan vast te knopen.

Pap en mam, ik weet niet hoe ik jullie moet bedanken. Bedankt dat jullie mij altijd hebben gesteund in de keuzes die ik gemaakt heb. Ook al begrepen jullie vast vaak niet waar ik het nu weer over had als ik het over mijn onderzoek sprak, jullie hebben mij altijd gesteund. Ik hoop dat dit nog heel lang zo blijft.

